UNIVERSITÀ DEGLI STUDI DI MILANO

Agriculture, Environment and Bioenergy
(code: R10)

Department of Agricultural and Environmental Sciences Production,
Landscape, Agroenergy (DISAA)

XXX cycle

FRUIT FLESH IN PEACH:
characterization of the 'slow softening' texture

Disciplinary sectors: AGR/03, AGR/07

Angelo Ciacciulli
R10941

Supervisor: Prof. Daniele Bassi
Co-supervisor: Prof. Laura Rossini
PhD School Coordinator: Prof. Daniele Bassi

2016-2017

Table of Contents

1 General abstract

The aim of this research was to deepen the knowledge about the slow softening texture in peach.

The texture is a synthesis of several parameters detected by senses, derived from the food structure. The paramount sense in the texture perception is the tactile one, principally perceived by hand and mouth. The tactile perception is a combination of four classes of mechanoreceptors, each one specialized to perceive mechanic deformation with different speed. This combined perception influences the consumer evaluation of food quality, giving the texture importance among food characteristics. The texture could also affect the taste perception through mechanical actions on food structure. The mechanical property linked to the texture is associated with the cellular organization and the cell wall strength. The main cell wall component affecting texture in fresh fruit is pectin, a polymer of galacturonic acid. The disassembly of pectin involves several enzymatic and non-enzymatic activities acting directly in pectin cleavage or indirectly disrupting non-covalent interactions. The gold standard of texture analyses is the sensorial one, however several issues make sensorial analyses inapplicable to breeding programs to select plant with improved fruit texture. Several efforts were made to achieve instrumental analyses capable of substitute humans in texture analyses. To mimic the tactile sense, a discipline studying the material response to an applied force, the rheology, is applied. The easiest instrumental measure of rheology parameters is the penetrometer test, diffused to measure the firmness, but exploitable to collect the Young's modulus and the slope of yield stress represented respectively elasticity and fracturability.

In peach, so far at least four textures were described, melting (M), stony hard (SH), non-melting (NM) and slow softening (SS). Prior to this work, no reliable objective nor fast tool were available to phenotype and select the SS trait in peach germplasm. The only reliable approach was a sensorial assessment done by a texture-trained panel, requiring repeated and time-consuming assessment. An objective, instrumental method, was set up by processing the data of a digital penetrometer test. The penetrometer itself, as reported in paragraph 2, does not support the ability to discriminate among the different texture types, as already reported in other works. In addition, this method appears to be affected by the fruit ripening season, since the early-ripening accessions tend to show faster loss of firmness, while the late-ripening exhibit a slower firmness loss.

Using the data collected in our experiment, the texture dynamic (TD) model was developed from the observation of differences in the rheogram shape due to the elasticity and fracturability parameters. The TD model, that excludes the firmness effect on the fracturability and elasticity parameters, was thus developed, after testing it on 20 accessions in three years, allowing for

reliable discrimination between SS and M phenotype. Differences in the TD were also found when comparing M vs SH and M vs NM textures. In particular, when comparing M and SS, TD value is explained for the 96% from the texture.

The developed method was then applied (together with sensorial evaluation) to genetically dissect the SS trait. Association and QTL mapping approaches were combined by analyzing a germplasm panel and a biparental progeny, and a single locus at the end of chromosome 8 was identified. RNA-seq analysis of 2 SS and 2 M accessions suggested some common features with the SH type described in literature. In both texture types a lower auxin response was found when compared to the M type. This agrees with the already known activity of auxin in the modulation of cell wall rearrangement and expansion. Therefore, slower softening could be associated to slower cell wall rearrangement. In future, comparison of auxin content in slow softening and melting type peaches might provide further insight into the validity of this hypothesis. In detail, by RNA-seq comparing M and SS a total of 64 differentially expressed genes were found in the genomic region harboring the SS locus. Out of these 64 genes, 16 are uncharacterized, while among the characterized ones, 4 are putatively involved in auxin response based on peach genome annotation. Analysis of polymorphisms in these 4 DEGs based on resequencing data of the ‘Max10’ and ‘Rebus 028’ parents of biparental population did not uncover any variants in agreement with the observed segregation. Analyzing 2kb gene models flanking regions, 16 genes were associated with polymorphisms outside the coding sequence: the possible regulatory effects of such variants require further evaluation by expression analyses.

In summary, the major results are the setup of a reliable tool to score objectively the SS texture and the detection of a major locus and his dominant mendelian inheritance. However, NGS and RNA-seq approaches are presented as a speculative data only, because they are not supported by hormones content in fruit, and the large locus detected did not allow indication of a putative variant.

These results will: a) give impetus in exploring SS genetic and physiology; b) support the design of future crosses and experiments; c) increase marker density in the locus; d) point out the possible central role of auxin (to validate the hypothesis of a similarity between SS and SH physiology); e) allow texture assessment of improved cultivars; and f) allow phenotyping of segregating progenies to develop molecular markers associated with the SS trait.

2 INTRODUCTION

2.1 The texture: a sensory property

A pioneer in food texture science and founding editor of the *Journal of Texture Studies*, Alina Szczesniak states [1] that "texture is the sensory and functional manifestation of the structural, mechanical and surface properties of foods detected through the senses of vision, hearing, touch and kinesthetics". She then postulated the following axioms:

a. "texture is a sensory property" which can only be perceived and described by humans and any instrumental measurements must be related to sensory responses.

b. "texture is a multi-parameter attribute."

c. "texture derives from the structure of the food."

d. "texture is detected by several senses."

Tactile texture can be divided into oral–tactile texture, mouth feel characteristics, phase changes in the oral cavity, and the tactile texture perceived when manipulating an object by hand (often used for fabric or paper and called "hand") or with utensils [2]. However, the tactile sense is perceived in humans at least from four different mechanoreceptors specialized on different deformation frequencies, the fast-adapting type I, the slowly-adapting type I, the fast-adapting type II and the slowly-adapting type II, involved in the perception of deformation with 5-50 Hz frequency, deformation with frequency lower than 5Hz, vibration of 40-400 Hz and the sensation of static force, respectively [3].

Texture is one of the most appreciated characteristics of food [4], enhancing or reducing flavor perception [5]. Experiments showed that foods are less recognizable after changes in texture, so the combination of taste and texture is considered a fingerprint of food in particular flavorless food like cucumber which are unrecognizable when blended [2].

Several experiments conducted in simplified models as artificial matrices [5,6], showed distinct phenomena modulating the perception of savors [7] by physical immobilization, increasing the contact area or the ability to change the releasing rate of aromas [5], juice and tasting molecules, affecting the biting time [8] and the receptor binding of the tasty molecules [9].

Regarding the relationship between texture and food structure, the basic structure of food is a carbon skeleton: commonly in fruit and vegetables a major component is represented by plant cell walls consisting of carbohydrates arranged in long and branched structures, called polysaccharides, interacting with other organic molecules and ions. Plant cell walls link together adjacent cells creating tissues and organs [4,10]. Considering edible fruits, non-lignified

parenchymatous cells are joined together by the middle lamella, composed mainly by pectin. Pectin is a polymer of galacturonic acid, branched with sundry substituents as sugars, probably the most complex macromolecule in nature [10]. Pectin plays a major role in texture perception [11] and its degradation is associated to changes in texture [12]. The pectin degradation pathway involves several enzymatic activities [13]. Polygalacturonase enzymes hydrolyze the poly galacturonic acid (pectin), cleaving the alpha-1,4 glycosidic bonds between galacturonic acid residues: exo-polygalacturonases cut molecules from the end, releasing galacturonic acid monomers, while endo-polygalacturonases cut the molecule randomly producing pectin fragments, i.e. oligogalacturonides. Pectin methylesterase catalyzes the demethoxylation of pectin, changing water affinity. Polygalacturonic transeliminase catalyzes an eliminative cleavage of (1->4)-alpha-D-galacturonan to give oligosaccharides with 4-deoxy-alpha-D-galact-4-enuronosyl groups at their non-reducing ends [14]. As recently demonstrated in tomato using genetic engineering approach, a bottleneck in pectin disassembly could be represented by the ability of the enzymes to move across extra-cellular matrix. The relaxation of extra-cellular matrix increasing the accessibility to the pectin matrix, a big part in relaxation is done by expansins disrupting non covalent interactions [15–18].

2.2 The gold standard for texture analysis

Since texture is defined as a sensory property that can be perceived and described only by humans, physical parameters detected and quantified by so-called texture testing instruments must be interpreted in terms of sensory perception [1,19]. For these reasons, sensorial analysis is the gold standard for texture studies. Sensory evaluation comprises a set of techniques for accurate measurement of human responses to foods and minimizes the potential bias effects of brand identity and other information influencing consumer perception [2].

Advanced protocols to describe different textures in food have been already published [6,20]. The use of humans as sensors involves several human abilities [1], tactile, acoustic and chemical perception, capacity to elaborate sensations from previous experience, communication capacity [19], known vocabulary (lexicon) and native language (compared to Americans, Japanese could use five times more words to describe the same textural property of foods) [2]. Each human ability involved in sensorial analysis may be a bottleneck for an objective and reproducible analysis [21].Other limits of sensory analysis could be to find standard foods, well trained panelists, homogeneity of the panelist age, culture and ethnicity [20,22]. Usually this time-consuming approach is inapplicable to breeding programs where a relatively large number of samples need to be assessed each day [23].

2.3 Objective analyses

Different scientific approaches have been applied to develop objective analyses to better understand texture, including: rheology [24–26], tribology [27] and acoustic-vibrational approaches [28,29], that are based on disciplines studying mechanical properties of matter; chemistry to study matter chemical composition [18]; optical approaches based on microscopy to visualize structural differences among samples with different textures [30]; and spectrophotometry to study optical properties of the material [31,32].

2.3.1 Mechanical properties

Different mechanical approaches intending to imitate the human tactile sense have been proposed to characterize food texture.

2.3.1.1 Rheology

Food rheology is the study of the manner in which food materials respond to an applied stress or strain [26]. Instrumental methods have been classified into three main categories: empirical, imitative and fundamental [28]. Among the empirical ones, the most used is the Penetrometer Test [22,24].

2.3.1.1.1 Penetrometer test

Penetrometer test is the easiest test to record a stress-strain curve [24]. The stress-strain curve of a material (where the stress is the compressive loading and the strain is the amount of deformation), is the relationship between the stress and strain recorded during the penetrometer test. The graphical representation of stress-strain curves is the rheogram, that is specific for each material and related with its mechanical properties [33]. Penetrometer test is usually performed at constant speed where the force is recorded [21]. Several plungers have been tested and adopted [34]: in the horticultural field the most used has a cylindrical shape with a flat head [22]. The test involves the compression force, applied by the central part of the plunger, and the shear force exercised by the edge of the plunger [35].

The most used mechanical parameter is the upper yield point (pag.18 Figure 2) that represents the firmness [2], one of the main maturity indices of fruits [36]. Other parameters that can be obtained are the Young's modulus that represents the elasticity, and the Slope of Yield Stress after the upper yield point, that represents the fracturability [37].

2.4 The texture in fruit

Texture is one of the main fruit quality attribute, influencing consumers degree of liking and marketability. All these aspects are well-described in several recent reviews [28,34,38].

In the horticulture field, the term “texture” has acquired a specific meaning, departing to some extent from its meaning in the food engineering field [34]. In contrast to the extemporary description of food texture used by food engineers, horticulturists define different texture types referring to the evolution of fruit structure-related characteristics during ripening or storage. This implies that fruit texture is somehow described as a dynamic concept linked to firmness evolution [38].

2.4.1 Fruit texture, improvement of consistency and shelf-life

The availability of fruits with satisfactory quality for fresh market requires the adoption of different solutions [39–41]. Most important examples are represented by the extension of the harvest season using cultivars with different ripening dates, combined with cultivation at different latitude and/or altitude; by the improving of storage technologies to preserve and control fruit texture (controlled temperature, atmosphere and light conditions); improving the maintenance of fruit consistency (reported in the sensory analysis vocabulary ISO 5492:2008, as "mechanical attribute detected by stimulation of the tactile or visual receptors") during storage, for example by tapping into a wide genetic diversity pool and combining texture type variants. Interesting, most of these variants were often discarded in the past, when the consumer trends and distribution chains were different [39,42].

2.5 Peach: Taxonomy and Botanical Overview

The domesticated peach (*Prunus persica* [L.] Batsch; synonym: *Amygdalus persica*) is a member of the *Rosaceae* family in the subgenus *Amygdalus* within the section Euamygdalus .*P.persica* is a self-compatible entomophilous species, with a small diploid genome (220Mb, 2n=16) almost twice the size of the Arabidopsis one [43]. The genus *Prunus* is a monophyletic group, which consists of ten subgenera and more than 200 species having certain morphological traits in common. They are deciduous shrubs and trees with simple leaves and glands at the base of a blade or at the top of the petiole. The inflorescence shows large variation among the groups but as common trait it has a calyx with a bell-shaped tube, inserted at the throat of flower [44].

Linné (1758) first named the species (*Amygdaluspersica*) with the specific epithet *persica* based on the opinion that the fruit was native to Persia (present day Iran) due to its widespread cultivation in this putative country of origin.

Written records and archaeological evidences discovered [45] between the 19th and the 20th century showed that the origin of peach domestication was the region of Northwest China between the Tarim Basin and the north slopes of the Kunlun Shan mountains, at least as far back as 3000 BC. More recent archaeological studies [46] (based on discovery of peach stones preserved in waterlogged context in the Zhejiang province) propose that the lower Yangzi River valley, in the East of China, was the region of early peach selection from the wild *P. persica* ancestor, in a process that began at least 7500 years ago and took over three millennia. This could help to explain the presence of peach in Japan around 2500 BC [45]. According to these data, the westward movement of peach could have brought it into Persia around the second century BC, by crossing the entire China in 3000 years.

Prunus is from the Latin for plums. Peaches were acquired by the Romans, probably along the Silk Road in the beginning of the Christian era, which had given rise to the European supposition that the fruit had originated in Persia. The fruit tree was introduced in Italy during the 1st century AD; soon it reached France, which became a second center of diversification of this species after China.

2.5.1 Macroeconomic Relevance

Globalization, decrease in transportation costs, rising incomes and technological improvements, in addition to development and evolution of commercial trades, have led to an enhancement of the global exchange of vegetables and fruits.

Peach has a prominent role in the global fruit farming production and is the most important in the genus Prunus [47].

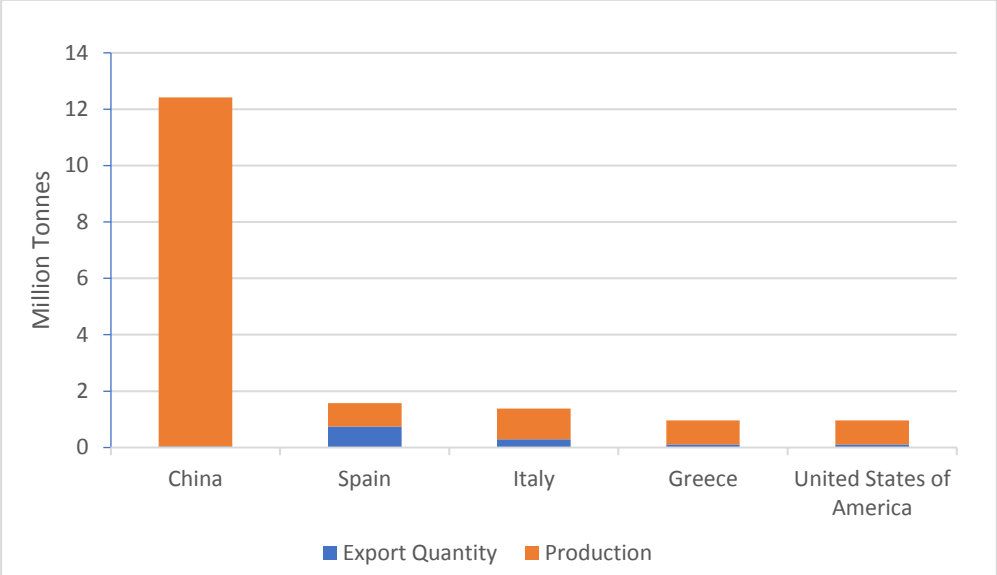

Figure 1 Production and export quantity (in millions of tons) of top five peach producer in the world (FAOSTAT 2013)

The global production of peaches is estimated around 21,6 million tons, which corresponds to 3,21% of the entire global fruit production, with a growth rate that has increased by approximately 3.93% every year since 2000 [48]. Worldwide, Italy is the third producer of peaches after China and Spain, producing 1.4 million tons of fresh fruit every year (Figure 1). Italy is also one of the major exporters (with Spain as leader), with almost a 300k tons exported in 2013 corresponding to an economic value of more than 363 million dollars [49].

2.5.2 Morphology

2.5.2.1 Growth Habit

Peach is a deciduous medium-high tree with a smooth and straight trunk and a dark grey bark. It can reach 4-8 m, depending on internode length [42]. The growth habit is characterized by the angle of insertion of the branches and the length of the internodes, which define the appearance of the tree canopy.

Buds are present at the base of leaves. Each node shows commonly two lateral flower buds and one vegetative bud in the middle [42]. One-year-old shoots have flower buds on their axis and one vegetative bud at the apex [42]. Fruit weight is positively correlated to the vigor of the shoot and

also depends on the season. For this reason, the production of fresh fruit needs a vigorous shoot, up to 100 cm in length. The production of canning fruit, instead, benefits from a weak shoot, 10-25 cm long [42] because the small fruit are more suitable for canning. Side shoots arising from a bud formed in the same year are called a “feather” [50].

2.5.2.2 Leaf

In peach, leaves are formed right after anthesis and present two temporary stipules at the base of the petiole [42]. The adaxial surface of the leaves is darker than the abaxial one, and the color of the veins is associated with the color of the flesh of the fruit: pale yellow in the yellow flesh fruit and pale green in the white flesh fruit. The margin can be smooth or crenate. There are usually a variable number of secreting glands near the bottom of the leaf margins. Their shape can be globose or reniform. They are absent in plants that are homozygous recessive for this trait [42].

2.5.2.3 Flower

Peach has hermaphroditic and perigynous flowers. The gamosepalous calix falls after the initial swelling of the fruitlet. Petals, normally five, are separated and two kinds of corolla are known: showy, with large rose-shaped petals, or non-showy, with bell-shaped smaller petals. This second shape is the dominant trait [51]. Petal color varies from white to dark red, but the most common is a shade of pink. The gynoecium is superior. The receptacle contains as many as 20 or 30 stamens and it carries reddish anthers, unless they are sterile: in this case, they look pale yellow; this is a monogenic recessive trait [42].

2.5.2.4 Phenological Stages

The time of flowering depends on the chilling units (see below) necessary to overcome endo-dormancy, and later, on the amount of “growing degree-hours” (GDH) required to reach a full blossom. The chilling requirement is the minimum period of cold below a certain threshold temperature that a flower needs to complete its morphological development. It is expressed in chilling units (CU), a measure of the exposure of plants to chilling temperature (latter depends on the adopted model) [52].The heat requirement is analogous to the chilling requirement: the flower needs an amount of heat to achieve organ development after endo-dormancy is fulfilled. Heat is the main driver of bloom timing [53][54].In winter, at the end of the dormancy period, microsporogenesis takes place: two 2-nucleated pollen grains, contained into the pollen sac, are generated from the microsporocytes [55]. A light brown color covers the swelling bud during meiotic division of the megasporocyte that leads to a tetrad of megaspores. Three of them ordinarily disintegrate, and the fourth one develops into an embryo sac. Following subsequent

nuclear divisions, the embryo sac contains eight nuclei, one of which becomes the female gamete; this usually happens a few days before full anthesis [53].

The ovary contains two ovules, but only one will be fertilized; the development of the ovary is conventionally divided into four phenological stages: cellular division (SI), pit hardening (SII), cell elongation and enlargement (SIII) and, finally, fruit ripening (SIV) [56].

The fruit development period may range from 55-60 to more than 220 days and is under polygenic control. A major locus for maturity date was located on chromosome 4 and associated to a variant in a NAC transcription factor gene [57].

2.5.2.5 Fruit

The peach drupe can have a globose, elongated or flat shape [58]. The weight can vary from 50g, up to 700g, depending on cultivars and agronomical management. The epicarp is thin and can be adherent to the flesh depending also on mesocarp texture. The skin can be pubescent or glabrous in the case of "nectarines", a mutation that occurred in China and has been imported in Europe in the XIV century [59–61].

Fruits are classified as climacteric or non-climacteric by the ability to increase respiration rate and ethylene production at the onset of ripening. The ethylene is a hormone synthesized in the plant from the amino acid methionine, by three enzymatic steps involving in order three enzymes: The S-adenosyl-L-methionine (SAM); 1-aminocyclopropane-1-carboxylic (ACC) acid synthase (ACS); and ACC oxidase (ACO). Several ACS and ACO genes are present in plant genomes [62]. The expression of these genes could be regulated by two different systems one autoinhibitory (in presence of exogenous ethylene the endogenous one decrease) and one autocatalytic (presence of exogenous ethylene induces endogenous ethylene production). The first (System 1) is induced in the normal plant development and in response to stress (such as cold), the second (System 2) plays a role in organ senescence and fruit ripening [62]. Peaches are described as climacteric fruit that ripe with a biphasic behavior, a first phase of slow flesh softening followed by a rapid decrease of firmness. The shift to a rapid loss of firmness is marked by a climacteric peak, with high ethylene production regulated by System 2 [63]. Notably, peach germplasm is characterized by the presence of non-climacteric accessions, such as the stony hard cultivars [64], unable to produce ethylene but reaching a sufficient degree of palatability.

2.5.2.6 Endocarp and Seed

The endocarp is lignified (in certain cultivars lignification can be so limited that the fruit is completely edible [42]) and shows a more or less furrowed surface. The suture presents a ridge and a pointed tip at the apex. The endocarp splitting trait (which is not a desirable trait) is believed to occur when a rapid mesocarp expansion leads to the splitting at the carpel suture or the shattering of the rigid endocarp. It is also associated to those agronomical practices that lead to a faster expansion of the mesocarp. In almonds (*P. dulcis*) the trait is associated to the presence of a site of a secondary ovule abortion [65]. Flesh and stone may adhere to each other or be separated. This trait seems to be controlled by a single locus, where the freestone allele is dominant over the clingstone allele [51]. Mesocarp and endocarp shapes are strictly related: in round shaped fruit, the stone is globose, while in flat fruits the stone is round-oblate or elliptic in elliptic fruits. The seed within the fruit is typically single (exceptionally, double) and may contain cyanogenic glycosides, that confer a bitter taste [42].

2.5.2.7 Fruit texture

Several texture variants have been described in peach flesh:

Melting (M) peaches are the most spread texture type in fresh market. They are characterized by a fast evolution from firm and crispy flesh to creamy and buttery on the tree and mealy during extended storage. Within this texture type, a quantitative variation exists for the rate of flesh melting. Several approaches were tested to measure differences in peach flesh texture: the rate of firmness loss, measured by penetrometer test, during ripening or storage, is the most commonly used to assess the quantitative variation in the M type [66].

Stony hard (SH) peaches have a crispy and consistent flesh characterized by the lack in ethylene and auxin production: they are able to melt and produce ethylene in cold storage or after ethylene or auxin exposure [67]. This trait originated in the far Est and was introduced in Italy from the Korean peach ‘Yumyeong’ used in an important Italian breeding program [68]. For the SH type, the production of ethylene can be assessed by head space gas chromatography of peach fruits. A recent molecular study of this texture type allowed the development of a genetic marker based on a microsatellite variant in the intron of *PpYUC11*, a gene involved in the auxin biosynthesis [69].

The non-melting (NM) type is characterized by a consistent flesh unable to melt, but able to produce ethylene [70]. This texture is associated to the lack of endopolygalacturonase activity [63], that gives resistance to mealiness during storage. This type is frequently used for canning [42]. For the NM type, knowledge of the molecular genetic basis of the trait produced reliable DNA markers allowing early prediction of the flesh texture already at the seedling stage [70].

Non-softening (NSF) texture is described as a crispy non-melting variant: this trait is controlled by a specific allele (called “f2”) of the same endoPG gene already described in non-melting texture [70].

Slow-ripening (SR) is described as a peach with a hard and pour quality flesh: it is a mutant unable to ripe properly, since fruit development arrests at the S3 stage [71]. First described in ‘Fantasia’ progeny, this texture type is insensitive to ethylene exposure [71].

Slow softening(SS) peaches are phenotypic variants of melting-type, characterized by a slower softening rate compared to the melting ones. Interesting, this type of texture was initially classified as stony hard types, although SS peaches were subsequently recognized as a distinct texture type for their ability to produce ethylene and melt [72]. The origin of this character is unknown, but was first described in the ‘Big Top’ variety, a nectarine licensed by Zaiger Genetics around 1980 [73].

2.5.3 Breeding

In breeding programs, breeders must be able to efficiently and inexpensively evaluate thousands of plants in a short time. In the case of fruit trees, phenotyping is made more complex by the high variability of fruits on the plant, so that a high number of replicated measurements/observations is required to obtain reliable data.

The inherent complexity of texture evaluation, the time and money required for advanced chemical/physical analysis to analyze cell wall structure, the inapplicability of panel tests for high numbers of genotypes, are stimulating the development of fast and low-cost techniques to phenotype different texture types. Combination of different mechanical properties with the appropriate interpretation could well represent the texture. As Harker argued, mechanical parameters are not the same for tactile or bite and instrumental detection: an example is the hardness (the force needed to compress the sample under a flat plate for 1cm), while the relation among instrumental and sensory has a good predictability on sample with different hardness but sharing the same matrix, compare samples with the same instrumental hardness, but different matrix, shows weaker relation between organoleptic hardness and instrumental ones [8,28].

2.5.3.1 Finding a reliable tool to phenotype the SS trait

The major relevance of texture types for the development of new peach cultivars requires reliable and efficient methods for texture evaluation, in order to be applied in breeding programs. Over the years our group's efforts were dedicated to find a reliable tool to score the SS texture type. Various approaches were tested including Time Resolved Spectroscopy (TRS), echography, computerized tomography (CT), expressible juice, penetrometer test by digital penetrometer [74], Fourier Transformed Near Infrared Spectroscopy in reflectance (FT-NIR), pectin analysis [72] and relaxation test by texturometer.

Herein it is reported the development and testing of an empirical method to score the SS texture type, incorporating an innovative interpretation approach and exploiting the relationship among rheological parameters as a predictor of fruit texture. This novel approach has been applied together with sensorial phenotyping in a genotyped progeny and germplasm collection to identify the genetic basis of the trait and genotypic markers associated to SS phenotype. A single locus was detected, suggesting a simple inheritance of SS texture. The gene models annotated within the target locus have been investigated through RNAseq approach by comparing 2 SS and 2 M accessions. Candidate variants were also investigated by whole-genome re-sequencing (WGRS) of cross parents.

The developing of a novel phenotyping approach for SS texture has been submitted to the *Journal of Texture Studies* with the title: **Identification of a melting type variant among peach (P. Persica L. Batsch) fruit textures by a digital penetrometer.** The manuscript is currently under review.

The genetic dissection of SS texture will be submitted to *Tree Genetics & Genomes*.

My contribution to the both studies was manifold, besides writing two papers. Both are ready to be submitted to referred journals.

In the first one, I contribute to the developing of the phenotyping approach, through the collection and analysis of the mechanical parameters from rheograms, and model development.

In the second paper, other than collecting and analyzing phenotypic data, I performed QTLs, RNA-seq and WGRS data analysis.

3 Identification of a melting type variant among peach (*P. Persica* L. Batsch) fruit textures by a digital penetrometer

3.1 Abstract

The increase of peach (*P. persica* L. Batsch) fruit shelf-life is one of the most important objectives of breeding activities, since peach is a highly perishable fruit which undergoes rapid softening during ripening. The loss of fruit firmness is accompanied by a modification of textural properties. At least four distinct textures were described in peach: *melting* (M), *non-melting* (NM), *stony hard* (SH) and *slow-melting* (better defined as '*slow-softening'*, SS). Flesh textures are usually discriminated using different approaches, specific for each type. Objective of this work was the development of a reliable method to assess flesh texture variants in peach fruit, with special attention to the SS type which is currently scored by sensorial evaluation. A puncture-based test using a digital penetrometer was performed on 20 accessions belonging to the four textural groups, obtaining a series of rheological measures related to mechanical flesh properties and including Young's Modulus, Upper Yield Point and Slope of Yield Stress. Among the components of elasto-plastic behavior of the fruits, the texture dynamic index (TD) was shown to be a reliable parameter to distinguish the group of M flesh texture from SS, NM and SH. The TD index can be applied to discriminate SS and M fruits, although variability within the different texture groups suggests the existence of genotypes with intermediate phenotypes and minor quantitative trait variation.

The availability of an objective method to clearly distinguish M and SS phenotypes paves the road to phenotype segregating progenies in order to find molecular markers associated to the SS trait.

3.1.1.1 Practical applications

The TD index could be considered to determine different textures in fleshy fruits in pre- and post-harvest, to support evaluation of quality for the intended use.

Key words: texture, firmness, slow softening, phenotyping, fruit quality, peach

3.2 Introduction

Fruit maturation is a coordinated and genetically programmed process, leading to the development of an edible fruit with desirable quality attributes [13]. In most fleshy fruits, softening is a ripening-related phenomenon. The softening process involves metabolic and physiological changes, which lead to the disassembly of the polysaccharide matrix composing the primary cell wall and middle lamella, and loss of turgor pressure [18]. Such changes impact shelf-life, so selection of slow softening cultivars is a major objective of current breeding activities, stimulating the search for textural characteristics able to increase fruit storability.

Peach [*Prunus persica* L. (Batsch)] is the most important cultivated species of the *Prunus* genus. Significant breeding efforts during the last decades have allowed the improvement of important fruit quality traits [42]. Currently, the increase of shelf-life is a primary breeding goal, since peach is a highly perishable fruit which undergoes a rapid softening during ripening [75]. In this context, the development of a quick and reliable method for assessing the range of textures present in peach is of utmost importance (see below). The rate of softening varies depending on genotype, environmental conditions and cultural practices [70]. Peach softening is also accompanied by a modification of fruit textural properties. Texture can only be perceived and described by humans and any instrumental measurements should be related to sensory responses because it is 'the sensory and functional manifestation of the structural, mechanical and surface properties of foods detected through the senses of vision, hearing, touch and kinesthetic' [2]. So far at least four distinct types of flesh texture have been identified in peach: ‘melting’ (M), ‘non-melting’ (NM), ‘stony hard’ (SH) and 'slow-melting' [42]. Most peach accessions are characterized by a melting flesh. NM peaches arise from a missense mutation in an *endo*-PG gene [34,76], coding for an endo-polygalacturonase enzyme, resulting in a slower decrease of firmness and the maintenance of a rubbery texture [77]. NM trait is typical of canning peaches. SH peaches also tend to remain firm, since they are unable to produce ethylene during ripening, although they can melt under appropriate storage conditions [78,79]. A reduced expression of the auxin biosynthesis gene *PpYUCCA11-like* has been recently suggested as the genetic base of the recessive SH trait [80]. A novel phenotype of qualitative origin has been recently characterized, the *slow-melting* (SM) texture, typical of 'Big Top'-like cultivars [81]. SM peach tend to soften slower compared to the melting ones, although the biochemical and physiological patterns are still largely unknown. In agreement with Contador et al. [82], we suggest renaming the SM texture in *slow-softening* (SS), since the term ‘slow-melting’ can be easily mistaken with the quantitative variability found within the melting type [72,83]. The different texture phenotypes are often discriminated using various

approaches, e.g. the evaluation of the softening rate during storage or other methods specific for each texture [66,82,84–86]. For the most interesting, the SS type, an objective and reliable method of phenotyping has not been developed yet.

The puncture test is one of the simplest methods to obtain a stress–strain curve. It is widely used in both solid and semi-solid foods [24], and thus very useful for measuring the textural qualities of fruits [21]. Puncture-based tests are commonly used in peach for firmness measurement, a crucial parameter for establishing the harvest time and for the monitoring of post-harvest storage [87,88]. However, the continuous evolution of firmness in peach flesh does not allow to phenotype a given texture by a simple pressure test. At the current state of the art, the NM accessions are mechanically indistinguishable from SH ones. Instead, SH accessions are usually identified by monitoring ethylene evolution, since both NM and M fruits release ethylene during maturation [89]. The SS phenotype is the most difficult to distinguish, particularly from very firm, unripe, M one. In some studies, SS accessions have been identified by comparing firmness decay during post-harvest storage, assuming a low rate of softening with respect to melting peach [66]. Nevertheless, this approach is hardly generalizable, since it is affected by the criteria adopted for the establishment of harvest time and the evaluation of maturity degree. Such difficulties are exacerbated in experimental studies involving many accessions or seedlings, often bearing a limited number of fruits.

The assessment of the different flesh phenotypes under variable conditions by using a simple and reproducible method and allowing a fast recording of many samples is highly desirable. The present study is aimed at the development of a reliable method to discriminate peach fruit texture using a digital penetrometer, with particular attention to the SS texture type.

3.3 Materials and Methods

3.3.1 Plant Material

The experiments were carried out with a total of twenty peach accessions belonging to the four different flesh phenotypes and the two skin types: peach (P, fuzzy surface) and nectarine (N, glabrous surface) (Table 1), harvested in seasons 2011, 2012 and 2014. Fruits were picked between June and August at the “Zabina” experimental orchard located in Castel San Pietro (Bologna, Italy). Fruits of each accession were harvested from different parts of the tree crown (lower,

medium and upper) to collect a full range of ripening degree. One hundred sixty-five fruits were harvested for each accession. Peaches were grouped into three maturity classes based on the I_{AD} parameter (see below) and divided into lots of 15 fruits for daily analysis, so that each lot included the full I_{AD} range. Each lot was composed by five fruits classified as less mature, five as medium mature and five as mature. Out of the one hundred sixty-five fruits for each accession, seventy-five were held at 20° C and ninety were put into 4° C storage for two weeks. After cold storage, fruits were held at 20° C for daily analysis. Every day one lot of fruit was taken out of storage and measured for I_{AD}, fruit weight and firmness. Shelf life evaluation was conducted after harvest and two weeks of cold storage.

3.3.2 Measure of the maturity stage by IAD

ΔAmeter instrument (Synteleia S.R.L., Italy) is a portable spectrometer that measures the index absorbance difference (IAD) between two wavelengths near the chlorophyll-A absorption peak [36]. I_{AD} was measured on the two sides of each fruit at harvest and daily during the analysis. The lower value of I_{AD} was taken as the expression of the physiological age the fruit, since the lower the parameter, the more advanced is the ripening evolution. The fruit classes are specific for each accession. For each accession, fruits were sorted using I_{AD} in three different classes, each representing about a third of the total number of fruits.

3.3.3 Penetrometer test

The penetrometer test was performed on the day of analysis. A 1.5 cm round portion of the skin was removed from the middle of each fruit cheek by a slicer. The penetrometer test was done using a constant rate digital penetrometer (Andilog Centor AC TEXT08) fitted with an 8mm diameter flat plunger for 1 cm puncture, motorized by a basic test stand (BATDRIVE) set at 5 mm/s speed. The rheogram data were acquired by the RSIC bundle software (Andilog Technology).

3.3.4 Rheogram processing

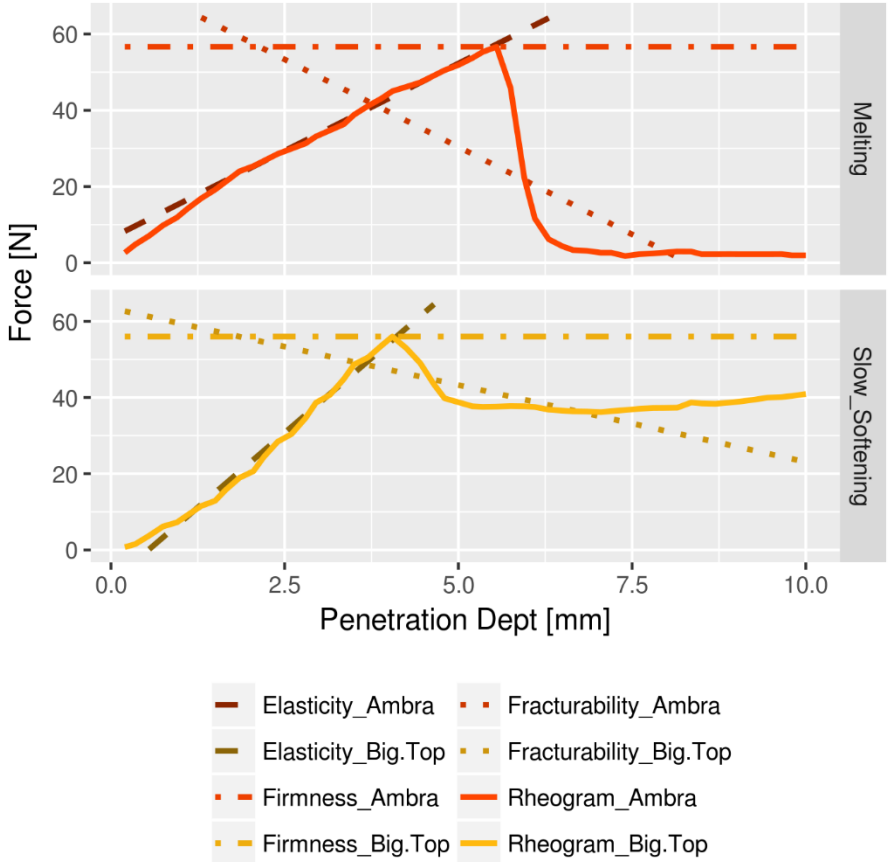

Figure 2 An example of rheogram (stress-strain curve) obtained using a digital penetrometer from sampled fruits of 'Big Top' (slow-softening, brown solid line) and 'Ambra' (melting, red solid line); the Young's modulus and the Slope of yield stress curve are indicated by dashed and dotted lines, respectively. The Young's modulus and the Slope of yield stress are calculated respectively on the 20 data points before and after the Upper yield point.

Young's modulus (Y_M), the upper yield point (the U_{YP}) and the slope of yield stress (S_{YS}) [9] were calculated from the rheogram of each sample (Figure 2). The upper yield point, and the Young's modulus are the maximum firmness and the elastic properties of the fruit, respectively. In a mechanical sense, the ripening process of fruit flesh can be described in terms of its elasto-plastic properties: elastic for the small deformations and plastic for the large ones. Modulus of elasticity (E), and modulus of fracturability (F) were evaluated by using the following formulas, respectively: $E = \Delta YM / \Delta UYP$ and $F = \Delta SYS / \Delta UYP$.

3.3.5 Statistical data analysis

To investigate the components of the elasto-plastic behavior in peach fruit, a regression approach was applied to rheological data. A linear regression for each accession was calculated using the *lmList* function of the R package *nlme*, according to the formula: $U_{YP} = E*Y_M + F*S_{YS} + k$, where E is the elasticity modulus, F the fracturability modulus and *k* the intercept. The *E:F ratio* was then defined as *texture dynamic* (TD) and calculated for each accession for each year and storage condition. ANOVA analysis was performed on TD data using as the *aov* function in R *stats* package. The data of each accession were analyzed by year and storage regime as blocks. Physical analyses were tested for distribution by Shapiro-Wilk test. Based on distribution, each parameter was analysed with a congruous test. Young's modulus was checked by Siegel-Tukey analysis for equal variability based on ranks. The upper yield point was analyzed by ANOVA for the variance analysis and the slope of yield stress was analyzed by Welch Two Sample t-test. An LSD ($\alpha<0.05$, p adjusted by Bonferroni) was done on TD, E and F using the texture phenotypes as blocks.

3.4 Results

A common problem when evaluating and comparing softening behavior, is to properly account for the variability in fruit physiological age, both within and among accessions. The maturity degree at harvest exerts a major effect on the dynamic of firmness loss during storage.

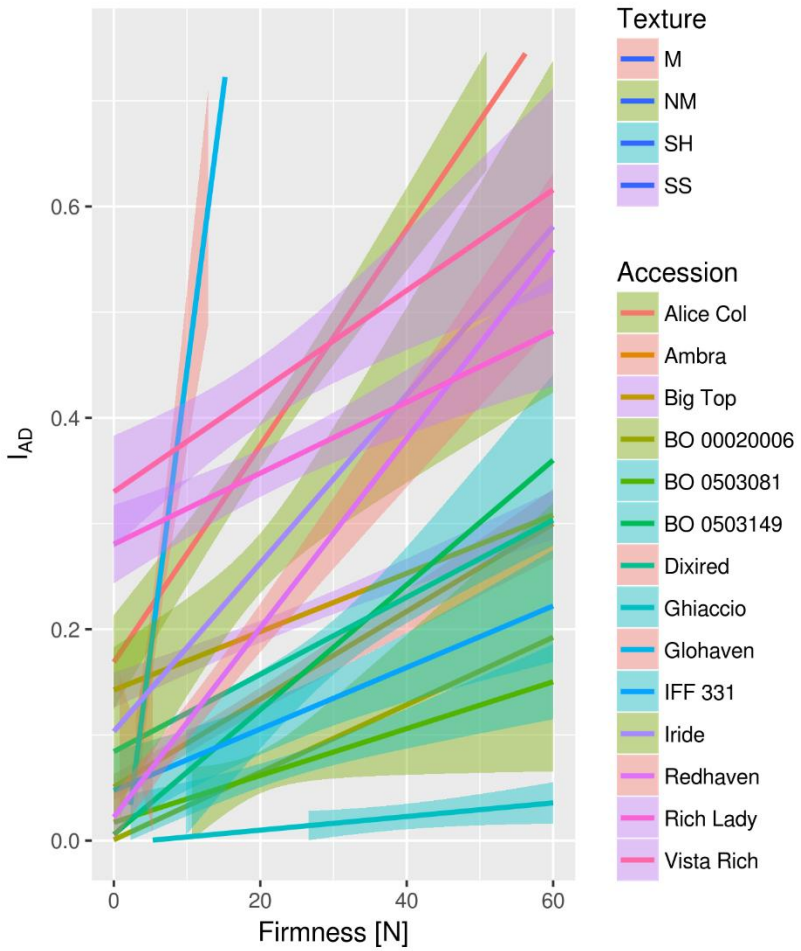

Figure 3 Rate of variation of the I_{AD} (maturity degree index) respect to the firmness, calculated using a linear regression model for each accession. Grey halo indicates the standard error.

Based on DA-meter measurement (I_{AD} as an estimate of fruit physiological age) and independently from the days of storage, firmness reduction (in terms of the I_{AD} *vs* U_{YP}) turned out to be highly variable, accession-specific and not correlated with the different textures types (Figure 3).

Also monitoring the temporal evolution of firmness (U_{YP} *vs* days of storage) does not reveal significantly different trends among the texture types, although NM accessions tend to display a slower decay (Figure 4). Indeed, the rate of firmness loss in each accession fits a logistic curve that largely depends on the criteria used for the establishment of harvest time. It is important to

remark that for this analysis, fruits were *a priori* sorted based on I_{AD} value into three maturity classes in order to remove confounding effects due to the heterogeneity in their physiological age.

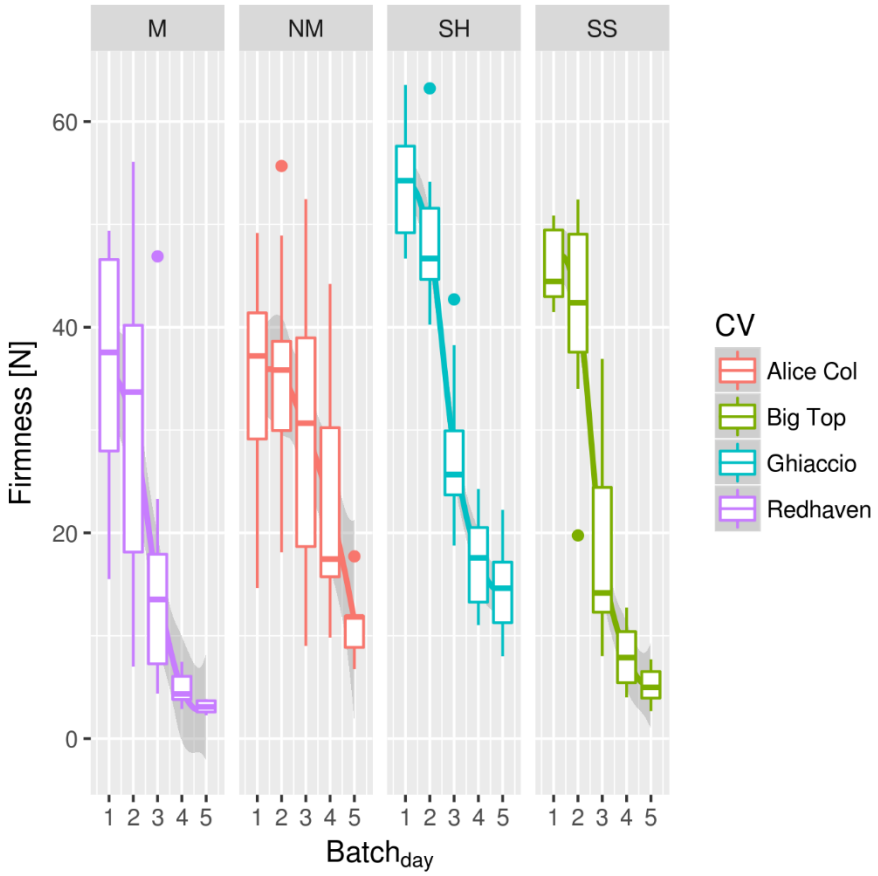

Figure 4. Rate of firmness loss during storage at 20° C for five days for four accessions representative of each texture group: 'Alice Col' (NM), 'Big Top' (SS), 'Ghiaccio' (SH) and 'Redhaven' (M). The regression model is smoothed using the Loess method, with a 0.8 span. The standard error is indicated by grey halo. The box plot represents the median and quartiles and for each day of analysis.

Therefore, none of the two above described approaches yielded a reliable classification of the different texture types within the considered panel of accessions. As described in Materials and Methods section, other rheological parameters can be used in addition to the U_{YP} to describe the changes of peach texture during ripening: the Young's modulus (Y_M), evaluating the elastic behavior, and the fracturability (F), dependent from the slope of yield stress and describing the plastic behavior [2] .

The Young's Modulus showed a bimodal distribution in M and SS accessions, being unimodal for the SH and NM ones (data not shown). The Y_M was strongly related with the U_{YP}, and the slope of this regression (E) was specific for each accession, representing the rate of variation in the elastic properties of the fruit (Supplemental Table 1). Nevertheless, the E parameter

was unable to significantly differentiate among the different textures, although a tendency to display low elasticity values was observed in M accessions (Table2).

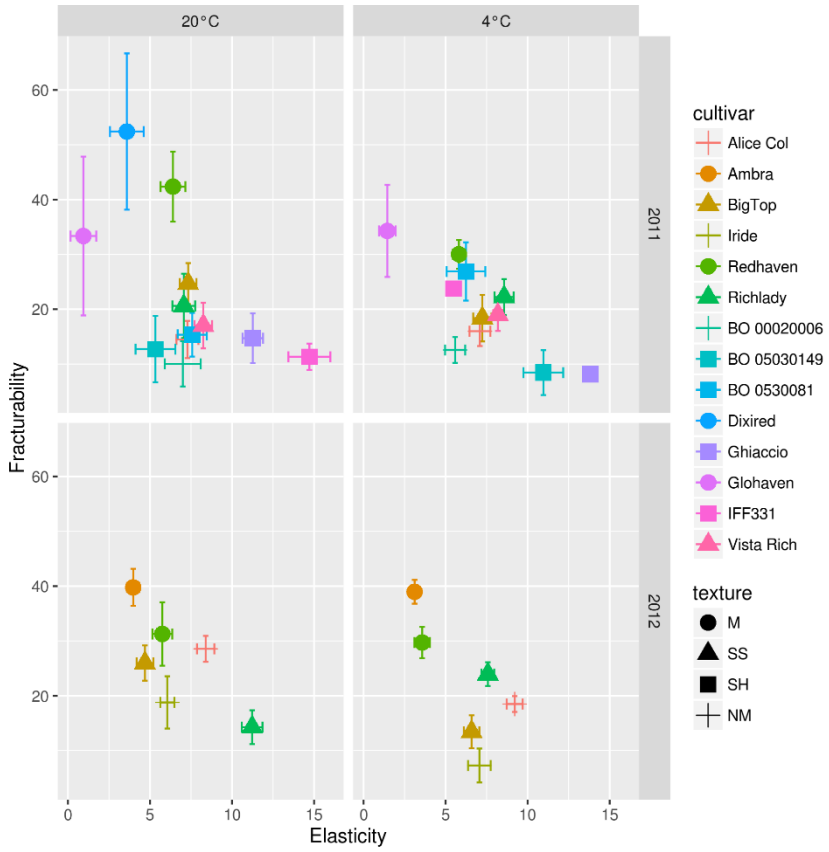

Figure 5. Relationship between Fracturability and Elasticity parameters in fruits collected during 2011-2012 seasons. The shape of the points indicates the texture group (M, melting; SS, slow-softening; SH, stony hard, and NM, non-melting). Colors indicates each cultivar. Horizontal and vertical error bars represent the standard error of the Fracturability (F) and the Elasticity(E) of the regression model: $U_{YP} = E*Y_M + F*S_{YS} + k$ (*see text for further details).*

The Slope of Yield Stress (S_{YS}) showed a studentized distribution, with a marked difference in the shape among the textures, while the statistical test showed significant differences for all pairs of combinations. The fracturability (F), calculated by the regression of the S_{YS} on the U_{YS}, was specific for each accession (Supplemental Table 1) and able to distinguish SS from M (showing high F value), but not from NM and SH (Table 2). As shown in Figure 5, E and F parameters tend to be inversely related i.e. the fracturability tend to decrease with the increase of elasticity and vice versa. Melting fruits show a higher fracturability and, thus, lower elasticity compared to the other texture types, particularly with respect to NM and SH fruits, in which the two parameters remain basically constant. In contrast to F, the E parameter was affected by storage conditions, particularly in SH accessions. However, the ability of F parameter to discriminate

between M and SS textures was not confirmed on 2014 season (Supplemental Table 2**).** For such reasons, novel indices were calculated: *Texture Dynamic* (TD) and *K-intercept*. The TD index is based on the ratio between the elasticity and the fracturability modulus (*E:F ratio*). The TD index, can be interpreted as the trend of variation in fruit consistency in function of the firmness, resulting significantly correlated to the texture, independently from the accession (including skin hairiness phenotype), year or storage regime. The texture explains 88% of the TD mean square error (MSE), whereas the M and SS phenotypes explained up to 96% of TD MSE. SH and NM add 8% of unexplained variance. The M phenotype can easily be separated from SS for TD value lower than 0.25 (Figure 6 and Supplemental Table 1). The discrimination ability of TD index was also validated on 2014 data, obtaining consistent results (Supplemental Figure 2 and Supplemental Table 2). Nevertheless, TD cannot distinguish NM from both SS and SH, since the index showed similar values for these three texture groups (Figure 6). The K-intercept is the intercept of the model and resulted well-correlated with the TD-index (data not shown).

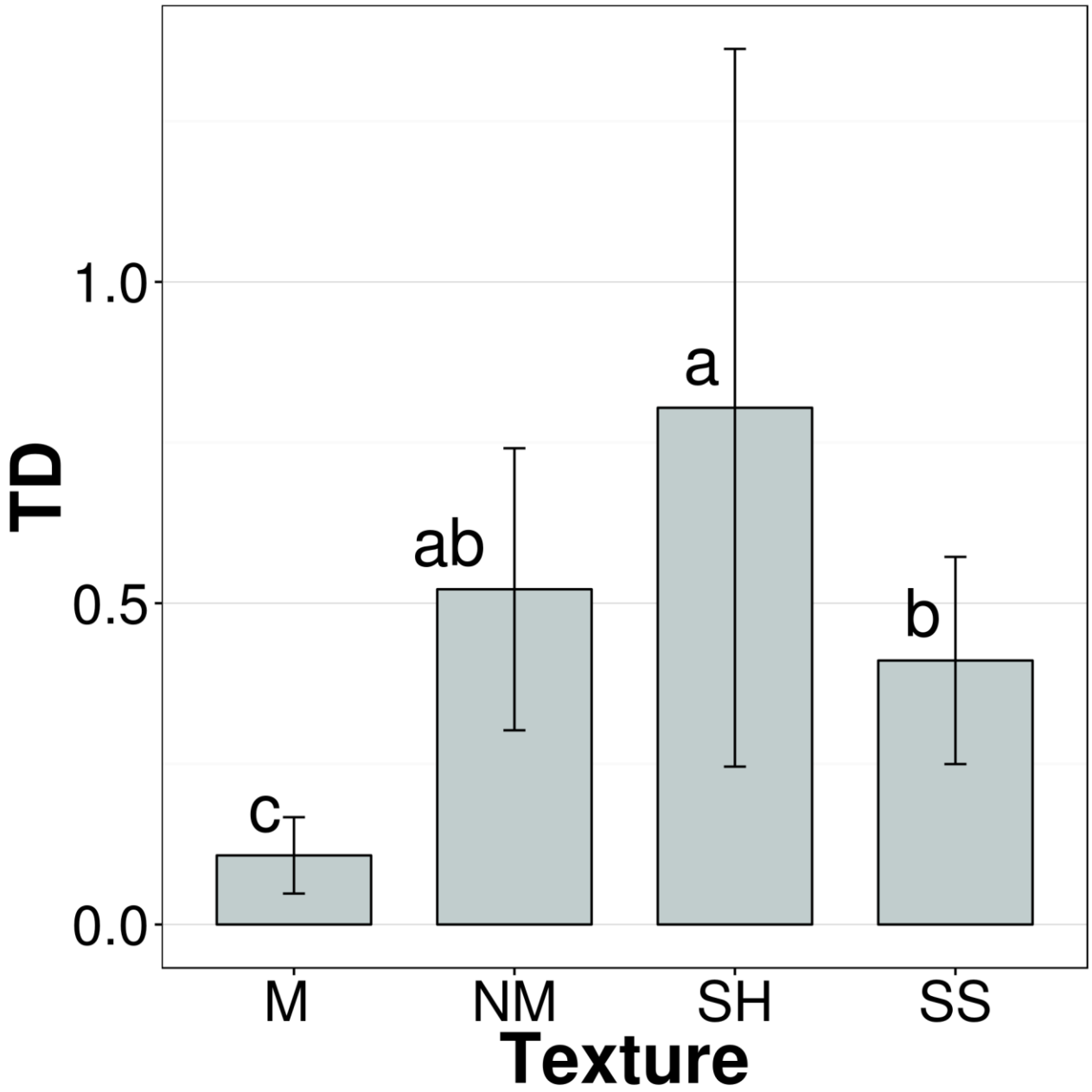

Figure 6Texture Dynamic (TD) values in each texture group as predicted by the model. Letters indicate the least significant differences (LSD) among textures for α<0.05 (p value adjusted by Bonferroni). The error bars represent the standard errors.

3.5 Discussion and Conclusions

Analyzing a diversified set of accessions, the difficulties of discriminating among different texture types by monitoring maximum firmness (U_{YP}) decay during storage became evident, in particular when comparing M and SS types. Comparison of the softening trend among accessions requires an accurate estimation of fruit physiological age. However, the main index used for assessing maturity degree (I_{AD}) was correlated to the firmness only in a genotype-dependent

manner, and therefore, not useful to standardize a diversified panel of accessions. This is in agreement with several other studies [66,90,91].

In addition to firmness, other mechanical properties of the fruit can be determined from rheological data, such as elasticity and fracturability. In the analyzed accessions, the E and F parameters were strongly interconnected and varied depending on the texture type. Fruit elasticity, calculated from the Young's Modulus, showed a unimodal behavior in NM and SH, and bimodal in M and SS. This is coherent with the typical biphasic pattern of firmness loss, because of the activation of the melting pathway [78]. Nevertheless, the E parameter was variable both within and among accessions, resulting in a reduced ability to distinguish the different textures. Such variability may be affected by the water status of flesh tissues and, thus, by changes in cell turgor pressure [92]. In contrast, the fracturability (F) appeared more specific and particularly able to discriminate M from the other textures: this is in agreement with the notion that the disassembly of cell wall structure (mainly responsible for fruit plasticity) plays a major role in the softening process in the melting type [93]. However, the F parameter was also affected by some variability, that in certain cases masks a reliable discrimination. The resolution of the F parameter can be increased by using the elasticity value to adjust for fruit water status, leading to a combination of both components in a unified index, TD, which is more stable and unaffected by season or storage regime. Indeed, this index measures inherent mechanical properties of the fruits, not dependent on the firmness. The texture phenotype can affect the rheological properties of the flesh but not the firmness, in agreement with some works in peach and other species [63,94]. While firmness represents just the ripening stage, TD allows to predict the evolution of the elasticity and fracturability during the softening process, thus identifying a specific phenotype. This index can be calculated through a one-step analysis, and only requires the sampling of fruits with an average firmness ≥15 N.

In this work, accessions have been considered as biological replicates of the four groups of textures. The rationale of this approach arose both from the need for a reliable method to discriminate predefined texture types (in particular SS) and from the opportunity to test a target modeling on well-outlined phenotypes (in the case of NM and SH, accompanied by the knowledge of genetic determinants). It is important to highlight that the analyzed rheological parameters (E, F and TD), irrespective of the greater or lesser predictive ability, all tend to distinguish the melting type from the other textures, and to group together NM, SH and SS, which tend to have similar mechanical properties of the flesh, as also previously hypothesized [81]. Moreover, the variability in TD values observed in each texture group suggests the existence of intermediate phenotypes

that may depend on the genetic background. The presence of a quantitative variability for flesh texture trait has been also observed in other studies [66,72,82]. Further studies are needed to confirm whether TD can be used as an effective approach to score the continuous phenotypic variability present in peach germplasm, in turn a crucial step for association and linkage mapping studies. However, we have to stress that the main goal of our work was achieved by setting up an objective method to clearly distinguish melting from slow softening phenotypes that so far was possible only by sensorial evaluation. This finding will pave the road to phenotype segregating progenies in order to find molecular markers associated to the slow softening trait.

3.6 Supplemental Materials and Tables

Table 1 Accession panel used in this study. Texture, skin hairiness (peach vs nectarine) and sampling season are reported.

Accession	Texture	Skin hairiness	Season
Alice Col	Non-Melting	Nectarine	2011-2012
Ambra	Melting	Nectarine	2012-2014
Amiga	Slow-Softening	Nectarine	2014
Big Top	Slow-Softening	Nectarine	2011-2012-2014
BO00020006	Non-Melting	Peach	2011
BO04020009	Melting	Peach	2014
BO0503149	Non-Melting	Peach	2011
BO0530081	Stony-Hard	Peach	2011
Dixired	Melting	Peach	2011
Ghiaccio1	Stony-Hard	Peach	2011-2014
Glohaven	Melting	Peach	2011
Grenat	Slow-Softening	Peach	2014
Honey Blaze	Slow-Softening	Nectarine	2014
Honey Kist	Slow-Softening	Nectarine	2014
IFF331	Stony-Hard	Peach	2011
IFF813	Non-Melting	Nectarine	2014
Iride	Non-Melting	Peach	2012
Pulchra	Slow-Softening	Peach	2014
Redhaven	Melting	Peach	2011-2012
Rich Lady	Slow-Softening	Peach	2011-2012-2014
Vistarich	Slow-Softening	Peach	2011-2014

Table 2. The average values of the Elasticity (E) and Fracturability (F) parameters are reported for each texture group for the seasons 2011 and 2012. Letters indicate significant different group based on Least Significant Difference (LSD) test (α<0.05, p value adjusted by Bonferroni).

Texture	**Elasticity**		**Fracturability**	
	E	**LSD**	**F**	**LSD**
Melting	3.84	b	36.90	a
Slow-Softening	7.67	ab	19.95	b
Non-Melting	7.21	a	15.77	b
Stony-Hard	9.42	a	15.13	b

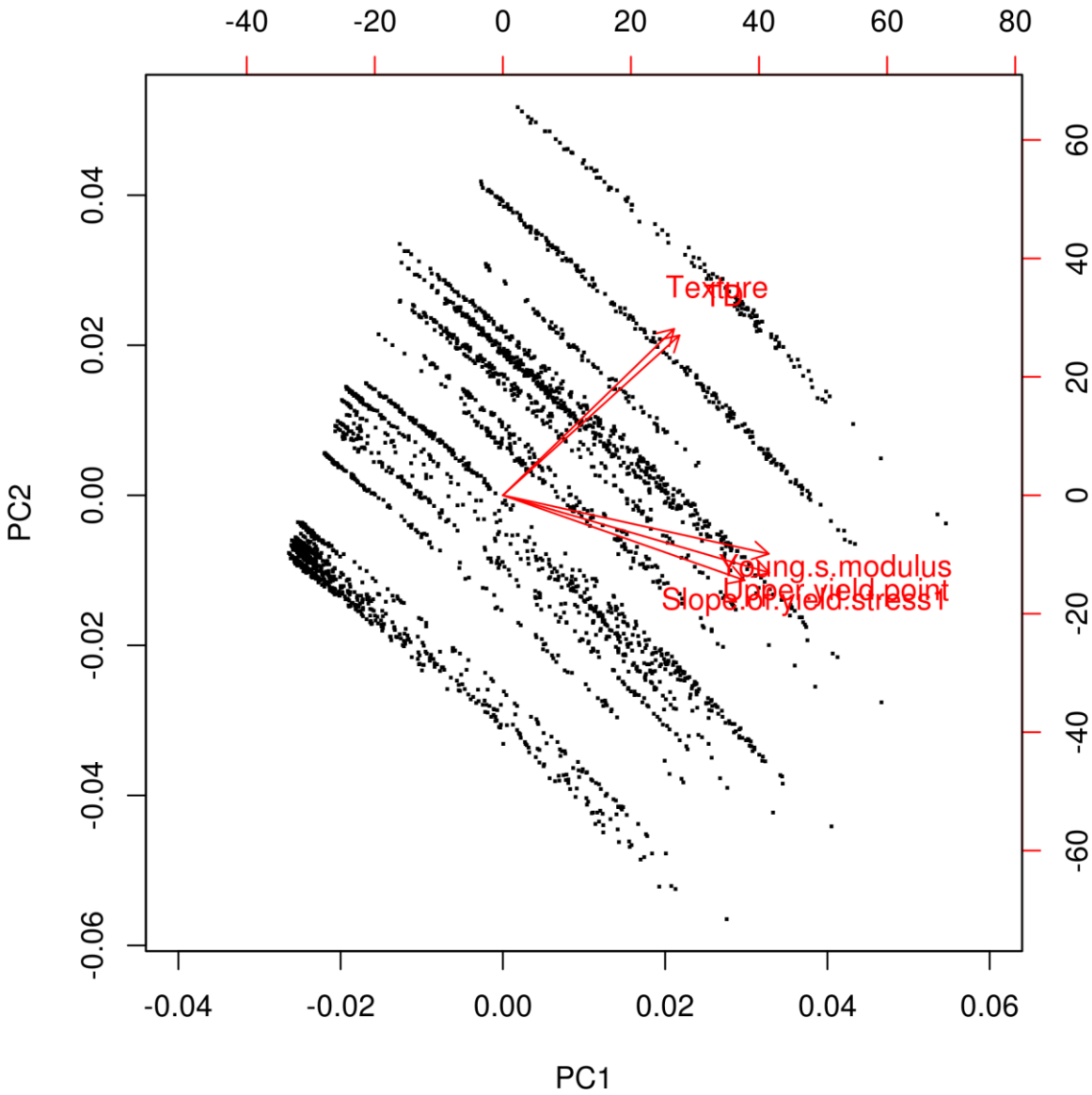

Supplemental Figure 1. Principal Component Analysis (PCA) performed on rheological data obtained from the analyzed panel of accessions. The first two components (PC1 and 2) explain 62 and 20% of the variance proportion, respectively, and 82% of the cumulative variation. Eigenvalues and eigenvectors relative to the texture, TD index, Young's modulus, Upper yield point and Slope of yield stress are highlighted in red.

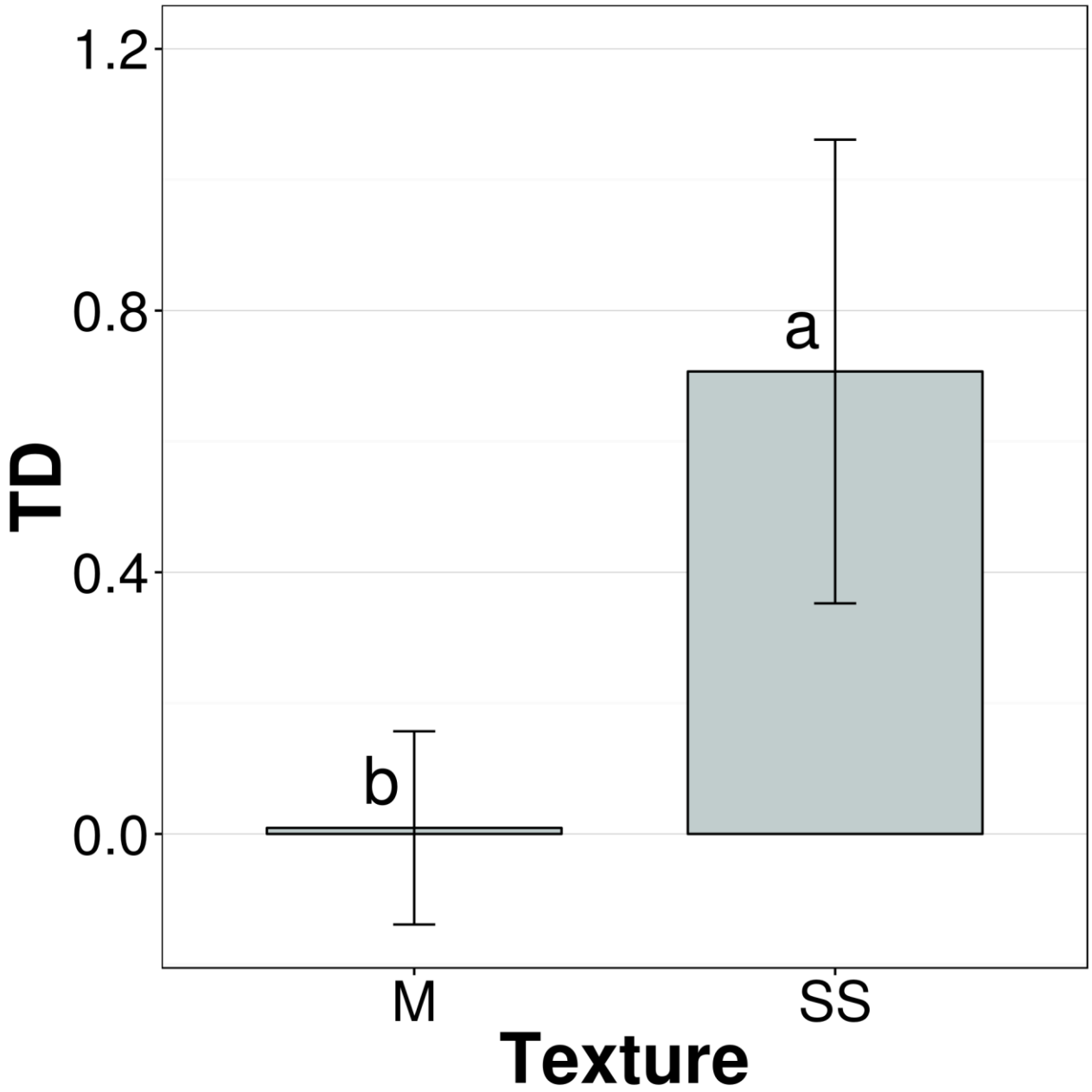

Supplemental Figure 2. TD index values for each texture group as determined on season 2014. Letters indicate the least significant differences (LSD) among melting and slow softening textures ($\alpha<0.05$, p adjusted by Bonferroni).

Supplemental Table 1. Rheological parameters recorded in two seasons (2011-2012) for 14 peach accessions. Fruits were stored at 4° and 20° C. All coefficients are expressed as average values. For the components K (intercept), E (elasticity), F (fracturability) the standard errors are also reported.

Accession	Year	Storage (°C)	Intercept	Elasticity	Fracturability	K		a		b		TD
						Estimate	Std.Error	Estimate	Std.Error	Estimate	Std.Error	
Alice Col	2011	20	-10.88	7.28	14.47	-10.88	1.37	7.28	0.65	14.47	3.30	0.50
Alice Col	2011	4	-11.62	7.09	15.99	-11.62	1.06	7.09	0.61	15.99	2.59	0.44
Alice Col	2012	20	-18.93	8.39	28.56	-18.93	0.93	8.39	0.516	28.56	2.30	0.29
Alice Col	2012	4	-14.72	9.21	18.49	-14.72	0.57	9.21	0.55	18.49	1.61	0.49
Ambra	2012	20	-21.85	3.97	39.77	-21.85	1.51	3.97	0.363	39.77	3.29	0.10
Ambra	2012	4	-20.95	3.11	38.96	-20.95	1.11	3.11	0.298	38.96	2.43	0.08
BigTop	2011	20	-15.97	7.32	24.67	-15.97	1.62	7.32	0.493	24.67	3.63	0.29
BigTop	2011	4	-12.64	7.24	18.37	-12.64	1.86	7.24	0.534	18.37	4.09	0.39
BigTop	2012	20	-15.29	4.69	25.97	-15.29	1.34	4.69	0.497	25.97	3.13	0.18
BigTop	2012	4	-9.96	6.58	13.43	-9.96	1.46	6.58	0.529	13.43	3.39	0.49
BO 00020006	2011	20	-8.84	6.99	10.02	-8.84	1.63	6.99	1.066	10.02	4.00	0.69
BO 00020006	2011	4	-9.06	5.58	12.56	-9.06	0.90	5.58	0.589	12.56	2.26	0.44
BO 05030149	2011	20	-8.60	5.33	12.72	-8.60	2.47	5.33	1.18	12.72	5.86	0.41
BO 05030149	2011	4	-10.98	10.96	8.44	-10.98	1.42	10.96	1.163	8.44	3.93	1.29
BO 0530081	2011	20	-12.16	7.57	15.34	-12.16	1.50	7.57	0.865	15.34	3.87	0.49
BO 0530081	2011	4	-17.21	6.24	26.89	-17.21	1.95	6.24	1.133	26.89	5.11	0.23
Dixired	2011	20	-27.92	3.59	52.41	-27.92	6.53	3.59	0.999	52.41	13.85	0.06
Ghiaccio	2011	20	-14.19	11.26	14.71	-14.19	1.94	11.26	0.61	14.71	4.40	0.76
Ghiaccio	2011	4	-13.00	13.81	8.158	-13.00	0.59	13.81	0.425	8.158	1.26	1.69
Glohaven	2011	20	-16.89	0.94	33.35	-16.89	6.78	0.94	0.758	33.35	14.07	0.02
Glohaven	2011	4	-17.61	1.45	34.28	-17.61	3.91	1.45	0.485	34.28	8.06	0.04
IFF331	2011	20	-16.40	14.71	11.32	-16.40	0.88	14.71	1.243	11.32	2.34	1.30
IFF331	2011	4	-15.13	5.47	23.73	-15.13	0.40	5.47	0.429	23.73	1.20	0.23
Iride	2012	20	-12.20	6.05	18.79	-12.20	2.22	6.05	0.418	18.79	4.64	0.32
Iride	2012	4	-7.18	7.06	7.27	-7.18	1.37	7.06	0.776	7.27	3.47	0.97

Supplemental Table 2. Rheological parameters recorded in 2014 season for 10 peach accessions. Fruits were stored at 4° C. All coefficients are expressed as average values. For the components K (intercept), E (elasticity), F (fracturability) the standard errors are also reported. The TD index shows lower values for the melting peach accessions 'Ambra' and 'BO 04020009'.

Accession	Year	Storage (° C)	U_{YP} (N)	Y_M	S_{YS}	K		E		F		TD
						Estimate	Std.Err	Estimate	Std.Err	Estimate	Std.Err	
Ambra	2014	4	31.79	0.10	0.21	0.36	0.12	1.51	0.52	14.53	0.66	0.1
Big Top	2014	4	48.11	0.23	0.10	2.08	0.40	6.54	1.55	13.24	3.92	0.4
BO 04020009	2014	4	42.48	0.17	0.28	0.07	0.43	1.70	1.17	14.21	1.48	0.1
Ghiaccio 1	2014	4	49.16	0.19	0.10	3.44	0.39	4.38	1.98	8.11	2.50	0.5
Grenat	2014	4	29.36	0.11	0.04	1.19	0.22	9.01	1.84	19.14	4.57	0.4
Honey Blaze	2014	4	32.00	0.11	0.07	2.09	0.57	11.59	4.87	1.53	5.93	7.5
Honey Kist	2014	4	25.42	0.10	0.06	0.58	0.17	12.71	2.03	11.31	2.62	1.1
IFF813	2014	4	40.27	0.14	0.14	1.60	0.17	11.59	1.90	6.92	1.67	1.6
Pulchra	2014	4	31.02	0.29	0.22	0.33	0.37	3.46	1.45	8.38	2.64	0.4
Vista Rich	2014	4	49.19	0.23	0.07	2.27	0.38	7.57	1.55	15.64	5.41	0.4

4 Genetic analysis of the slow softening trait in peach

4.1 Abstract

Texture is one of the main quality attributes of peach fruit. A germplasm panel and a segregating progeny were genotyped with the Illumina 9k peach SNP array and phenotyped for fruit texture (Slow-softening *vs* Melting) using a sensorial evaluation and by measuring mechanical properties, respectively. Combining association and linkage mapping a locus for the Slow-softening trait was located in the distal part of chromosome 8 (spanning an interval of about 2.3 Mb and 1.6Mb, respectively using GWA and QTL-mapping). The most significantly associated SNPs in Genome Wide-Association and QTL-mapping are spaced about 257kb apart on the reference peach genome sequence, suggesting that the same locus might be segregating both in progeny and association panel. Among 804 gene models fall in the locus, 517 were expressed in the fruit flesh. A preliminary investigation of putative candidate genes was performed by inspecting annotated transcripts within the identified interval, by comparing fruit gene expression data between two slow-softening and two melting accessions and whole-genome re-sequencing data of parents in search of sequence variants possibly associated with the trait: 7 variants were identified in coding regions of differentially expressed genes, Prupe.8G257900 (coding for tetratricopeptide repeat (TPR)-containing protein), Prupe.8G224000 (coding for Protein of unknown function, DUF647) and Prupe.8G206600 (coding for UDP-Glycosyltransferase superfamily protein) (1, 2 and 4 variants, respectively), while 33 were identified in regulatory regions of 16 differentially expressed genes. This is the first description of slow-softening locus, his inheritance resulting consistent with previous works fasting objective method and molecular biology. It is expected that applying texture dynamic model on a similar or an even wider peach progeny or collection will support precise QTL mapping or genome wide association studies. This would allow to identify genes involved in peach texture control.

4.2 Introduction

The limited shelf-life of peach fruit has stimulated an increasing interest for the characterization of the natural phenotypic variability associated to texture and softening behavior [42]. The vast majority of peach cultivars are characterized by a melting flesh (M) texture type, manifested through an initial slow decrease of firmness followed by a rapid softening (melting phase), concomitant to the climacteric respiration and ethylene burst [95]. The loss of turgor pressure and cell-to-cell adhesion in pericarp tissues have been proposed as the main physiological mechanisms

regulating the melting process in peach [63]. At genetic level, the M trait is regulated by a major locus located on linkage group 4 [76], and harboring a cluster of genes belonging to the endopolygalacturonase family (endo-PG), under the control of ethylene signaling pathways [96]. Copy number variation at the *M* locus involving the presence/absence of two endo-PG genes (endoPGM and endoPGF), has been recently proposed as the genetic bases of the monogenic recessive non-melting flesh (NM) trait [97]. NM peaches are characterized by the maintenance of a rubbery texture, characteristic which makes them suitable for canning [70]. The stony-hard (SH) texture is a monogenic recessive trait first reported by Yoshida (1976) [83]. The flesh of SH peaches remains firm and consistent at full ripening, evolving null or very low ethylene amount during ripening [79,84]. The inability to produce ethylene is determined by a low expression of the main fruit-related ethylene biosynthesis gene, the 1-aminocyclopropane-1-carboxylic acid synthase isoform *PpACS1* [98], in turn caused by the lack of auxin increase at the onset of ripening [67]. The ppa008176m gene, coding for an auxin biosynthesis protein similar to the Arabidopsis YUCCA11 (AtYUC11) has been recently proposed as a candidate gene for the recessive SH trait [80].

Apart from these texture variants, the genetic basis of the quantitative behavior associated to the melting flesh phenotype is poorly understood, mainly hampered by environmental effects and intra-genotype variability [72]. Understanding variation within the melting group is especially important because of its relevance for the fresh market [87]. An interesting melting-variant, the slow-softening type, has been recognized in 'Big Top'-like cultivars [73,81]. The Slow-softening trait is manifested through a delay of the melting phase, resulting in a prolonged shelf-life and a crispy texture compared to the melting flesh. The genetic and physiological mechanisms regulating this phenotype still remain largely unknown [42]. A dominant Mendelian inheritance has been suggested for the SS trait, observing the segregation pattern in several bi-parental progenies derived from the ‘Big Top’ parent [73]. However, the inherent complexity of SS trait does not allow to exclude a co-dominant or even quantitative inheritance.

Aim of this work is the genetic dissection of the slow-softening trait and the identification of molecular markers to be used for marker assisted selection and putative candidate genes and/or pathways involved.

4.3 Materials and methods

4.3.1 Plant materials

A panel of 119 accessions and 70 F1 progenies from cross ‘Max10’ x ‘Rebus 028’ (MxR028) were analyzed in this study. Plants were grown under integrated pest management in the “Centro Ricerche Produzioni Vegetali” (CRPV) experimental orchard, located at Imola. Eleven fruits per plant were assessed by DA-meter [36] and visual inspection in order to select representative fruits at commercial ripening stage. Of the 119 accessions 41 are nectarines, (21 acid and 20 sub-acid), while 78 accessions are peaches (63 acids and 15 sub-acid). MxR028 F1 seedlings are all nectarines, but segregate 1:1 for the *D* locus controlling the acid/sub-acid trait (32 sub-acid, 38 acid). Rebus 028 is a SS early ripening nectarine belonging from a cross between SS ‘Big Top’ and M ‘May Fire’ cultivars. Max10 is a M late ripening nectarine the pedigree is unknown.

4.3.2 Genotyping

The panel of 119 accessions and 70 individuals from F1 cross-population MxR028 were genotyped by using the IPSC peach 9K SNP array [99], using previously described SNP selection criteria [51]. SNP positions within the array were recalibrated based on the Peach Genome assembly V2.0 [100]. For the germplasm panel, genotyping data were further filtered for marker missing rate < 10% and minor allele frequency (MAF) > 5%, finally retaining a total of 6104 SNPs for GWA analysis.

4.3.3 Phenotyping

Accessions and MxR028 seedlings were screened for fruit texture through sensorial analysis classifying them as melting (M) or slow-softening (SS). Organoleptic data were collected for at least 5 years through the scoring of tactile and mouthfeel attributes during SIV ripening stage and post-harvest (room temperature). For mechanical analysis, fruits of MxR seedlings were selected based on maturity degree (established through IAD index measurement) and firmness value (above 15 N threshold) and analyzed through a digital penetrometer (Andilog Centor) after peel removal as detailed in paragraph 3 (page 17). Rheograms data were analyzed as described in paragraph 3 (page 18). Fruit acidity, fresh weight, SSC, skin overcolor and maturity date were also measured and evaluated. Statistical analyses were performed in R using *nmle* and *stat* packages.

4.3.4 Genome Wide Association Study

The panel used for GWA analysis was established by including a total of 119 accessions, of which 34 with SS phenotype and the remaining with MF. Population structure was inferred by using

ADMIXTURE v1.22 [101,102] by using a value of K = 3, chosen based on a 10-fold cross-validation procedure with 10 different fixed initial seeds. For association analysis, Mixed Linear Model (MLM) was performed in GAPIT R package [103]. Random effects were included in the mixed models as kinship matrix computed using Identical-By-State (IBS) algorithm, as implemented in EMMAX package [104]. For fixed effects, a Q-matrix using a value of K = 3 was used as covariate for association analysis. The Fixed and random model Circulating Probability Unification (FarmCPU) method was used to further confirm association signals [105]. The performance of all tested GWA algorithms was evaluated by comparing the observed *vs* expected *p*-values under null hypothesis, through quantile-quantile (QQ)-plot inspection and considering statistical power against False-Discovery Rate (FDR). A conservative threshold for assessing SNP significance was calculated based on Bonferroni correction for a type I error rate of 0.05. Intra-chromosomal LD patterns were measured and visualized using HAPLOVIEW v4.2 [106].

4.3.5 Map construction and QTL-mapping

Genetic map construction was performed with JoinMap 4.1 [107], using the Monte Carlo Maximum Likelihood mapping with a spatial sampling threshold of 0.01 and 3 rounds, using 70 F1 seedlings and 479 SNP markers: 199 *hkxhk* (heterozygous in both parents), 114 *lmxll* (heterozygous in ‘Max10’ and homozygous in ‘Rebus028’), 166 *nnxnp* (homozygous in ‘Max10’ and heterozygous in ‘Rebus028’) according to JoinMap and MapQTL manuals. Markers showing segregation distortion were excluded. The map was built using as fixed order the recalibration of SNP positions based on the current assembly of the peach reference genome v2.1 [100]. A nearest-neighbour fit parameter higher than 0.11 was set as threshold for marker exclusion[108]. QTL analyses were carried out using the software MapQTL 6.0 [108]. The nonparametric Kruskal–Wallis (KW) rank sum test was used to search phenotype–marker associations. The association was accepted as significant if the significance level was under the *p*-value threshold of 0.005.

4.3.6 RNA sequencing and data processing

Fruits from two SS cultivars, ‘Big Top’ (BT) and ‘Rich Lady’ (RL), and two melting cultivars, ‘Bolero’ (BL) and ‘Red Haven’ (RH) were collected. Trees were grown under integrated pest management growing systems at the “Centro Ricerche Produzioni Vegetali” (CRPV) (Imola, Italy) experimental orchard. Representative fruits of each accessions were harvested along the SIII and SIV stage of ripening. Maturity degree was assessed through the measuring of IAD index using DA-meter instrument (Sintéleia, Bologna, Italy). For each accession 9 fruits (3 fruits from 3 trees) were collected, immediately peeled, sliced in wedges, quickly frozen and ground using liquid nitrogen. Total RNA was obtained following the protocol of Dal Cin et al. [109]. Total RNA concentration was evaluated examining aliquots of samples in a Nanodrop spectrophotometer (Thermo Scientific) while the quality was assessed by gel electrophoresis on a 1% agarose gel in TAE buffer and stained with ethidium bromide. Samples were sequenced using Illumina RNA-Seq technology (HiSeq 2000) at IGA Technology Services (Udine, Italy) in 6-plex with a 50 bp single end module. Quality of raw data was checked using the FastQC tool for high throughput sequence data [110] . About 98% of the cleaned reads were aligned against the ‘Lovell’ peach genome version 2.0 using bowtie2 and TopHat2 [111,112]. About 90% of the reads were uniquely mapped and counted by HTSeq [113]. For subsequent analyses, only features with more than one read per million in at least three samples were retained, for a total of 15 672 genes expressed across the different texture types. Expression of each gene was normalized in RPKM (reads per kilobase of exon model per million mapped reads), calculated based on the length of the gene and reads mapped [114]. To compare the M accessions to SS accessions a gene by gene non-parametric analysis was done by *nparcomp* package. Heatmap data visualization was obtained with the heatmap.2::R software package [115].

4.3.7 Next-generation sequencing whole-genome resequencing

Whole-genome sequence (WGS) libraries of ‘Max10’ and ‘Rebus 028’ parents were prepared by the Genomics Platform of Parco Tecnologico Padano (Lodi, Italy) with the Illumina Truseq DNA Nano sample prep kit (Illumina, San Diego) following manufacturer's protocol and sequenced on the Hiseq2000 with paired-end sequencing module using the Truseq SBS kit v3. FASTQ files were obtained with the Illumina CASAVA Pipeline. After cleaning and filtering, reads were trimmed with Trimmomatic v0.32 and mapped using default parameters onto the peach reference genome v2.0 using BWA-MEM algorithm, implemented in BWA v.0.6.1 tool [116]. After alignment, mean coverage was estimated by using Samtools *mpileup* tool, obtaining a value of 31.6x and 28.9x respectively for ‘Max10’ and ‘Rebus 028’. For variant identification, after duplicate removal and reads indexing with PICARD, a joint-calling approach was performed using Haplotype Caller algorithm in GATK, following Best Practice guidelines. Sequences for predicted peach gene models were retrieved from the Phytozome database [117]. Functional annotation of the variants was performed using SNPEffect v2.0 [118].

4.4 Results

4.4.1 Phenotyping for fruit texture

The slow-softening trait is a phenotypic variant of melting flesh texture characterized by a delay of softening processes. At the start of this work, an objective method to identify this trait was not yet available, while firmness measurement through maximum force tests were shown not to correlate to texture properties (see paragraph 3 for more details and references on this topic). The identification of SS trait was (and still is) largely based on sensorial analysis by trained experts, through tactile evaluation and mouthfeel sensations, and in comparison, with reference phenotypes (i.e 'Big Top'-like varieties). The accession panel and MxR028 progeny were phenotyped for at least 5 years using sensorial analysis throughout SIV stage of fruit development and in post-harvest. In addition to the 'Big Top' variety, the panel includes well-known series of SS accessions, including 'Honey' and 'Romagna' for nectarines, and 'Rich' and 'Royal' series for peach and some breeding selections derived from them (Table 3). The MxR028 progenies was obtained from the cross of two SS nectarine parents, 'Max10' and 'Rebus 028' ('Big Top' x 'Mayfire'). Seedlings of this progeny (Table 4) were phenotyped through the approach proposed in the previous chapter. This method is based on the use of synthetic indices (Texture Dynamics, TD and K-intercept, K) derived from the measurement of the mechanical properties (Elasticity and Fracturability) of pulp tissues through penetration-based tests.

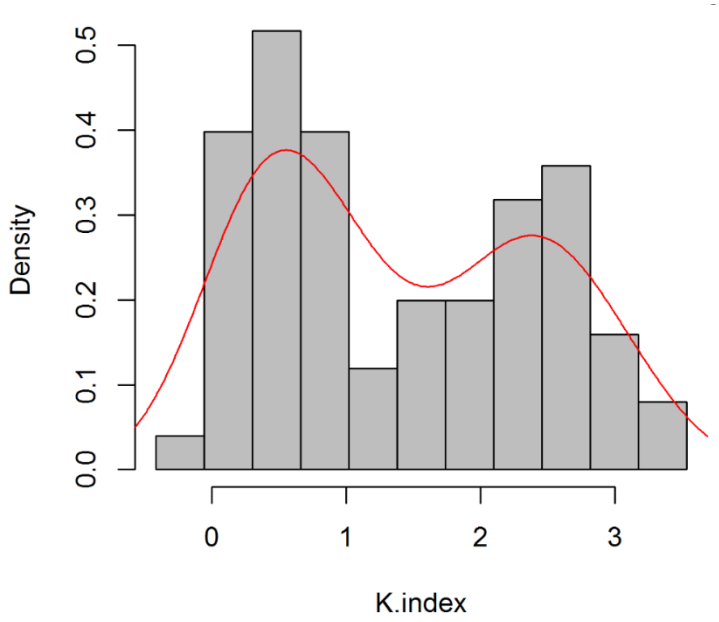

Figure 7 The bimodal distribution of the index K.intercept in the MxR028, on the left the M seedlings and on the right the SS seedlings.

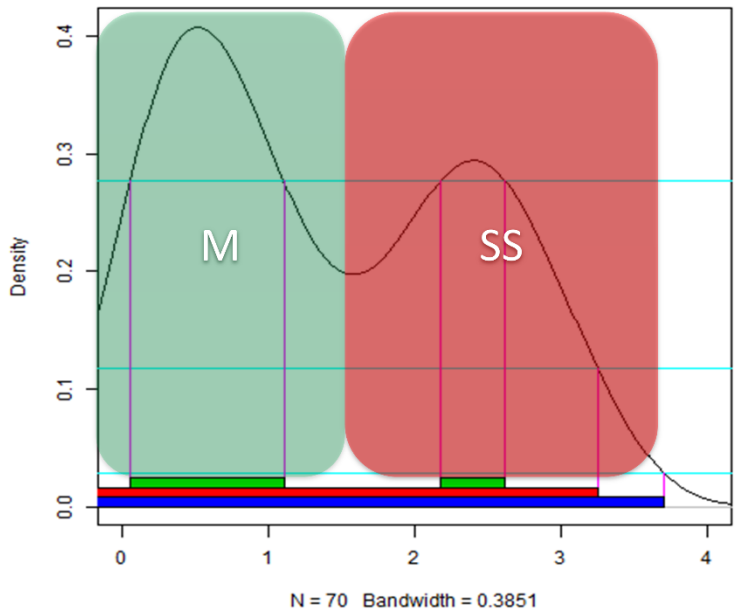

Figure 8 The bimodal distribution of the index K.intercept in the MxR028, under the green halo on the left the M seedlings and under the red halo on the right the SS seedlings; the horizontal bars represent respectively in green the 50% of the data, in red the 95% and in blue the 99%.

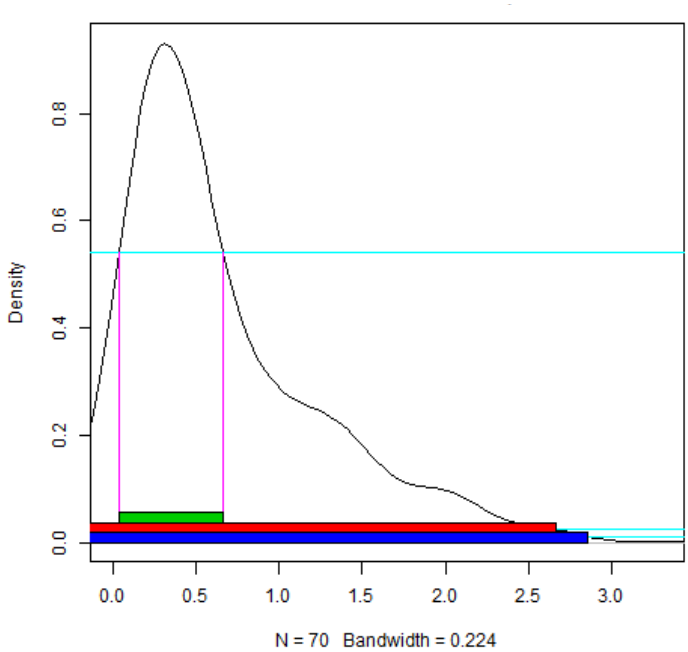

Figure 9 The not normal distribution of the TD index in the MxR028; horizontal bars represent respectively in green the 50% of the data in red the 95% and in blue the 99%.

As a result of the application of this method on MxR028 seedlings, the K-intercept value showed a bimodal distribution, varying between a minimum of -0.08 and a maximum of 3.20, with 2th and 3rd quartiles included within the intervals 0.1-1.1 and 2.2-2.6, respectively Figure 7). The K-index is able to cluster seedlings into two groups of similar sample size, supporting the hypothesis of a mendelian trait (Figure 8). The TD index showed instead a continuous and not normal distribution (SW-test $p < 0.05$), with a maximum peak ranged between 0.1-0.65, typical of a quantitative behavior (Figure 9). No significant ($p<0.05$) correlation was found between the K and TD indices and the other tested parameters, such as I_{AD}, acidity, SSC, fruit overcolor, maturity date and fresh weight (Figure 10).

Supporting the phenotypical data, the already described pleiotropic effect of the maturity date on the SSC were found[119].

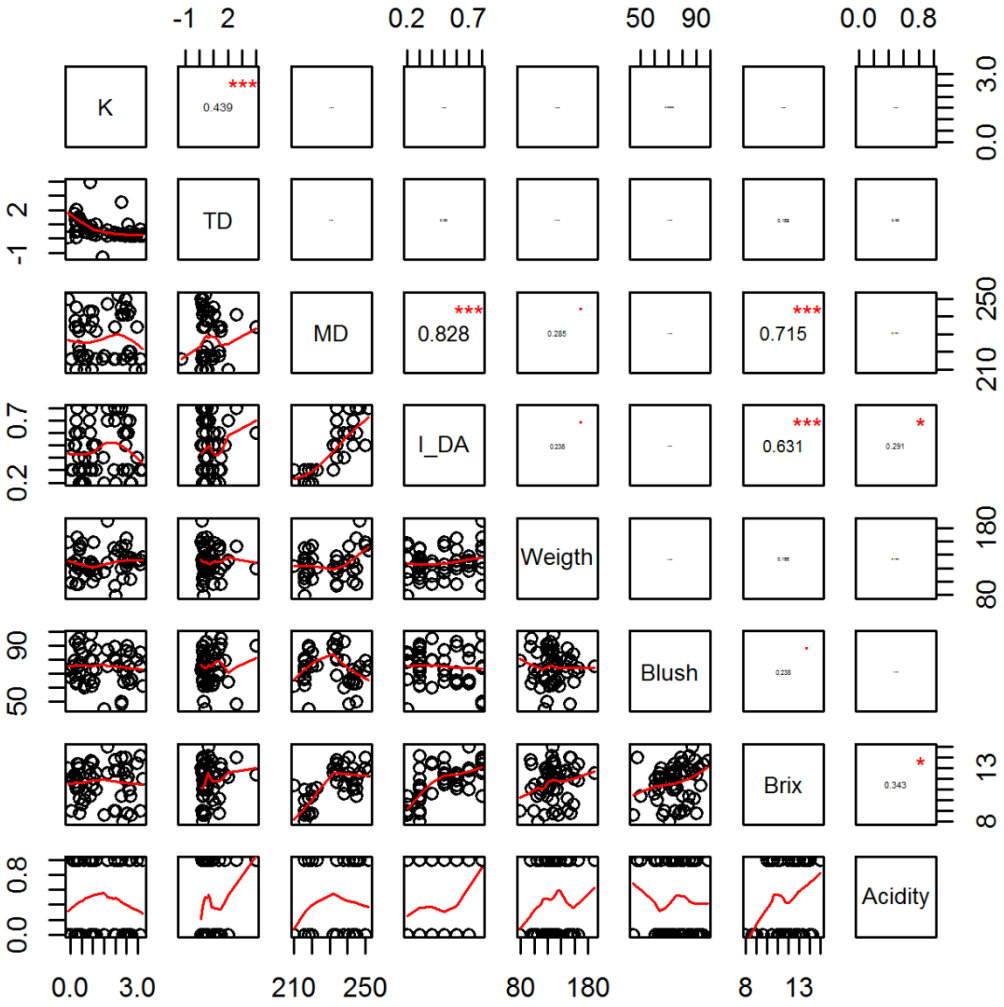

*Figure 10 Pearson correlation among the TD equation parameters (TD and Intercept) and other fruit attributes. The numbers represent the Pearson correlation coefficient, * mark significant values ('***': p < 0.001 -- '**': p < 0.01 -- '*': p < 0.05 -- '.': p < 0.1).*

4.4.2 Genome-wide association and LD analysis

The 119 accessions used for GWA analysis included: 35 slow softening accessions (2 acid nectarines, 10 acid peaches, 19 sub-acid nectarines, 4 sub-acid peaches); 84 melting accessions (19 acid nectarines, 53 acid peaches, 1 sub-acid nectarine and 11 sub acid peaches) (Figure 11, Table 5). Prior to GWA analysis, the genetic structure of the panel was inferred by ADMIXTURE software.

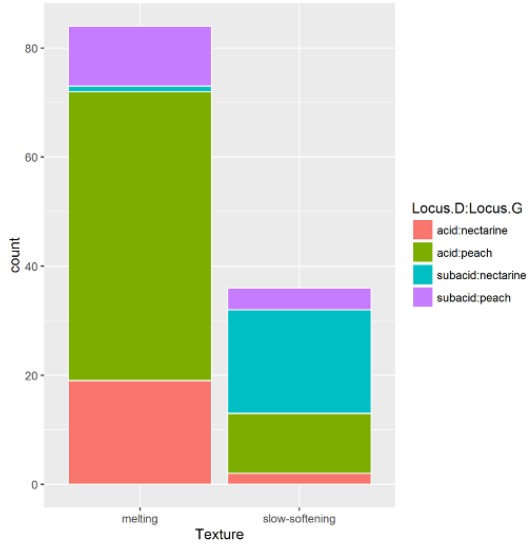

	melting	slow-softening	tot.
acid	72	12	84
subacid	12	23	35
nectarine	20	21	41
peach	64	14	78
acid:nectarine	19	2	21
acid:peach	53	10	63
subacid:nectarine	1	19	20
subacid:peach	11	4	15
tot.	84	35	119

Figure 11 The counting of the pubescence and acidity mendelian traits between the M and SS accessions used for GWA analysis.

A value of K = 3 minimized cross-validation error, explaining most of the ancestry within the panel. The clusters of Oriental, Occidental and breeding-derived (the most represented) Figure 13, accessions agreed with the already suggested pattern of peach domestication. As a proof-of-concept of the statistical power of the GWA approach, the panel was used to map the monogenic

trait acid/sub-acid (D/*d* locus). For this analysis, phenotypes were coded as a binary trait, assigning 0 - 1 to acid and sub-acid accessions, respectively (Figure 11).

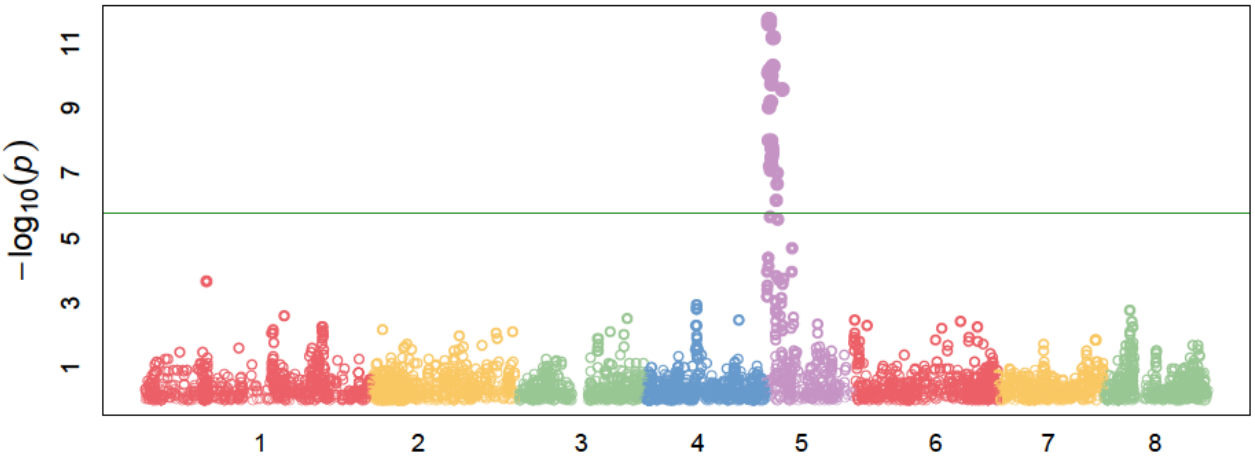

Figure 12Manhattan plot of the GWAS analysis for the low acidity trait (MLM algorithm in the GAPIT software, corrected using the kinship matrix). In the different color the chromosome reported on the x axis. On the y the log10 of the probability (p). Green line is the threshold calculated using Bonferroni.

Using FarmCPU algorithm adjusted for population structure, a strong significant signal (p-value 1.95e-12 was detected on the proximal regions of chromosome 5 (SNP_IGA_544657, at 635,222 bp), in agreement with previous studies [51,120].

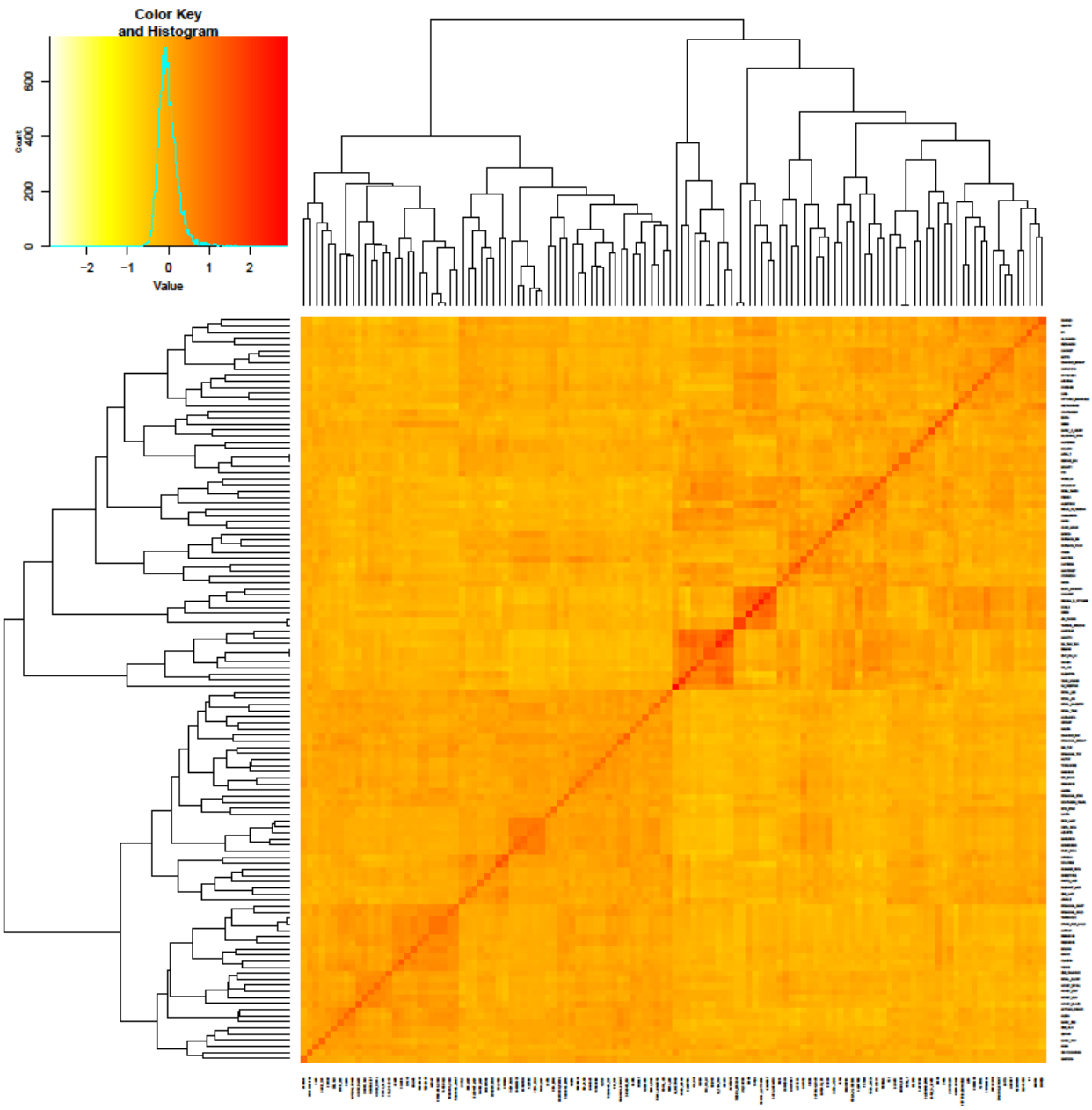

Figure 13 The kinship matrix representing the genetic structure of the panel of accessions. In small on the top left the color key and the color frequency.

The same approach (FarmCPU algorithm adjusted for population structure) was used for detecting genome-wide associations for the SS trait. A highly significant signal was detected on

chromosome 8, corresponding to the marker SNP_IGA_881722, with a *p*-value of 4.0e-7), above to the Bonferroni threshold (Figure 13).

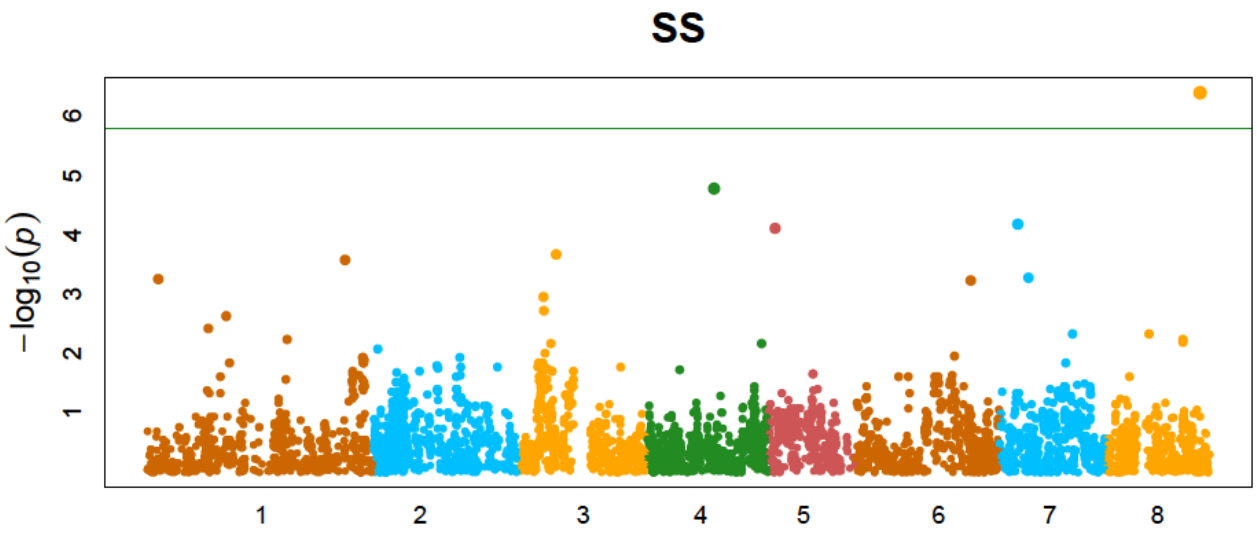

Figure 14 Manhattan plot of the GWAS analysis for the Slow Softening trait, made using the FarmCPU software. In the different colors, the chromosome reported on the x axis. On the y the log10 of the probability (p). Green line is the threshold calculated using Bonferroni.

A less significant signal p-value of 6.8e-05 was also detected on chromosome 7, at SNP_IGA_707848. As deduced by QQ-plot inspection, the p-values distribution suggests a reduced background inflation and low number of false positive associations (Figure 14).

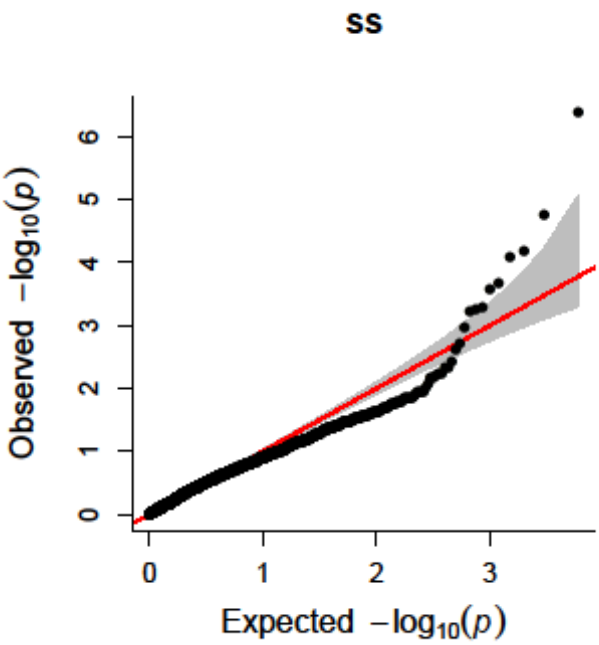

Figure 15 QQ-plot for the SNPs association to the SS trait

SNP_IGA_881722 is located at 19,889,620 bp in a distal region of chromosome 8 and with a MAF (minor allele frequency) of 0.21. Linkage disequilibrium (LD) analysis of the regions surrounding the SNP_IGA_881722 estimated an extended LD block, which encompasses a region of about 2.3 Mb in physical size, roughly comprised between SNP_IGA_881120 (19,710,170 bp) and SNP_IGA_885740 (21,948,219 bp).

4.4.3 QTL-mapping of SS trait

In order to verify the significance of the locus detected by GWA, a QTL-mapping approach was performed in an F1 MxR028 progeny, using mechanical properties. A genetic map of the MxR028 progeny was built from IPSC 9k SNP array data. A total of 479 markers were arranged in 12 linkage groups which were anchored to the 8 chromosomes of the peach genome sequence: chromosomes 1, 2 and 6 were subdivided in 3, 2 and 2 linkage groups, respectively (Figure 19). A total distance of 172.6Mb (165.4Mb without counting the gap >20cM) of the peach genome is covered by the map with a mean physical/genetic distance ratio of 216Kb/cM, (maximum ratio of 459 Kb/cM in MxR_1b and a minimum of 71 Kb/cM MxR_2b). As a first validation of the obtained genetic map for genetic dissection of fruit quality traits, a QTL analysis for fruit acidity was performed: a major QTL was identified in agreement with the already known *D* locus on chromosome 5 (Figure 19). Mechanical properties obtained from rheological analyses were then used for QTL analysis. All the parameters coming from TD equation including the logistic K-intercept parameters showed a single and significant ($p<0.005$) association on chromosome 8 with K* of Kruskal-Wallis non-parametric test>19 (significance < 0.0001), and a maximum association of the logistic K-intercept of 47.9 K* (Figure 16).

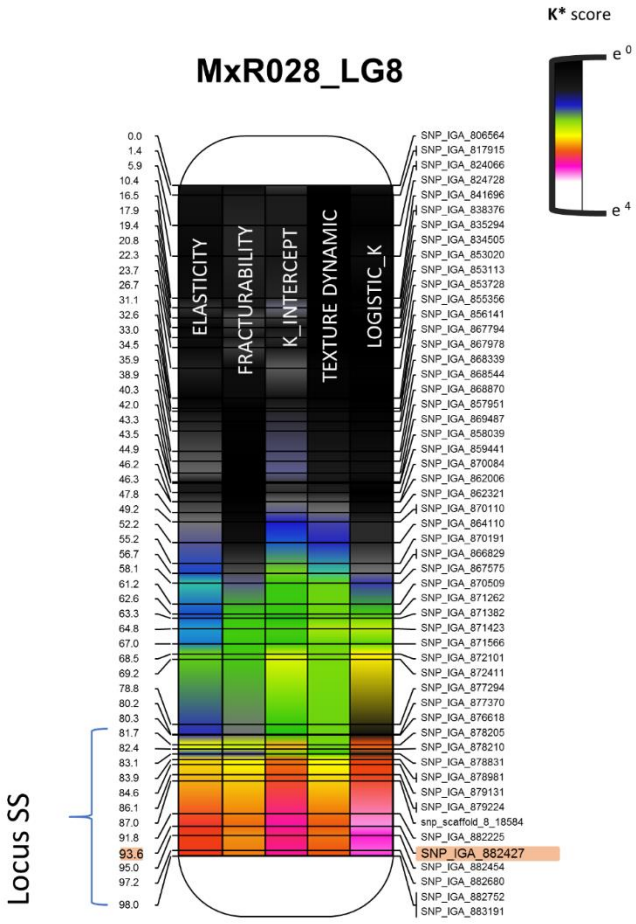

Figure 16 The genetic map of the chromosome 8 showing in color the K score of the Kruskal-Wallis analysis made using MapQTL software and colored by the Harry Plotter software [41]

The mapped interval spans a region of about 1.63Mb on chromosome 8, roughly comprised between SNP_IGA_878205 (18.675.130 bp) and SNP_IGA_882809 (20.308.888 bp), being

SNP_IGA_882427 the most associated (20.146.776 bp). The interval is composed by *hkxhk* marker type (heterozygous in both parents), which do not allow the tracing of SS allele in the donor parent Rebus028, although individuals bearing *kk* markers were all characterized by M texture. Although the SS texture has been reported as dominant over M, QTL analysis do not allow to exclude the hypothesis of a recessive inheritance i.e. Rebus028 parent is homozygous recessive and Max10 heterozygous for the SS allele. Using an interval mapping (IM) approach to map the logistic K-intercept, the identified interval spans 1.64Mb, comprised between SNP_IGA_877294 (18.438.875 bp and LOD 5.61) and SNP_IGA_883291 (20.478.408 bp and LOD of 14.91), and a maximum peak corresponding to SNP_IGA_882225 (20.084.243 and LOD of 100).

4.4.4 Gene mining and transcriptome analysis

The large size of mapped intervals, respectively of 2.3 Mb and 1.6Mb using GWA and QTL-mapping, hampers the identification of candidate genes or variants potentially associated to the SS trait. Despite this, a preliminary investigation was performed, by exploring the annotated gene inventory, transcriptome data of two SS and two M accessions and whole-genome re-sequencing data of 'Max10' and 'Rebus 028' parents.

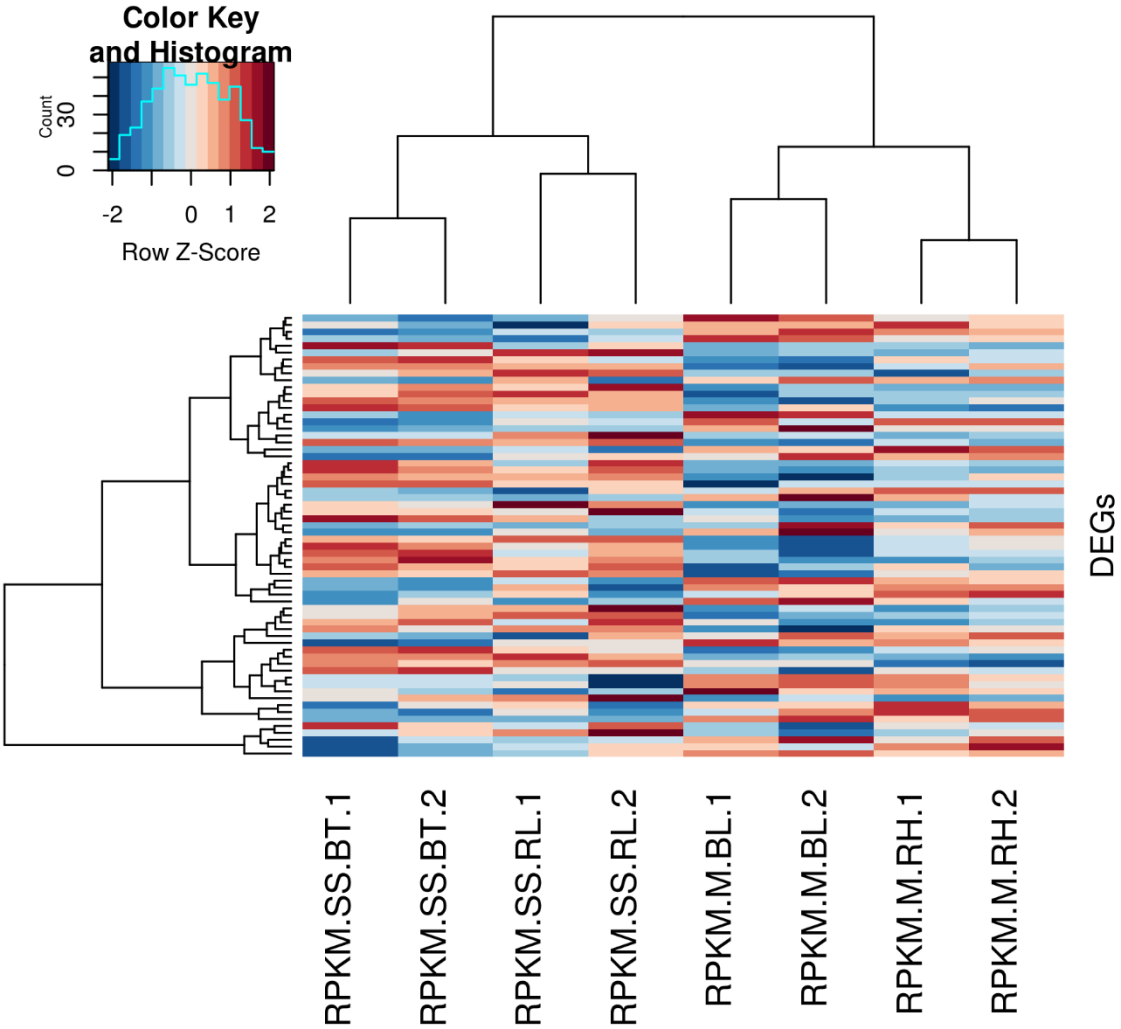

Figure 17 The Z-normalization of RPKM of 64 genes differentially expressed in the non-parametrical contrast gene by gene performed using the npar.t.test of the nparcomp::r package. The heatmap was obtained using the heatmap.2 function of the gplot::r package, Top, hierarchical clustering of the cultivar.Left, gene clustering according to the expression in RPKM. On the bottom the texture type the cultivar (BT 'Big Top' SS, RL 'Rich Lady' SS, BL 'Bolero' M, RH 'Red Haven' M) and the replica (1 first replica, 2 the second). In small on the top left the color key and the class frequency.

A total of 806 transcripts were annotated in the interval between the SNP_IGA_878205 (18 Mb) and the distal part of chromosome 8 (22.5Mb). The region from 20.1 to 22.5Mb was not covered by any markers but is in linkage with the identified regions, as deduced by LD measure in the

accession panel (data not shown). Based on the assumption that the gene(s) controlling the SS trait is expressed in ripening fruit tissues, analysis of transcriptome data allowed to reduce the number of candidates to 517 genes. In order to evaluate the potential association between differential expression of any of these genes and the SS trait, their expression pattern was compared by a non-parametric contrast, identifying a total of 64 genes with a significant differential expression between SS and M fruits at SIV ripening stage (Figure 17). Based on peach reference transcripts annotation v2.1a, these transcripts were mainly involved in auxin response, fatty acid biosynthesis, cell-wall metabolism, regulation of transcription and RNA metabolism, while 16 were uncharacterized or unknown.

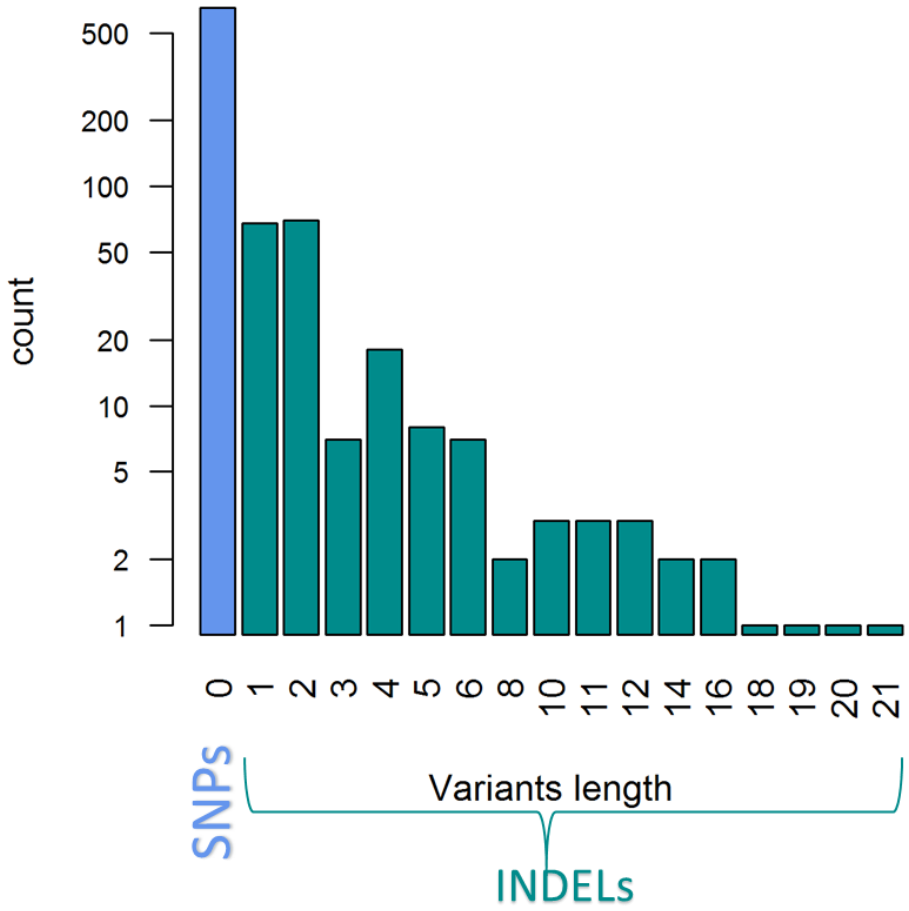

Figure 18 The count of the SNPs (length 0) and INDELs (length between 1-21) in the SS locus in according these in agree with the observed pattern of segregation.

Differentially expressed genes (DEGs) were further investigated by the analysis of re-sequencing data of 'Max10' and 'Rebus028'. Within the identified interval, a total of 10680 variants were

found in ‘Max10’ and ‘Rebus 028’: of these,853 were in agreement with the observed pattern of trait segregation. Most of them (656) are SNPs, while 197 are INDELs ranging from 1 to 22 bp (Figure 17). Furthermore, 7 variants were identified in coding regions of DEGs, Prupe.8G257900 (coding for tetratricopeptide repeat (TPR)-containing protein), Prupe.8G224000 (coding for Protein of unknown function, DUF647) and Prupe.8G206600 (coding for UDP-Glycosyltransferase superfamily protein) (1, 2 and 4 variants, respectively), while 33 were identified in regulatory regions of 16 DEGs (Table 5).

4.5 Discussion

Maintenance of an elevated consistency is necessary for the storage and the handling of ripe fruits [39]. Due to the commercial success of ‘Big Top’ nectarine[73], the SS texture has been increasingly studied in the last 20 years[81,82,121–123]. The penetrometer itself, as reported in paragraph 3, does not support the ability to discriminate among the different texture types, as already reported in other works [63,66,122]. In addition, this method appears affected by the fruit ripening season, since the early-ripening accessions tend to show a faster loss of firmness, while the late-ripening a more slower firmness loss. Using the firmness loss method, Serra et al. [121] found major QTLs overlapping with the major QTLs for maturity date.

Nevertheless, the lack of an easy and cheap tool to phenotype this melting texture variant hampered its full exploitation in breeding activities [73]. The most widely used method to score the SS trait is based on sensorial evaluation, based on mouthfeel and tactile sensation assessed by expert breeders. However, this approach is limited by its low throughput, requiring several years of observation for a reliable assessment. Clearly, sensorial evaluation suffers from a certain degree of subjectivity, which makes observation not generalizable to all experimental conditions. In the previous chapter, novel indices have been developed, the TD and K-intercept, which allows a more objective evaluation of fruit textural properties. These methods rely on the measurement of the mechanical properties of the flesh, which are able to distinguish between SS and M textures. In the present work, a panel of accessions and a biparental population were phenotyped by sensorial evaluation and instrumental measures of mechanical parameters, and used in association and linkage mapping experiment. A major locus was identified in the distal part of chromosome 8, between 18.4Mb and 20.5 Mb. The distance between the most associated signals in GWAS and QTL-mapping is 257.156 bp, suggesting the same locus segregates in both populations. Association and linkage mapping results support the hypothesis of a Mendelian inheritance of the trait, although this hypothesis should be further verified in other genetic backgrounds. Our results are consistent with a dominant effect of the allele conferring the SS trait, as early reported[73]. In

the MxR028 progeny, most associated SNPs in the identified interval are heterozygous in both parents, thus not useful for an application in marker assisted selection. The mapped interval spans a region of about 2 Mb, too large to confidently identify causal variants. In order to increase genetic resolution of the target locus and restrict the list of candidate genes, a higher number of segregating progenies should be analyzed, taking advantage of the high degree of molecular polymorphism of the identified genomic region. Despite the low resolution of the current chromosomal position, the locus was further explored by using RNA-seq and whole-genome re-sequencing data as a preliminary step to evaluate possible associations with candidate genes. A total of 64 DEG transcripts were identified by the comparison of fruit flesh at SIV ripening stage transcriptome of two SS and two M cultivars: genes related to auxin metabolism and response were detected. As recently found in peach, auxin homeostasis is crucial for fruit ripening, stimulating ethylene biosynthesis[69]. Moreover, an auxin biosynthesis gene, *YUC11*-like, has been recently proposed as a candidate gene for the stony hard texture trait in peach. Thus, auxin metabolism and/or response may a play a role in SS trait as well [80].

4.6 Conclusions

In this work a novel approach based on processed mechanical parameters (see paragraph 3), the texture dynamics index (TD), was applied to phenotype fruit texture types in a segregating progeny (MxR028). The K-intercept of TD model was able to distinguish melting and slow-softening individuals, allowing the identification of a major locus on the distal part of chromosome 8. QTL-mapping was coupled with GWA analysis in a wide peach collection characterized by sensorial evaluation of fruit texture. Most associated SNPs detected by association mapping confirmed the presence of a single locus in the same region of chromosome 8, albeit with a broader genetic interval compared to QTL analysis. Nevertheless, the size of the associated interval is still too extended for a preliminary screening of candidate gene variants.

This study is the first reporting a major locus associated to the SS trait in peach, supporting early observations of a simple inheritance of the trait. Furthermore, results demonstrated the suitability of the TD index for a quick and reliable phenotyping of peach texture in segregating progenies, even of relative small size. Considering the complexity of sensorial assessment, this aspect is of fundamental importance for fine-mapping experiments, which will require a wider progeny or wide germplasm collections. A more precise mapping would allow the identification of the gene(s) involved in peach texture and the development of efficient markers for assisted selection of new cultivars with optimum textural performance, a crucial aspects for increasing peach fruit competitiveness in the fresh market.

Map

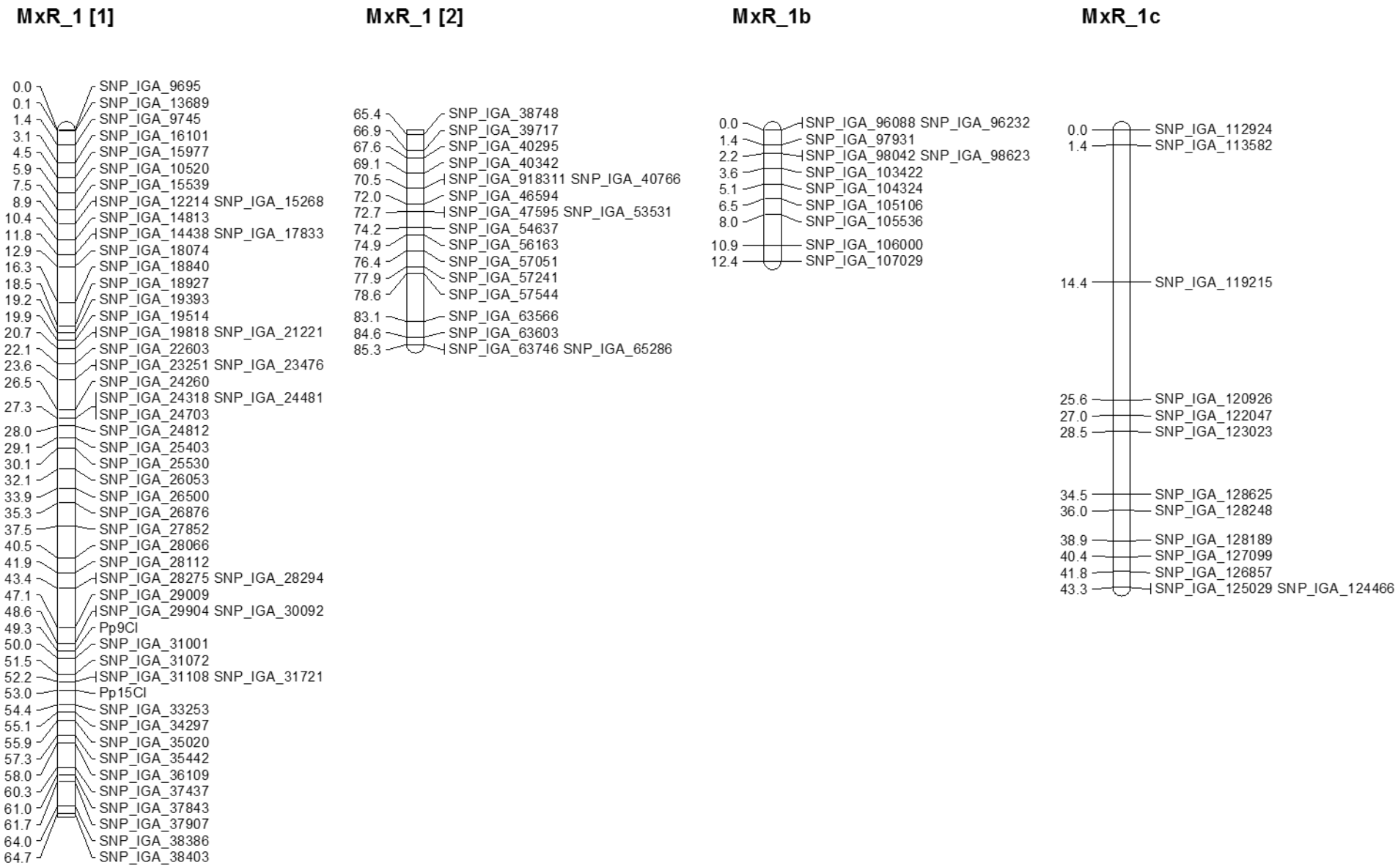
MxR_1 [1]
0.0 SNP_IGA_9695
0.1 SNP_IGA_13689
1.4 SNP_IGA_9745
3.1 SNP_IGA_16101
4.5 SNP_IGA_15977
5.9 SNP_IGA_10520
7.5 SNP_IGA_15539
8.9 SNP_IGA_12214 SNP_IGA_15268
10.4 SNP_IGA_14813
11.8 SNP_IGA_14438 SNP_IGA_17833
12.9 SNP_IGA_18074
16.3 SNP_IGA_18840
18.5 SNP_IGA_18927
19.2 SNP_IGA_19393
19.9 SNP_IGA_19514
20.7 SNP_IGA_19818 SNP_IGA_21221
22.1 SNP_IGA_22603
23.6 SNP_IGA_23251 SNP_IGA_23476
26.5 SNP_IGA_24260
27.3 SNP_IGA_24318 SNP_IGA_24481
SNP_IGA_24703
28.0 SNP_IGA_24812
29.1 SNP_IGA_25403
30.1 SNP_IGA_25530
32.1 SNP_IGA_26053
33.9 SNP_IGA_26500
35.3 SNP_IGA_26876
37.5 SNP_IGA_27852
40.5 SNP_IGA_28066
41.9 SNP_IGA_28112
43.4 SNP_IGA_28275 SNP_IGA_28294
47.1 SNP_IGA_29009
48.6 SNP_IGA_29904 SNP_IGA_30092
49.3 Pp9CI
50.0 SNP_IGA_31001
51.5 SNP_IGA_31072
52.2 SNP_IGA_31108 SNP_IGA_31721
53.0 Pp15CI
54.4 SNP_IGA_33253
55.1 SNP_IGA_34297
55.9 SNP_IGA_35020
57.3 SNP_IGA_35442
58.0 SNP_IGA_36109
60.3 SNP_IGA_37437
61.0 SNP_IGA_37843
61.7 SNP_IGA_37907
64.0 SNP_IGA_38386
64.7 SNP_IGA_38403
MxR_1 [2]
65.4 SNP_IGA_38748
66.9 SNP_IGA_39717
67.6 SNP_IGA_40295
69.1 SNP_IGA_40342
70.5 SNP_IGA_918311 SNP_IGA_40766
72.0 SNP_IGA_46594
72.7 SNP_IGA_47595 SNP_IGA_53531
74.2 SNP_IGA_54637
74.9 SNP_IGA_56163
76.4 SNP_IGA_57051
77.9 SNP_IGA_57241
78.6 SNP_IGA_57544
83.1 SNP_IGA_63566
84.6 SNP_IGA_63603
85.3 SNP_IGA_63746 SNP_IGA_65286
MxR_1b
0.0 SNP_IGA_96088 SNP_IGA_96232
1.4 SNP_IGA_97931
2.2 SNP_IGA_98042 SNP_IGA_98623
3.6 SNP_IGA_103422
5.1 SNP_IGA_104324
6.5 SNP_IGA_105106
8.0 SNP_IGA_105536
10.9 SNP_IGA_106000
12.4 SNP_IGA_107029
MxR_1c
0.0 SNP_IGA_112924
1.4 SNP_IGA_113582
14.4 SNP_IGA_119215
25.6 SNP_IGA_120926
27.0 SNP_IGA_122047
28.5 SNP_IGA_123023
34.5 SNP_IGA_128625
36.0 SNP_IGA_128248
38.9 SNP_IGA_128189
40.4 SNP_IGA_127099
41.8 SNP_IGA_126857
43.3 SNP_IGA_125029 SNP_IGA_124466

Map

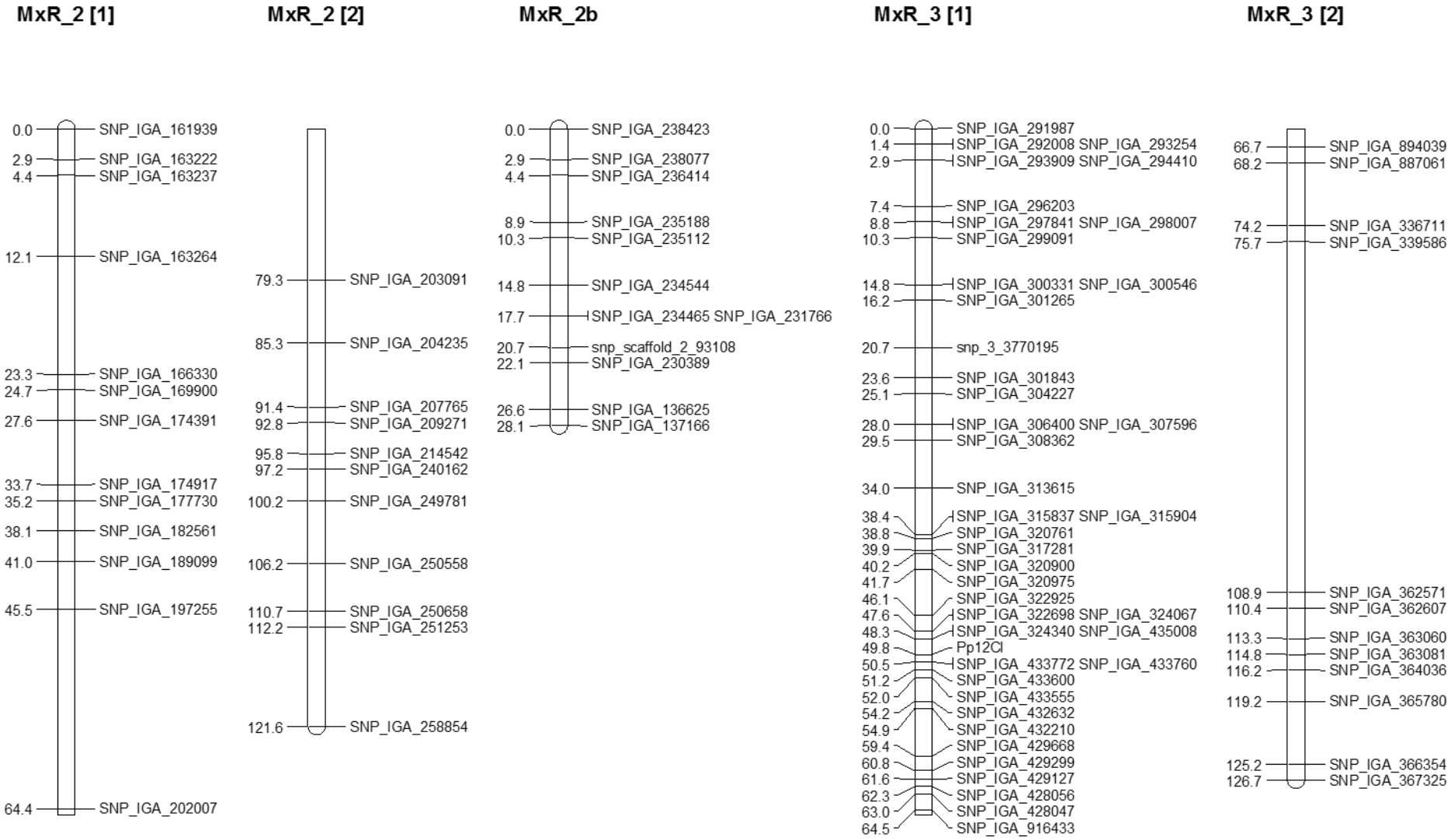
MxR_2 [1]
0.0 SNP_IGA_161939
2.9 SNP_IGA_163222
4.4 SNP_IGA_163237
12.1 SNP_IGA_163264
23.3 SNP_IGA_166330
24.7 SNP_IGA_169900
27.6 SNP_IGA_174391
33.7 SNP_IGA_174917
35.2 SNP_IGA_177730
38.1 SNP_IGA_182561
41.0 SNP_IGA_189099
45.5 SNP_IGA_197255
64.4 SNP_IGA_202007
MxR_2 [2]
79.3 SNP_IGA_203091
85.3 SNP_IGA_204235
91.4 SNP_IGA_207765
92.8 SNP_IGA_209271
95.8 SNP_IGA_214542
97.2 SNP_IGA_240162
100.2 SNP_IGA_249781
106.2 SNP_IGA_250558
110.7 SNP_IGA_250658
112.2 SNP_IGA_251253
121.6 SNP_IGA_258854
MxR_2b
0.0 SNP_IGA_238423
2.9 SNP_IGA_238077
4.4 SNP_IGA_236414
8.9 SNP_IGA_235188
10.3 SNP_IGA_235112
14.8 SNP_IGA_234544
17.7 SNP_IGA_234465 SNP_IGA_231766
20.7 snp_scaffold_2_93108
22.1 SNP_IGA_230389
26.6 SNP_IGA_136625
28.1 SNP_IGA_137166
MxR_3 [1]
0.0 SNP_IGA_291987
1.4 SNP_IGA_292008 SNP_IGA_293254
2.9 SNP_IGA_293909 SNP_IGA_294410
7.4 SNP_IGA_296203
8.8 SNP_IGA_297841 SNP_IGA_298007
10.3 SNP_IGA_299091
14.8 SNP_IGA_300331 SNP_IGA_300546
16.2 SNP_IGA_301265
20.7 snp_3_3770195
23.6 SNP_IGA_301843
25.1 SNP_IGA_304227
28.0 SNP_IGA_306400 SNP_IGA_307596
29.5 SNP_IGA_308362
34.0 SNP_IGA_313615
38.4 SNP_IGA_315837 SNP_IGA_315904
38.8 SNP_IGA_320761
39.9 SNP_IGA_317281
40.2 SNP_IGA_320900
41.7 SNP_IGA_320975
46.1 SNP_IGA_322925
47.6 SNP_IGA_322698 SNP_IGA_324067
48.3 SNP_IGA_324340 SNP_IGA_435008
49.8 Pp12Cl
50.5 SNP_IGA_433772 SNP_IGA_433760
51.2 SNP_IGA_433600
52.0 SNP_IGA_433555
54.2 SNP_IGA_432632
54.9 SNP_IGA_432210
59.4 SNP_IGA_429668
60.8 SNP_IGA_429299
61.6 SNP_IGA_429127
62.3 SNP_IGA_428056
63.0 SNP_IGA_428047
64.5 SNP_IGA_916433
MxR_3 [2]
66.7 SNP_IGA_894039
68.2 SNP_IGA_887061
74.2 SNP_IGA_336711
75.7 SNP_IGA_339586
108.9 SNP_IGA_362571
110.4 SNP_IGA_362607
113.3 SNP_IGA_363060
114.8 SNP_IGA_363081
116.2 SNP_IGA_364036
119.2 SNP_IGA_365780
125.2 SNP_IGA_366354
126.7 SNP_IGA_367325

Map

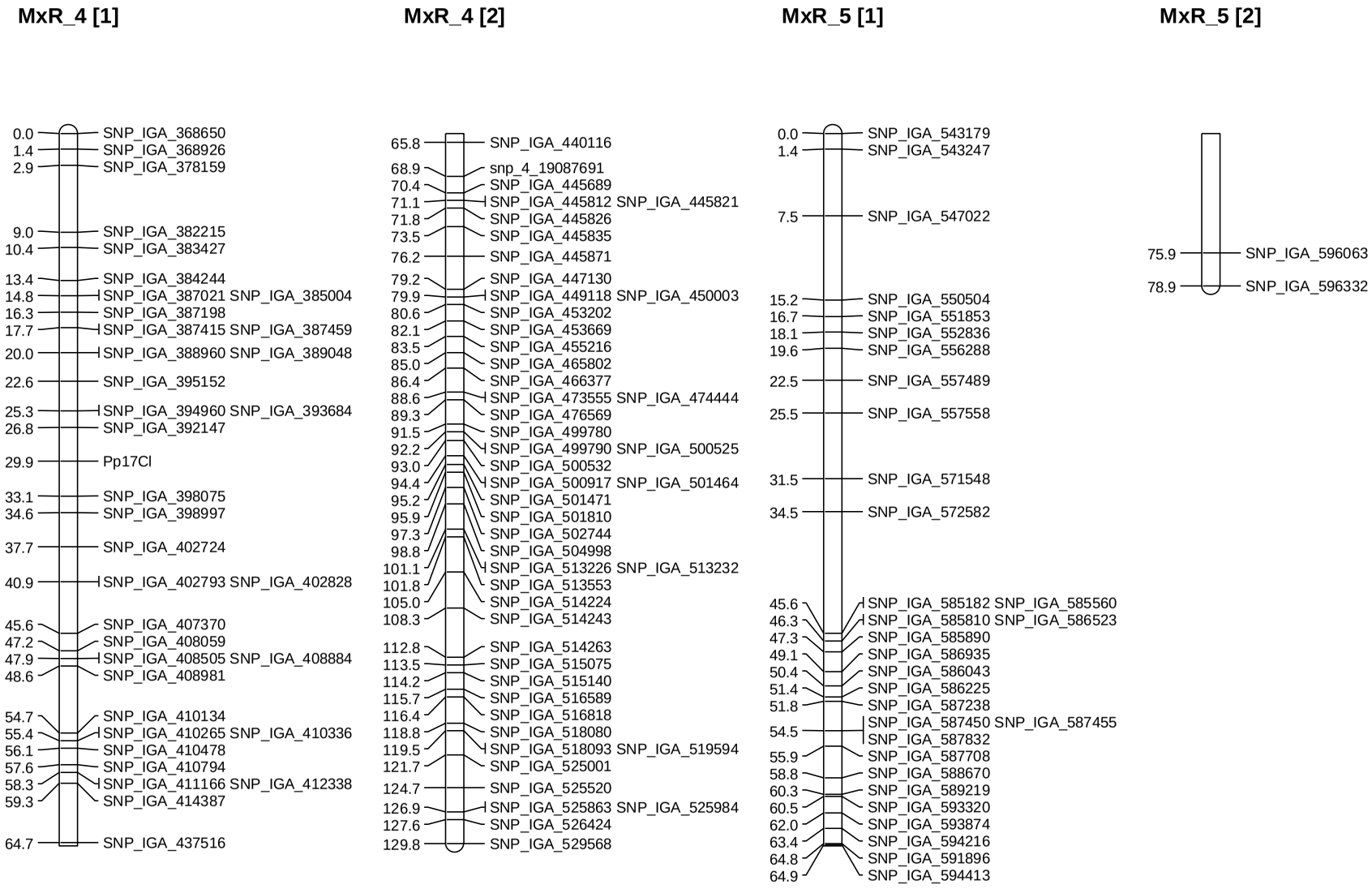
MxR_4 [1]
0.0 SNP_IGA_368650
1.4 SNP_IGA_368926
2.9 SNP_IGA_378159
9.0 SNP_IGA_382215
10.4 SNP_IGA_383427
13.4 SNP_IGA_384244
14.8 SNP_IGA_387021 SNP_IGA_385004
16.3 SNP_IGA_387198
17.7 SNP_IGA_387415 SNP_IGA_387459
20.0 SNP_IGA_388960 SNP_IGA_389048
22.6 SNP_IGA_395152
25.3 SNP_IGA_394960 SNP_IGA_393684
26.8 SNP_IGA_392147
29.9 Pp17Cl
33.1 SNP_IGA_398075
34.6 SNP_IGA_398997
37.7 SNP_IGA_402724
40.9 SNP_IGA_402793 SNP_IGA_402828
45.6 SNP_IGA_407370
47.2 SNP_IGA_408059
47.9 SNP_IGA_408505 SNP_IGA_408884
48.6 SNP_IGA_408981
54.7 SNP_IGA_410134
55.4 SNP_IGA_410265 SNP_IGA_410336
56.1 SNP_IGA_410478
57.6 SNP_IGA_410794
58.3 SNP_IGA_411166 SNP_IGA_412338
59.3 SNP_IGA_414387
64.7 SNP_IGA_437516
MxR_4 [2]
65.8 SNP_IGA_440116
68.9 snp_4_19087691
70.4 SNP_IGA_445689
71.1 SNP_IGA_445812 SNP_IGA_445821
71.8 SNP_IGA_445826
73.5 SNP_IGA_445835
76.2 SNP_IGA_445871
79.2 SNP_IGA_447130
79.9 SNP_IGA_449118 SNP_IGA_450003
80.6 SNP_IGA_453202
82.1 SNP_IGA_453669
83.5 SNP_IGA_455216
85.0 SNP_IGA_465802
86.4 SNP_IGA_466377
88.6 SNP_IGA_473555 SNP_IGA_474444
89.3 SNP_IGA_476569
91.5 SNP_IGA_499780
92.2 SNP_IGA_499790 SNP_IGA_500525
93.0 SNP_IGA_500532
94.4 SNP_IGA_500917 SNP_IGA_501464
95.2 SNP_IGA_501471
95.9 SNP_IGA_501810
97.3 SNP_IGA_502744
98.8 SNP_IGA_504998
101.1 SNP_IGA_513226 SNP_IGA_513232
101.8 SNP_IGA_513553
105.0 SNP_IGA_514224
108.3 SNP_IGA_514243
112.8 SNP_IGA_514263
113.5 SNP_IGA_515075
114.2 SNP_IGA_515140
115.7 SNP_IGA_516589
116.4 SNP_IGA_516818
118.8 SNP_IGA_518080
119.5 SNP_IGA_518093 SNP_IGA_519594
121.7 SNP_IGA_525001
124.7 SNP_IGA_525520
126.9 SNP_IGA_525863 SNP_IGA_525984
127.6 SNP_IGA_526424
129.8 SNP_IGA_529568
MxR_5 [1]
0.0 SNP_IGA_543179
1.4 SNP_IGA_543247
7.5 SNP_IGA_547022
15.2 SNP_IGA_550504
16.7 SNP_IGA_551853
18.1 SNP_IGA_552836
19.6 SNP_IGA_556288
22.5 SNP_IGA_557489
25.5 SNP_IGA_557558
31.5 SNP_IGA_571548
34.5 SNP_IGA_572582
45.6 SNP_IGA_585182 SNP_IGA_585560
46.3 SNP_IGA_585810 SNP_IGA_586523
47.3 SNP_IGA_585890
49.1 SNP_IGA_586935
50.4 SNP_IGA_586043
51.4 SNP_IGA_586225
51.8 SNP_IGA_587238
54.5 SNP_IGA_587450 SNP_IGA_587455
SNP_IGA_587832
55.9 SNP_IGA_587708
58.8 SNP_IGA_588670
60.3 SNP_IGA_589219
60.5 SNP_IGA_593320
62.0 SNP_IGA_593874
63.4 SNP_IGA_594216
64.8 SNP_IGA_591896
64.9 SNP_IGA_594413
MxR_5 [2]
75.9 SNP_IGA_596063
78.9 SNP_IGA_596332

Map

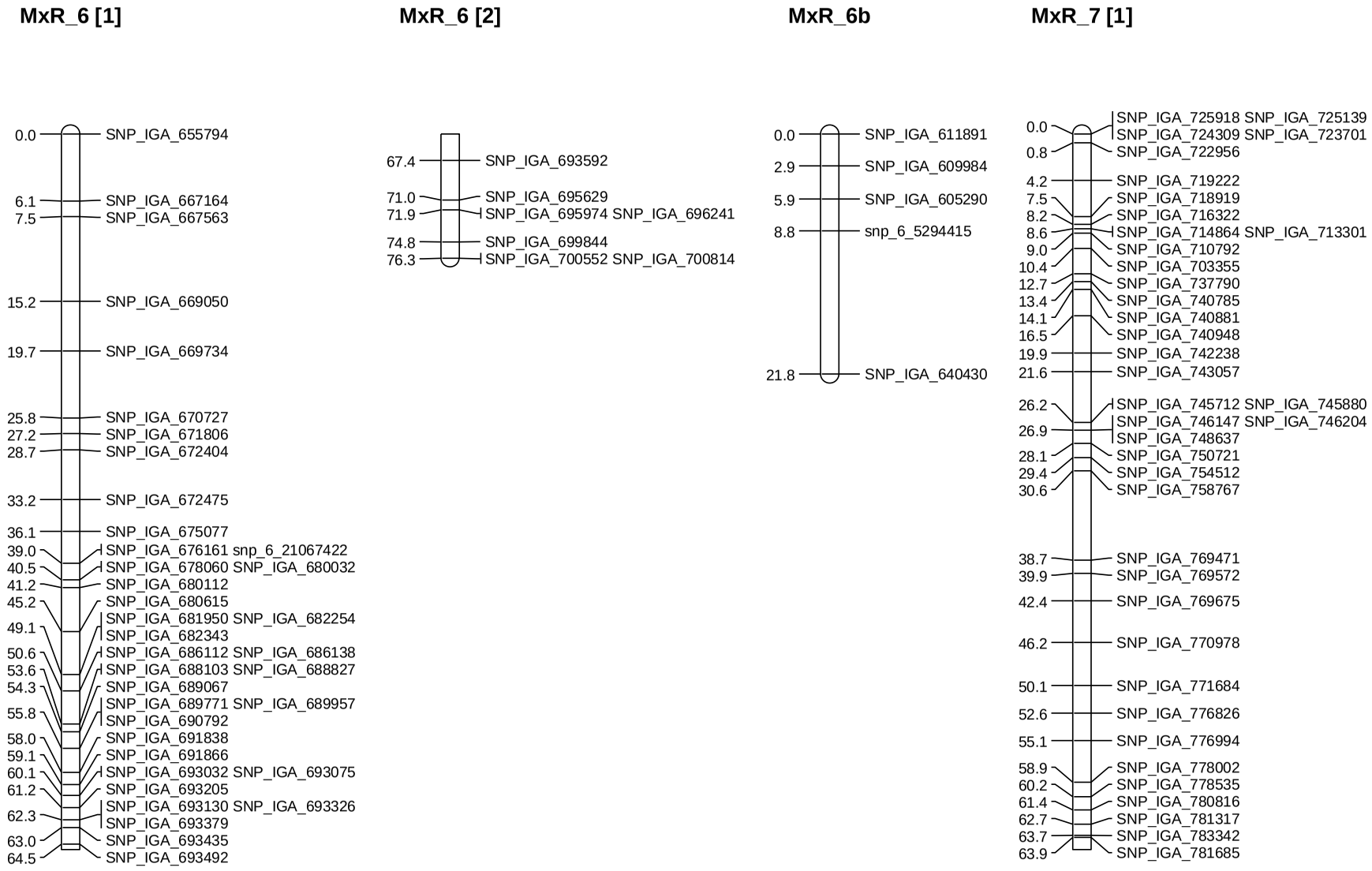
MxR_6 [1]
0.0 SNP_IGA_655794
6.1 SNP_IGA_667164
7.5 SNP_IGA_667563
15.2 SNP_IGA_669050
19.7 SNP_IGA_669734
25.8 SNP_IGA_670727
27.2 SNP_IGA_671806
28.7 SNP_IGA_672404
33.2 SNP_IGA_672475
36.1 SNP_IGA_675077
39.0 SNP_IGA_676161 snp_6_21067422
40.5 SNP_IGA_678060 SNP_IGA_680032
41.2 SNP_IGA_680112
45.2 SNP_IGA_680615
49.1 SNP_IGA_681950 SNP_IGA_682254
SNP_IGA_682343
50.6 SNP_IGA_686112 SNP_IGA_686138
53.6 SNP_IGA_688103 SNP_IGA_688827
54.3 SNP_IGA_689067
55.8 SNP_IGA_689771 SNP_IGA_689957
SNP_IGA_690792
58.0 SNP_IGA_691838
59.1 SNP_IGA_691866
60.1 SNP_IGA_693032 SNP_IGA_693075
61.2 SNP_IGA_693205
62.3 SNP_IGA_693130 SNP_IGA_693326
SNP_IGA_693379
63.0 SNP_IGA_693435
64.5 SNP_IGA_693492
MxR_6 [2]
67.4 SNP_IGA_693592
71.0 SNP_IGA_695629
71.9 SNP_IGA_695974 SNP_IGA_696241
74.8 SNP_IGA_699844
76.3 SNP_IGA_700552 SNP_IGA_700814
MxR_6b
0.0 SNP_IGA_611891
2.9 SNP_IGA_609984
5.9 SNP_IGA_605290
8.8 snp_6_5294415
21.8 SNP_IGA_640430
MxR_7 [1]
0.0 SNP_IGA_725918 SNP_IGA_725139
SNP_IGA_724309 SNP_IGA_723701
0.8 SNP_IGA_722956
4.2 SNP_IGA_719222
7.5 SNP_IGA_718919
8.2 SNP_IGA_716322
8.6 SNP_IGA_714864 SNP_IGA_713301
9.0 SNP_IGA_710792
10.4 SNP_IGA_703355
12.7 SNP_IGA_737790
13.4 SNP_IGA_740785
14.1 SNP_IGA_740881
16.5 SNP_IGA_740948
19.9 SNP_IGA_742238
21.6 SNP_IGA_743057
26.2 SNP_IGA_745712 SNP_IGA_745880
26.9 SNP_IGA_746147 SNP_IGA_746204
SNP_IGA_748637
28.1 SNP_IGA_750721
29.4 SNP_IGA_754512
30.6 SNP_IGA_758767
38.7 SNP_IGA_769471
39.9 SNP_IGA_769572
42.4 SNP_IGA_769675
46.2 SNP_IGA_770978
50.1 SNP_IGA_771684
52.6 SNP_IGA_776826
55.1 SNP_IGA_776994
58.9 SNP_IGA_778002
60.2 SNP_IGA_778535
61.4 SNP_IGA_780816
62.7 SNP_IGA_781317
63.7 SNP_IGA_783342
63.9 SNP_IGA_781685

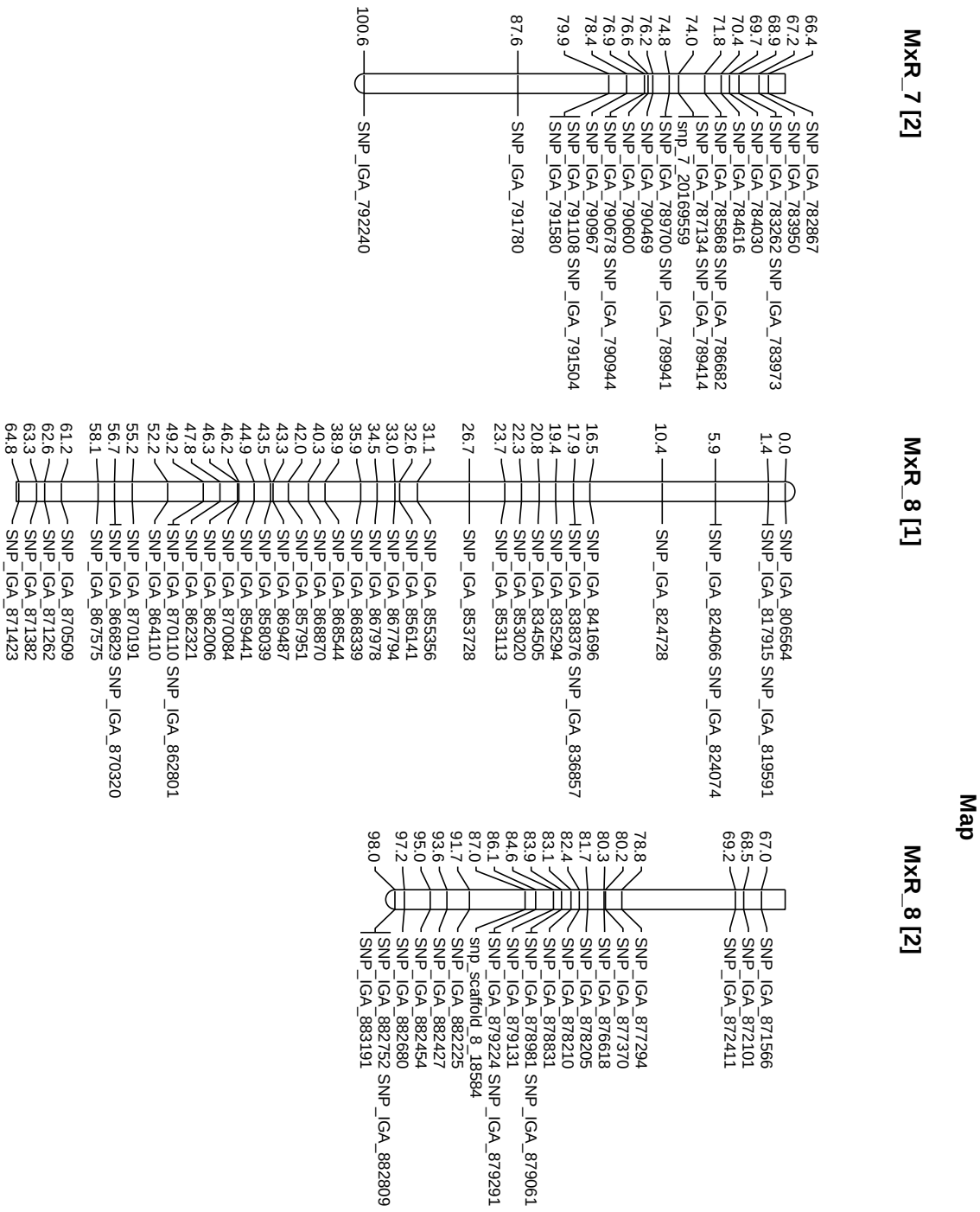

Figure 19 Genetic map of MxR028 population, 12 linkage groups (anchored to the 8 chromosomes) represented with integrated map, plotted using JoinMap 4.1.

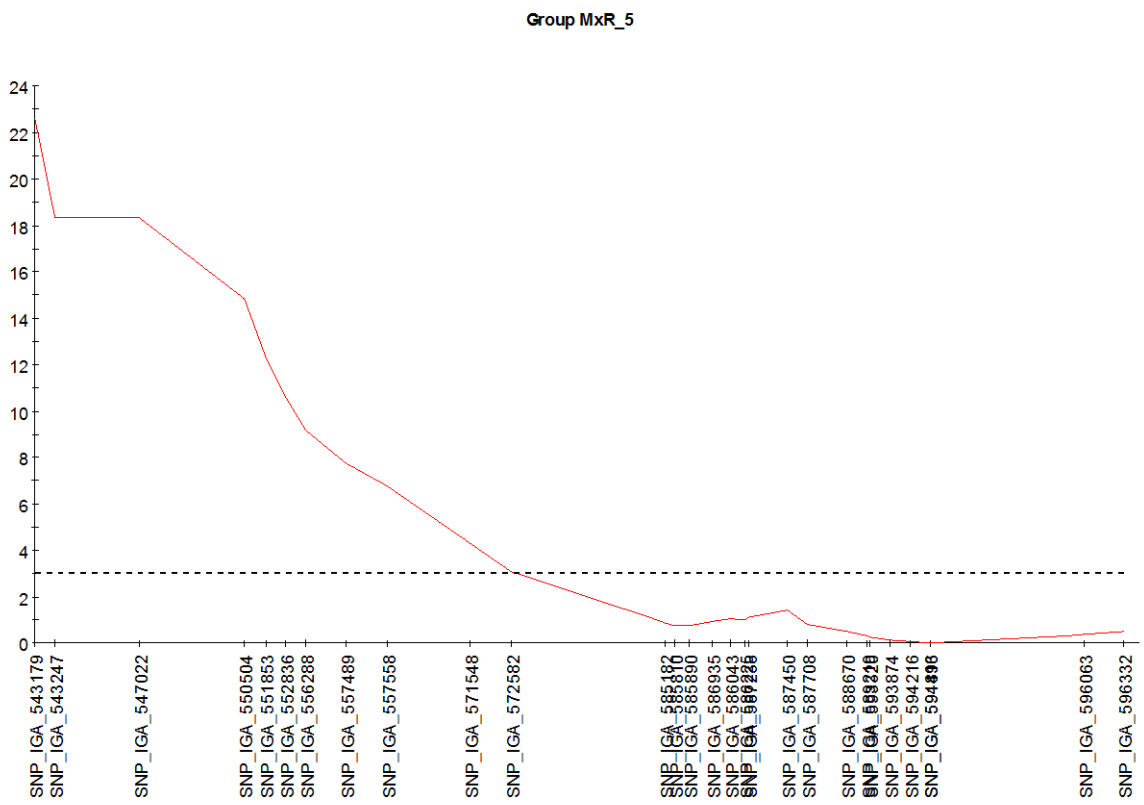

Figure 20 QTL mapping of acidity, recovering the Locus D. In red the LOD value, the dashed line represents the threshold obtained by permutation test (3.1 LOD).

Table 3 phenotypes collected in MxR28 seedlings

individualnames_	K.Intercept	TD	Elasticity	Fracturabi	Logistic_K	MD	I_DA	Weight	Blush	RSR	TDy2	Acidity Type
MxR28-003	2,12	0,38	1,82	4,85	2	252	0,8	147	75	12,8	0,22	1
MxR28-004	3,11	0,64	1,84	2,86	2	NA	0,3	126	85	14,2	0,22	0
MxR28-006	0,38	0,51	2,59	5,1	1	223	0,3	121	76	11,2	0,24	1
MxR28-007	1,49	0,38	2,15	5,73	1	218	0,2	115	45	8,6	NA	0
MxR28-014	1,13	0,27	1,81	6,81	1	216	0,3	110	73	11	0,25	1
MxR28-016	2,52	0,22	1,84	8,24	2	218	0,3	128	90	8,8	NA	0
MxR28-018	2,58	0,22	1,82	8,38	2	220	0,3	134	75	11	NA	1
MxR28-023	0,38	1,49	2,99	2	1	232	0,3	119	91	13	NA	0
MxR28-034	2,45	0,21	1,44	6,93	2	250	0,5	154	79	14	0,22	0
MxR28-042	2,55	1,02	2,48	2,42	2	241	0,6	131	65	12,2	0,23	0
MxR28-045	0,87	0,55	2,45	4,49	1	NA	NA	NA	NA	NA	NA	NA
MxR28-049	3,21	0,17	1,69	9,66	2	210	NA	NA	NA	NA	NA	NA
MxR28-051	0,9	0,86	2,36	2,75	1	NA	0,8	129	98	13,7	0,25	1
MxR28-052	0,18	1,77	3,65	2,06	1	NA	0,5	126	79	12,4	0,23	1
MxR28-055	2,61	0,5	1,5	3,01	2	243	0,7	129	63	11	0,21	0
MxR28-057	0,31	0,49	2,86	5,89	1	NA	0,8	166	74	13,4	0,22	1
MxR28-061	0,84	0,67	2,5	3,73	1	243	0,7	116	65	13	NA	1
MxR28-064	0,24	0,46	3,73	8,15	1	238	0,6	124	93	11,4	0,24	0
MxR28-066	2,88	0,19	1,76	9,01	2	210	NA	NA	NA	NA	NA	NA
MxR28-069	2,81	0,2	1,77	8,87	2	NA	NA	NA	NA	NA	NA	NA
MxR28-077	0,21	1,3	3,37	2,6	1	234	0,5	113	69	11,7	0,27	0
MxR28-080	0,38	1,49	2,99	2	1	234	0,4	96	95	13,4	NA	0
MxR28-081	0,64	-4,62	2,91	-0,63	1	238	0,4	109	60	10,6	0,23	1
MxR28-089	0,28	2,03	3,17	1,56	1	NA	0,7	132	64	12,2	NA	0
MxR28-097	2,38	0,24	1,87	7,94	2	241	0,6	132	64	12,6	NA	0
MxR28-103	1,92	0,29	2	6,85	2	216	0,3	150	81	9	NA	0
MxR28-106	0,41	1,37	2,94	2,14	1	220	0,2	154	78	8,8	NA	0
MxR28-107	0,41	1,37	2,94	2,14	1	218	0,3	149	88	10,2	NA	1
MxR28-108	3,21	0,3	1,32	4,46	2	NA	0,3	137	61	12	0,22	1
MxR28-109	0,44	1,27	2,89	2,27	1	NA	NA	NA	NA	NA	NA	NA
MxR28-117	0,11	5,01	3,72	0,74	1	NA	0,3	128	75	12	NA	1
MxR28-118	0,28	0,08	1,67	20,6	1	210	NA	NA	NA	NA	0,42	NA
MxR28-120	0,97	0,58	2,42	4,17	1	210	0,3	123	61	11,4	NA	0
MxR28-123	0,28	1	2,72	2,72	1	245	0,6	96	63	11,1	0,27	0
MxR28-126	1,96	0,4	1,63	4,05	2	234	0,7	138	81	12,8	0,2	1
MxR28-128	1	0,56	2,39	4,27	1	238	0,4	126	79	13,6	NA	1
MxR28-132	2,28	2,57	2,61	1,02	2	241	0,8	153	48	14	0,21	1
MxR28-133	0,87	0,65	2,48	3,84	1	NA	0,3	119	80	10,4	NA	0
MxR28-136	0,28	2,03	3,17	1,56	1	210	NA	NA	NA	NA	NA	NA
MxR28-138	0,41	1,37	2,94	2,14	1	NA	0,6	148	71	12,4	NA	1
MxR28-139	1,03	0,54	2,38	4,38	1	NA	0,5	159	64	12	NA	0
MxR28-141	0,64	0,46	2,17	4,73	1	210	0,2	NA	NA	NA	0,28	NA
MxR28-147	2,71	0,21	1,79	8,66	2	216	0,2	136	66	8,6	NA	0
MxR28-148	1,99	0,23	1,71	7,3	2	234	0,8	94	89	13,8	0,22	1
MxR28-149	2,35	0,24	1,88	7,87	2	NA	NA	NA	NA	NA	NA	NA
MxR28-152	-0,09	0,09	2,3	25,27	1	250	0,5	159	72	13	0,26	0
MxR28-159	2,02	0,28	1,97	7,1	2	216	0,2	79	79	9	NA	0
MxR28-160	2,94	0,32	1,22	3,8	2	234	0,4	130	80	13,5	0,23	1
MxR28-163	2,65	0,21	1,81	8,52	2	220	0,2	104	85	10,4	NA	1
MxR28-164	2,22	0,25	1,91	7,57	2	NA	NA	NA	NA	NA	NA	NA
MxR28-165	1,46	0,38	2,17	5,64	1	NA	0,4	NA	NA	NA	NA	NA
MxR28-171	0,28	2,03	3,17	1,56	1	210	NA	NA	NA	NA	NA	NA
MxR28-173	1,43	-1,29	2,32	-1,81	1	216	NA	NA	NA	NA	0,37	NA
MxR28-176	1,99	0,28	1,98	7,02	2	216	NA	NA	NA	NA	NA	NA
MxR28-178	2,48	0,23	1,85	8,17	2	NA	0,7	123	86	12,9	NA	0
MxR28-179	1,66	0,6	2,35	3,95	2	NA	0,7	128	87	15	0,2	1
MxR28-191	0,05	12,16	4,26	0,35	1	216	0,3	99	67	9	NA	0
MxR28-192	2,32	0,24	1,89	7,8	2	216	0,3	105	71	8	NA	0
MxR28-204	0,77	0,79	2,4	3,03	1	218	NA	NA	NA	NA	0,24	NA
MxR28-206	2,48	0,23	1,85	8,17	2	245	0,6	165	71	11,9	NA	0
MxR28-208	0,77	0,44	2,36	5,35	1	218	NA	NA	NA	NA	0,29	NA
MxR28-210	1,66	0,17	1,63	9,75	2	247	0,8	190	75	12,6	0,23	1
MxR28-213	1,13	0,97	3,53	3,65	1	232	0,5	119	87	12,6	0,23	0
MxR28-218	2,28	0,27	1,62	5,96	2	245	0,8	119	50	10,4	0,21	1
MxR28-221	3,11	0,18	1,71	9,47	2	216	0,3	132	75	9	NA	0
MxR28-227	0,87	3,95	3,65	0,92	1	234	0,6	120	90	12,4	0,25	1
MxR28-228	0,51	1,11	2,81	2,54	1	NA	0,2	158	84	9,6	NA	0
MxR28-229	0,61	0,93	2,7	2,91	1	216	0,3	127	62	10	NA	1
MxR28-231	1	0,28	2,13	7,64	1	243	0,5	100	73	11,5	0,21	0
MxR28-242	0,54	1,04	2,77	2,66	1	218	0,2	NA	NA	NA	NA	NA

Table 4DEGs in SS locus between the M and SS accessions.

Gene	Position	foldchange	CDS variants	Variants Flanking (2k)	Annotation
Prupe.8G192500.v2.1	18643902-18646172	2,71	0	0	Auxin-responsive family protein
Prupe.8G192700.v2.1	18651621-18652697	1,58	0	0	auxin-responsive family protein
Prupe.8G196600.v2.1	18815103-18816216	-1,49	0	8	
Prupe.8G196900.v2.1	18829145-18831138	2,82	0	8	cytochrome P450, family 82, subfamily G, polypeptide 1
Prupe.8G200200.v2.1	18962947-18967387	-1,28	0	0	GPI transamidase component PIG-S-related
Prupe.8G202800.v2.1	19101309-19102983	-1,82	0	1	Ribosomal protein L13 family protein
Prupe.8G202900.v2.1	19103722-19105639	-1,49	0	0	cytochrome B5 isoform B
Prupe.8G203200.v2.1	19114472-19117029	-1,35	0	0	BSD domain-containing protein
Prupe.8G203400.v2.1	19124862-19128400	-3,7	0	0	proteolysis 1
Prupe.8G204600.v2.1	19182750-19185601	-1,22	0	0	homolog of bacterial PANC
Prupe.8G205200.v2.1	19212279-19212973	4,29	0	0	
Prupe.8G206400.v2.1	19321695-19324805	1,24	0	0	peroxisomal 3-ketoacyl-CoA thiolase 3
Prupe.8G210900.v2.1	19510008-19512968	-1,39	0	3	Glutaredoxin family protein
Prupe.8G211800.v2.1	19567128-19577259	3,67	0	0	global transcription factor group B1
Prupe.8G215400.v2.1	19776926-19780643	2,03	0	0	indole-3-acetic acid inducible 11
Prupe.8G216200.v2.1	19816130-19818295	-1,59	0	0	plasmodesmata-located protein 2
Prupe.8G216400.v2.1	19826510-19828518	1,79	0	0	Glutathione S-transferase family protein
Prupe.8G219000.v2.1	19953927-19959169	1,21	0	0	no pollen germination related 2
Prupe.8G220500.v2.1	20027790-20030920	-1,23	0	0	vacuolar protein sorting-associated protein 2.3
Prupe.8G220800.v2.1	20041459-20047260	-1,75	0	0	Ypt/Rab-GAP domain of gyp1p superfamily protein
Prupe.8G221000.v2.1	20062678-20065027	-1,37	0	0	
Prupe.8G222400.v2.1	20145270-20150752	1,2	0	1	ARM repeat superfamily protein
Prupe.8G222700.v2.1	20160344-20164335	-1,33	0	0	Peptidase S24/S26A/S26B/S26C family protein
Prupe.8G223500.v2.1	20189766-20190797	1,92	0	0	
Prupe.8G223600.v2.1	20191345-20195989	-1,2	0	1	translocase inner membrane subunit 44-2
Prupe.8G224100.v2.1	20213330-20216347	-1,22	0	2	
Prupe.8G225000.v2.1	20254913-20257736	1,39	0	1	
Prupe.8G229700.v2.1	20527683-20532213	-1,61	0	0	IND1(iron-sulfur protein required for NADH dehydrogenase)-like
Prupe.8G230700.v2.1	20573325-20576549	1,26	0	0	WRKY DNA-binding protein 21
Prupe.8G232400.v2.1	20653624-20655672	1,59	0	0	AUX/IAA transcriptional regulator family protein
Prupe.8G232500.v2.1	20655080-20657037	-1,67	0	0	Primosome PriB/single-strand DNA-binding
Prupe.8G233400.v2.1	20711762-20715713	2,47	0	0	
Prupe.8G233500.v2.1	20724576-20727588	1,68	0	0	Ggamma-subunit 1
Prupe.8G236700.v2.1	20916860-20917895	-1,32	0	0	
Prupe.8G237300.v2.1	20955842-20957155	1,59	0	0	Protein of unknown function (DUF581)
Prupe.8G238200.v2.1	20984438-20987946	-1,43	0	1	Transducin/WD40 repeat-like superfamily protein
Prupe.8G238300.v2.1	20991186-20993923	-1,39	0	1	Protein of unknown function (DUF581)
Prupe.8G238900.v2.1	21011896-21014402	-1,35	0	1	Ribosomal protein S13/S18 family
Prupe.8G239300.v2.1	21041987-21043487	1,92	0	1	Plant protein of unknown function (DUF868)
Prupe.8G240900.v2.1	21114323-21118055	-1,37	0	0	RAN GTPase activating protein 1
Prupe.8G241400.v2.1	21137506-21139618	1,86	0	1	Protein of unknown function (DUF3049)
Prupe.8G242600.v2.1	21199953-21203790	-1,54	0	0	TRICHOME BIREFRINGENCE-LIKE 11
Prupe.8G245000.v2.1	21310320-21318203	1,22	0	1	REF4-related 1
Prupe.8G247100.v2.1	21399627-21404706	-1,89	0	0	oxidoreductase, 2OG-Fe(II) oxygenase family protein
Prupe.8G247600.v2.1	21415077-21417619	-1,41	0	0	ribosomal RNA processing 4
Prupe.8G248600.v2.1	21474403-21479245	-1,41	0	0	Major facilitator superfamily protein
Prupe.8G253000.v2.1	21670736-21673787	1,21	0	0	tubby like protein 3
Prupe.8G254700.v2.1	21759740-21761601	-1,69	0	1	
Prupe.8G257400.v2.1	21914479-21916328	1,29	0	1	Seven transmembrane MLO family protein
Prupe.8G259800.v2.1	21998521-22007097	1,66	0	0	multidrug resistance-associated protein 4
Prupe.8G261000.v2.1	22055341-22057371	1,28	0	0	
Prupe.8G261100.v2.1	22057662-22058465	-1,3	0	0	complex 1 family protein / LVR family protein
Prupe.8G263800.v2.1	22155178-22158557	3,19	0	0	AtL5
Prupe.8G265300.v2.1	22219511-22224016	-1,45	0	0	fumarase 1
Prupe.8G266200.v2.1	22269906-22276951	-1,2	0	0	SET domain-containing protein
Prupe.8G267300.v2.1	22313937-22317753	-1,54	0	0	
Prupe.8G267400.v2.1	22319209-22322641	1,11	0	0	NAD+ transporter 1
Prupe.8G267800.v2.1	22334771-22338301	1,38	0	0	nodulin MtN21 /EamA-like transporter family protein
Prupe.8G270100.v2.1	22426303-22428517	-1,28	0	0	ADP-ribosylation factor family protein
Prupe.8G270200.v2.1	22429206-22433386	-1,33	0	0	DNAJ heat shock family protein
Prupe.8G270600.v2.1	22454004-22457476	1,7	0	0	Heat shock protein DnaJ with tetratricopeptide repeat
Prupe.8G257900.v2.1	21932617-21936030	-1,28	1	0	tetratricopeptide repeat (TPR)-containing protein
Prupe.8G224000.v2.1	20209396-20213267	-1,23	2	0	Protein of unknown function, DUF647
Prupe.8G206600.v2.1	19334972-19340609	1,14	4	0	UDP-Glycosyltransferase superfamily protein

Table 5 germplasm phenotypes for texture (melting/slow softening), skin pubescence (Locus G), and flesh acidity (Locus D)

Accession	Texture	Locus G	Locus D	Accession	Texture	Locus G	Locus D
391C12XXXIV86	melting	nectarine	subacid	MAILLARA	slow-softening	nectarine	subacid
AFRA T	melting	peach	acid	MARLI	melting	peach	subacid
AKATSUKI	melting	peach	subacid	MAURA	slow-softening	peach	acid
ALBATROS	melting	peach	acid	MAX10	slow-softening	nectarine	acid
ALEXA	melting	nectarine	acid	MAYCREST	melting	peach	acid
ALIBLANCA	melting	peach	acid	MAYFIRE	melting	peach	acid
ALIPERSIE	melting	peach	acid	NADIA	melting	peach	acid
ALITOP	slow-softening	nectarine	subacid	NECTAGRAND	melting	nectarine	acid
ALMA	melting	nectarine	acid	NJ WEEPING	melting	peach	acid
AMBRA	melting	nectarine	acid	OKUBO	melting	peach	subacid
ANTONY	melting	nectarine	acid	OURO IAPAR	melting	peach	subacid
AUTUMN GRAND	melting	nectarine	acid	PIERI81	melting	peach	acid
AZURITE	slow-softening	peach	acid	PZ1	melting	peach	acid
BEICME BIN	melting	peach	acid	REBUS38	slow-softening	nectarine	subacid
BEIJING	melting	peach	subacid	REBUS195	slow-softening	nectarine	subacid
BELLA DI CESENA	melting	peach	acid	REBUS28	slow-softening	nectarine	subacid
BIG TOP	slow-softening	nectarine	subacid	REDHAVEN	melting	peach	acid
BLUSHING STAR	melting	peach	acid	REGINA D OTTOBRE	melting	peach	acid
BO96025035	melting	peach	acid	RICH LADY	slow-softening	peach	acid
BOLIVIA	melting	peach	acid	RITA STAR	melting	nectarine	acid
BORDO	slow-softening	peach	acid	ROMAGNA BRIGHT	slow-softening	nectarine	subacid
BOTTO	melting	peach	acid	ROMAGNA GIANT	slow-softening	nectarine	subacid
BOUNTY	melting	peach	acid	ROMAGNA GOLD	slow-softening	nectarine	subacid
BUCO INCAVATO	melting	peach	acid	ROMAGNA STAR	slow-softening	nectarine	subacid
CAPUCCI18	melting	peach	acid	ROMAGNA TOP	slow-softening	nectarine	subacid
CHIMARRITA	melting	peach	subacid	ROSA DARDI	melting	peach	acid
CINZIA	melting	peach	acid	ROSELLA	melting	peach	acid
CLAUDIA	melting	nectarine	acid	ROYAL GLORY	slow-softening	peach	subacid
CONTENDER	melting	peach	acid	ROYAL JIM	slow-softening	peach	acid
CORINDON	melting	peach	acid	ROYAL LEE	slow-softening	peach	subacid
DA TIAN TAO	melting	peach	subacid	ROYAL MAJESTIC	slow-softening	peach	acid
DIAMOND BRIGHT	melting	nectarine	acid	ROYAL TIME	slow-softening	peach	acid
DIXIRED	melting	peach	acid	RUBY RICH	slow-softening	peach	acid
DOLORES	melting	peach	acid	S5898	melting	nectarine	acid
EARLY O HENRY	melting	peach	acid	S6699	melting	nectarine	acid
EARLY TOP	melting	nectarine	acid	SOUTHERN PEARL	melting	peach	acid
EARLY ZEE	melting	nectarine	acid	SPLENDOR	melting	nectarine	acid
ELBERTITA	melting	peach	acid	STARK RED GOLD	slow-softening	nectarine	acid
ELEGANT LADY	melting	peach	acid	SUMMER RICH	slow-softening	peach	acid
FFF7910001	melting	peach	acid	SUPEACH FOUR	melting	peach	acid
FORLI1	melting	peach	acid	SUPEACH SIX	melting	peach	acid
GARCICA	slow-softening	nectarine	subacid	SWEETFIRE	slow-softening	peach	subacid
GLOHAVEN	melting	peach	acid	TARDIGOLD	melting	nectarine	acid
GRENAT	slow-softening	peach	subacid	TARDIVA SPADONI	melting	peach	acid
HAKUTO	melting	peach	subacid	TURQUOISE	slow-softening	nectarine	subacid
HONEY BLAZE	slow-softening	nectarine	subacid	VENUS	melting	nectarine	acid
HONEY GLO	slow-softening	nectarine	subacid	VISTARICH	slow-softening	peach	acid
HONEY KIST	slow-softening	nectarine	subacid	VITTORIO EMANUELE	melting	peach	acid
HONEY ROYAL	slow-softening	nectarine	subacid	WHITE LADY	melting	peach	subacid
IP1	melting	peach	acid	XIA HUI	melting	peach	subacid
ISKRA	melting	peach	acid	YANG HUANG	melting	peach	acid
JIN CHUNG	melting	peach	subacid	ZAO XIA LU	melting	peach	acid
KAMARAT	melting	peach	acid	ZEE DIAMOND	melting	peach	acid
KAWEAH	melting	peach	acid	ZEE LADY	melting	peach	acid
KV930455	melting	peach	acid	ZEPHIR	slow-softening	nectarine	subacid
LAURA	melting	nectarine	acid	ORION	melting	nectarine	acid
LIMONET	melting	peach	acid	SENTRY	melting	peach	acid
LUCREZIA	melting	peach	acid	J.H.HALE	melting	peach	acid
MAGIQUE	slow-softening	nectarine	subacid	SPRINGCREST	melting	peach	acid
QUETTA	melting	nectarine	acid				

5 General conclusions

The aim of this research was to deepen the knowledge about the slow softening texture in peach.

Two major goals achieved are the setup of the texture dynamics models (TD) as a reliable tool to score difference in texture and the detection of SS major locus and his dominant mendelian inheritance.

Results from RNA-seq and NGS approaches as speculative data, because: a) not supported by measure of fruit hormones content; b) the so wide locus found did not allow to indicate a putative variant.

TD model could be applied to deep the knowledge about texture in peach, with the possibility to find new textures or to dissect the already known textures to find modulatory genes.

Findings the locus and the mendelian inheritance of the SS trait will help to design future experiments and would allow a more precise mapping and identification of the gene(s) involved in peach texture. Additionally, the new tool (TD) will help the development of efficient markers for assisted selection in breeding for optimum textural performance, a crucial aspect for increasing peach fruit competitiveness in the fresh market.

6 References

1. Szczesniak AS. Texture is a sensory property. Food Qual Prefer. 2002;13: 215–225. doi:10.1016/S0950-3293(01)00039-8
2. Lawless HT, Heimann H. Sensory Evaluation of Food 2nd Ed. Science. 2010. doi:10.1007/978-1-4419-6488-5
3. Johansson RS, Flanagan JR. Coding and use of tactile signals from the fingertips in object manipulation tasks. Nat Rev Neurosci. 2009;10: 345–359. doi:10.1038/nrn2621
4. Waldron KW, Smith AC, Parr AJ, Ng A, Parker ML. New approaches to understanding and controlling cell separation in relation to fruit and vegetable texture. Trends Food Sci Technol. 1997;8: 213–221. doi:10.1016/S0924-2244(97)01052-2
5. Boland AB, Delahunty CM, Van Ruth SM. Influence of the texture of gelatin gels and pectin gels on strawberry flavour release and perception. Food Chem. 2006;96: 452–460. doi:10.1016/j.foodchem.2005.02.027
6. Rosenthal AJ. Texture Profile Analysis - How Important Are the Parameters? J Texture Stud. 2010;41: 672–684. doi:10.1111/j.1745-4603.2010.00248.x
7. Tournier C, Sulmont-Rosse C, Guichard E. Flavour perception: aroma, taste and texture interactions. Food. 2007;1: 246–257. Available: http://www.globalsciencebooks.info/Journals/images/GSB_EditorBoards.pdf
8. Foster KD, Woda a, Peyron M a. Effect of texture of plastic and elastic model foods on the parameters of mastication. J Neurophysiol. 2006;95: 3469–79. doi:10.1152/jn.01003.2005
9. Rao MA. Rheology of Fluid, Semisolid, and Solid Foods [Internet]. Boston, MA: Springer US; 2014. doi:10.1007/978-1-4614-9230-6
10. Voragen AGJ, Coenen GJ, Verhoef RP, Schols HA. Pectin, a versatile polysaccharide present in plant cell walls. Struct Chem. 2009;20: 263–275. doi:10.1007/s11224-009-9442-z
11. Kim Y, Yoo YH, Kim KO, Park JB, Yoo SH. Textural properties of gelling system of low-methoxy pectins produced by demethoxylating reaction of pectin methyl esterase. J Food Sci. 2008;73: 367–372. doi:10.1111/j.1750-3841.2008.00771.x
12. Paniagua C, Posé S, Morris VJ, Kirby AR, Quesada M a, Mercado J a. Fruit softening and pectin disassembly: an overview of nanostructural pectin modifications assessed by atomic force microscopy. Ann Bot. 2014;114: 1375–83. doi:10.1093/aob/mcu149
13. Prasanna V, Prabha TN, Tharanathan RN. Fruit Ripening Phenomena–An Overview. Crit Rev Food Sci Nutr. 2007;47: 1–19. doi:10.1080/10408390600976841
14. Kanehisa M, Furumichi M, Tanabe M, Sato Y, Morishima K. KEGG: New perspectives on

genomes, pathways, diseases and drugs. Nucleic Acids Res. 2017;45: D353–D361. doi:10.1093/nar/gkw1092

15. Hayama H, Ito A, Moriguchi T, Kashimura Y. Identification of a new expansin gene closely associated with peach fruit softening. Postharvest Biol Technol. 2003;29: 1–10. doi:10.1016/S0925-5214(02)00216-8

16. Brummell DA, Harpster MH. Cell wall metabolism in fruit softening and quality and its manipulation in transgenic plants. Plant Mol Biol. 2001;47: 311–340. doi:10.1023/A:1010656104304

17. Hayama H, Shimada T, Fujii H, Ito A, Kashimura Y. Ethylene-regulation of fruit softening and softening-related genes in peach. J Exp Bot. 2006;57: 4071–4077. doi:10.1093/jxb/erl178

18. Brownleader MD, Jackson P, Mobasheri A, Pantelides a T, Sumar S, Trevan M, et al. Molecular aspects of cell wall modifications during fruit ripening. Crit Rev Food Sci Nutr. 1999;39: 149–164. doi:10.1080/10408399908500494

19. Wilkinson C, Dijksterhuis GB, Minekus M. From food structure to texture. 2001;11: 442–450.

20. Varela P, Ares G. Sensory profiling, the blurred line between sensory and consumer science. A review of novel methods for product characterization. Food Res Int. Elsevier Ltd; 2012;48: 893–908. doi:10.1016/j.foodres.2012.06.037

21. Essex E. Objective measurements for texture in foods. J Texture Stud. 1969;1: 19–37. Available: http://onlinelibrary.wiley.com/doi/10.1111/j.1745-4603.1969.tb00953.x/abstract

22. Harker FR, Redgwell RJ, Hallett IC, Murray SH, Carter G. Texture of Fresh Fruit. Horticultural Reviews. Oxford, UK: John Wiley & Sons, Inc.; 2010. pp. 121–224. doi:10.1002/9780470650646.ch2

23. Otegbayo B, Aina J, Abbey L, Sakyi-Dawson E, Bokanga M, Asiedu R. Texture Profile Analysis Applied To Pounded Yam. J Texture Stud. 2007;38: 355–372. doi:10.1111/j.1745-4603.2007.00101.x

24. Tabilo-Munizaga G, Barbosa-Cánovas G V. Rheology for the food industry. J Food Eng. 2005;67: 147–156. doi:10.1016/j.jfoodeng.2004.05.062

25. Rao MA. Rheology of Fluid, Semisolid, and Solid Foods. 2014; doi:10.1007/978-1-4614-9230-6

26. Barbosa-Cánovas G V., Kokini JL, Ma L, Ibarz A. The Rheology of Semiliquid Foods. Adv Food Nutr Res. 1996;39: 1–69. doi:10.1016/S1043-4526(08)60073-X

27. Prakash S, Tan DDY, Chen J. Applications of tribology in studying food oral processing and texture perception. Food Res Int. Elsevier Ltd; 2013;54: 1627–1635. doi:10.1016/j.foodres.2013.10.010
28. Kilcast D. Texture in Food. Texture in Food: Solid Foods v. 2. 2004. doi:10.1533/9781855737082.1.3
29. Costa F, Cappellin L, Longhi S, Guerra W, Magnago P, Porro D, et al. Assessment of apple (Malus×domestica Borkh.) fruit texture by a combined acoustic-mechanical profiling strategy. Postharvest Biol Technol. Elsevier B.V.; 2011;61: 21–28. doi:10.1016/j.postharvbio.2011.02.006
30. Varela P, Salvador A, Fiszman S. Changes in apple tissue with storage time: Rheological, textural and microstructural analyses. J Food Eng. 2007;78: 622–629. doi:10.1016/j.jfoodeng.2005.10.034
31. Kj??lstad L, Isaksson T, Rosenfeld HJ. Prediction of sensory quality by near infrared reflectance analysis of frozen and freeze dried green peas (Pisum sativum). J Sci Food Agric. 1990;51: 247–260. doi:10.1002/jsfa.2740510212
32. Martens M, Martens H. NEAR-INFRARED REFLECTANCE DETERMINATION OF SENSORY QUALITY OF PEAS. Appl Spectrosc. 1986;40: 303–310. doi:10.1366/0003702864509114
33. Roylance D. Stress-Strain Curves. Test. 2001; 1–14. doi:10.1361/aac
34. Harker FR, Redgwell RJ, Hallett IC, Murray SH, Carter G. Texture of Fresh Fruit. In: Janick J, editor. Horticultural Reviews. Oxford, UK: John Wiley & Sons, Inc.; 2010. pp. 121–224. doi:10.1002/9780470650646.ch2
35. Bourne MCC. Food texture and viscosity: concepts and measurements. 2002.
36. Ziosi V, Noferini M, Fiori G, Tadiello a., Trainotti L, Casadoro G, et al. A new index based on vis spectroscopy to characterize the progression of ripening in peach fruit. Postharvest Biol Technol. 2008;49: 319–329. doi:10.1016/j.postharvbio.2008.01.017
37. Finney EE, Abbott JA. METHODS FOR TESTING THE DYNAMIC MECHANICAL. 1978;2: 55–74.
38. Contador L, Díaz M, Hernández E, Shinya P, Infante R. The relationship between instrumental tests and sensory determinations of peach and nectarine texture. Eur J Hortic Sci. 2016;81: 189–196. doi:10.17660/eJHS.2016/81.4.1
39. Byrne DH. Trends in stone fruit cultivar development. Horttechnology. 2005;15: 494–500.
40. Thompson AK. Fruit and Vegetable Storage: Hypobaric, Hyberbaric and Controlled Atmosphere. 2016.

41. Thompson AK. Fruit and Vegetables [Internet]. Chichester, UK: John Wiley & Sons, Ltd; 2014. doi:10.1002/9781118653975
42. Layne D, Bassi D. The peach: botany, production and uses [Internet]. Layne D, Bassi D, editors. The peach: botany, production and uses. Wallingford: CABI; 2008. doi:10.1079/9781845933869.0000
43. Baird WV, Estager AS, Wells JK. Estimating Nuclear DNA Content in Peach and Related Diploid Species Using Laser Flow Cytometry and DNA Hybridization. J Am Soc Hortic Sci. 1994;119: 1312–1316.
44. Shi S, Li J, Sun J, Yu J, Zhou S. Phylogeny and Classification of Prunus sensu lato (Rosaceae). J Integr Plant Biol. 2013;55: 1069–1079. doi:10.1111/jipb.12095
45. Alphonse De Candolle. Origine des plantes cultivées. Germer-Baillière. 1886; 1689–1699.
46. Zheng Y, Crawford GW, Chen X. Archaeological evidence for peach (Prunus persica) cultivation and domestication in China. PLoS One. 2014;9. doi:10.1371/journal.pone.0106595
47. Dirlewanger E, Cosson P, Boudehri K, Renaud C, Capdeville G, Tauzin Y, et al. Development of a second-generation genetic linkage map for peach [Prunus persica (L.) Batsch] and characterization of morphological traits affecting flower and fruit. Tree Genet Genomes. 2006;3: 1–13. doi:10.1007/s11295-006-0053-1
48. FAOSTAT. FAOSTAT. Food and Agricultural Organization of the United Nations. 2014.
49. FAOSTAT. FAOSTAT Database on Agriculture. In: FAO - Food and Agriculture Organization of the United Nations. 2015.
50. Giovannini D, Liverani A, Sartori A, Cipriani G. Botanical and Pomological Aspects of Stone Fruits Physiology, Agronomy and Orchard Management. Agric Food Biotechnol Olea Eur Stone Fruit. 2015; 161–242. doi:10.2174/97816080599351150101
51. Micheletti D, Dettori MT, Micali S, Aramini V, Pacheco I, Da Silva Linge C, et al. Whole-genome analysis of diversity and SNP-major gene association in peach germplasm. PLoS One. 2015;10: 1–19. doi:10.1371/journal.pone.0136803
52. Anderson J V. Advances in Plant Dormancy. Sunflower and Plant Biology Research. 2015. doi:10.1017/CBO9781107415324.004
53. Reinoso H, Luna V, Pharis RP, Bottini R. Dormancy in peach (Prunus persica) flower buds. V. Anatomy of bud development in relation to phenological stage Article. Can J Bot. 2002;80: 656–663. doi:10.1139/b02-052
54. Citadin I, Raseira MCB, Herter FG, Baptista Da Silva J. Heat requirement for blooming and leafing in peach. HortScience. 2001;36: 305–307. doi:10.1590/S0100-29452003000100034

55. Szalay L, Timon B, Szabo Z, Papp J. Microsporogenesis of peach (Prunus persica L. Batsch) varieties. Int J Hortic Sci. 2002;8: 7–10.

56. Mounzer OH, Conejero W, Nicolás E, Abrisqueta I, García-Orellana Y V., Tapia LM, et al. Growth pattern and phenological stages of early-maturing peach trees under a Mediterranean climate. HortScience. 2008;43: 1813–1818.

57. Pirona R, Eduardo I, Pacheco I, Da Silva Linge C, Miculan M, Verde I, et al. Fine mapping and identification of a candidate gene for a major locus controlling maturity date in peach. BMC Plant Biol. BMC Plant Biology; 2013;13: 166. doi:10.1186/1471-2229-13-166

58. López-Girona E, Zhang Y, Eduardo I, Mora JRH, Alexiou KG, Arús P, et al. A deletion affecting an LRR-RLK gene co-segregates with the fruit flat shape trait in peach. Sci Rep. 2017;7: 6714. doi:10.1038/s41598-017-07022-0

59. Li X, Meng X, Jia H, Yu M, Ma R, Wang L, et al. Peach genetic resources: diversity, population structure and linkage disequilibrium. BMC Genet. 2013;14: 84. doi:10.1186/1471-2156-14-84

60. Yoon J, Liu D, Song W, Liu W, Zhang A, Li S. Genetic diversity and ecogeographical phylogenetic relationships among peach and nectarine cultivars based on simple sequence repeat (SSR) markers. J Amer Soc Hort Sci. 2006;131: 513–521. Available: http://journal.ashspublications.org/content/131/4/513.abstract?related-urls=yes&legid=jashs;131/4/513

61. Vendramin E, Pea G, Dondini L, Pacheco I, Dettori MT, Gazza L, et al. A unique mutation in a MYB gene cosegregates with the nectarine phenotype in peach. PLoS One. 2014;9. doi:10.1371/journal.pone.0090574

62. Pech JC, Purgatto E, Bouzayen M, Latché A. Ethylene and Fruit Ripening. Plant Horm Ethyl. 2012;44: 275–304. doi:10.1002/9781118223086.ch11

63. Ghiani a., Onelli E, Aina R, Cocucci M, Citterio S. A comparative study of melting and non-melting flesh peach cultivars reveals that during fruit ripening endo-polygalacturonase (endo-PG) is mainly involved in pericarp textural changes, not in firmness reduction. J Exp Bot. 2011;62: 4043–4054. doi:10.1093/jxb/err109

64. Haji T. Inheritance of flesh texture in peach and effects of ethylene treatment on softening of the stony hard peach. Japan Agric Res Q. 2014;48: 57–61. doi:10.6090/jarq.48.57

65. Gradziel TM, Martinez-Gomez P. Shell seal breakdown in almonds is associated with the site of secondary ovule abortion. J Amer Soc Hort Sci. 2002;127: 69–74.

66. Reig G, Alegre S, Cantín CM, Gatius F, Puy J, Iglesias I. Tree ripening and postharvest firmness loss of eleven commercial nectarine cultivars under Mediterranean conditions. Sci

Hortic (Amsterdam). Elsevier B.V.; 2017;219: 335–343. doi:10.1016/j.scienta.2017.03.001

67. Tatsuki M, Nakajima N, Fujii H, Shimada T, Nakano M, Hayashi KI, et al. Increased levels of IAA are required for system 2 ethylene synthesis causing fruit softening in peach (Prunus persica L. Batsch). J Exp Bot. 2013;64: 1049–1059. doi:10.1093/jxb/ers381

68. Nicotra A, Conte L, Moser L, Fantechi P. New types of high quality peaches: Flat peaches (P. Persica var. Platicarpa) and ghiaccio peach series with long on tree fruit life. Acta Horticulturae. 2002. pp. 131–135.

69. Fang W, Cai Z, Li G, Wang Z. PpYUC11 , a strong candidate gene for the stony hard phenotype in peach (Prunus persica L . Batsch), participates in IAA biosynthesis during fruit ripening Lei Pan , Wenfang Zeng , Liang Niu , Zhenhua Lu , Hui Liu , Guochao Cui , Yunqin Zhu , Jinfang Ch.

70. Sandefur P, Clark JR, Peace C. Peach Texture. Horticultural Reviews. 2013. pp. 241–302. doi:10.1002/9781118707418.ch06

71. Brecht JK, Kader AA, Ramming DW, Brecht, Jeffrey K. and Kader AA. Description and postharvest physiology of some slow-ripening nectarine genotypes. Journal of the American Society for Horticultural Science. 1984. pp. 596–600.

72. Mignani I, Ortugno C, Bassi D. Biochemical parameters for the evaluation of different peach flesh types. Acta Horticulturae. International Society for Horticultural Science (ISHS), Leuven, Belgium; 2006. pp. 441–448. doi:10.17660/ActaHortic.2006.713.65

73. Vaio C Di, Damiano C, Fideghelli C, Vaio C Di, Damiano C. VI CONVEGNO N AZIONALE SULLA P ESCHICOLTURA M ERIDIONALE SULLA P ESCHICOLTURA M ERIDIONALE A cura di : 2008.

74. Attanasio (Department of Agricultural and Environmental Sciences Production, Landscape A (DISAA). Graduate School in Molecular Sciences and Plant , Food and Enviromental Biotechnology Department of Agricultural and Environmental Sciences Production , Landscape , Agroenergy (DISAA) Plant Biology and Production XXV cycle Assessment of flesh texture in. 2012.

75. Lurie S, Crisosto CH. Chilling injury in peach and nectarine. Postharvest Biol Technol. 2005;37: 195–208. doi:10.1016/j.postharvbio.2005.04.012

76. Peace CP, Crisosto CH, Gradziel TM. Endopolygalacturonase: A candidate gene for Freestone and Melting Flesh in peach. Mol Breed. 2005;16: 21–31. doi:10.1007/s11032-005-0828-3

77. Pressey R, Avants JK. Difference in polygalacturonase composition of clingstone and freestone peaches. J Food Sci. Blackwell Publishing Ltd; 1978;43: 1415–1417.

doi:10.1111/j.1365-2621.1978.tb02507.x

78. Begheldo M, Manganaris GA, Bonghi C, Tonutti P. Different postharvest conditions modulate ripening and ethylene biosynthetic and signal transduction pathways in Stony Hard peaches. Postharvest Biol Technol. 2008;48: 84–91. doi:10.1016/j.postharvbio.2007.09.023

79. Hayama H, Tatsuki M, Ito A, Kashimura Y. Ethylene and fruit softening in the stony hard mutation in peach. Postharvest Biol Technol. 2006;41: 16–21. doi:10.1016/j.postharvbio.2006.03.006

80. Pan L, Zeng W, Niu L, Lu Z, Liu H, Cui G, et al. PpYUC11, a strong candidate gene for the stony hard phenotype in peach (Prunus persica L. Batsch), participates in IAA biosynthesis during fruit ripening. J Exp Bot. 2015;66: 7031–7044. doi:10.1093/jxb/erv400

81. Ghiani A, Negrini N, Morgutti S, Baldin F, Nocito FF, Spinardi A, et al. Melting of "Big Top" nectarine fruit: Some physiological, biochemical, and molecular aspects. J Am Soc Hortic Sci. 2011;136: 61–68. Available: http://www.scopus.com/inward/record.url?eid=2-s2.0-78651519484&partnerID=tZOtx3y1

82. Contador L, Díaz M, Millanao M, Hernández E, Shinya P, Sáenz C, et al. A proposal for determining the flesh softening of peach and nectarine in postharvest through simplified targeted modeling. Sci Hortic (Amsterdam). Elsevier B.V.; 2016;209: 47–52. doi:10.1016/j.scienta.2016.06.015

83. Yoshida M. Genetical studies on the fruit quality of peach varieties, 3: Texture and keeping quality. Bull Fruit Tree Res Station Ser A Hiratsuka. 1976; Available: http://agris.fao.org/agris-search/search.do?recordID=JP19760099806#.WV-YBeKCPK4.mendeley

84. Haji T, Yaegaki H, Yamaguchi M. Inheritance and expression of fruit texture melting, non-melting and stony hard in peach. Sci Hortic (Amsterdam). 2005;105: 241–248. doi:10.1016/j.scienta.2005.01.017

85. Rizzolo A, Vanoli M, Eccher Zerbini P, Jacob S, Torricelli A, Spinelli L, et al. Prediction ability of firmness decay models of nectarines based on the biological shift factor measured by time-resolved reflectance spectroscopy. Postharvest Biol Technol. 2009;54: 131–140. doi:10.1016/j.postharvbio.2009.05.010

86. Giné-Bordonaba J, Cantín CM, Echeverría G, Ubach D, Larrigaudiére C. The effect of chilling injury-inducing storage conditions on quality and consumer acceptance of different Prunus persica cultivars. Postharvest Biol Technol. Elsevier B.V.; 2016;115: 38–47. doi:10.1016/j.postharvbio.2015.12.006

87. Infante R. Harvest maturity indicators in the stone fruit industry. Stewart Postharvest Rev. 2012; doi:10.2212/spr.2012.1.4

88. Zhang L, Chen F, Yang H, Sun X, Liu H, Gong X, et al. Changes in firmness, pectin content and nanostructure of two crisp peach cultivars after storage. LWT - Food Sci Technol. Elsevier Ltd; 2010;43: 26–32. doi:10.1016/j.lwt.2009.06.015

89. Goffreda JC. Stony hard gene of peach alters ethylene Biosynthesis. Respiration, and other ripening-related characteristics. HortScience. 1992: 27:610 (Abstr.).

90. Iglesias I, Echeverría G. Differential effect of cultivar and harvest date on nectarine colour, quality and consumer acceptance. Sci Hortic (Amsterdam). 2009;120: 41–50. doi:10.1016/j.scienta.2008.09.011

91. Bonora E, Noferini M, Costa G, Vidoni S. Modeling fruit ripening for improving peach homogeneity in planta. Sci Hortic (Amsterdam). Elsevier B.V.; 2013;159: 166–171. doi:10.1016/j.scienta.2013.05.011

92. Matthews MA, Thomas TR, Shackel KA. Fruit ripening in Vitis vinifera L.: Possible relation of veraison to turgor and berry softening. Aust J Grape Wine Res. 2009;15: 278–283. doi:10.1111/j.1755-0238.2009.00060.x

93. King GA, Henderson KG, Lill RE. Ultrastructural changes in the nectarine cell wall accompanying ripening and storage in a chilling-resistant and chilling-sensitive cultivar. New Zeal J Crop Hortic Sci. 1989;17: 337–344. doi:10.1080/01140671.1989.10428054

94. Giovannoni JJ, DellaPenna D, Bennett a B, Fischer RL. Expression of a chimeric polygalacturonase gene in transgenic rin (ripening inhibitor) tomato fruit results in polyuronide degradation but not fruit softening. Plant Cell. 1989;1: 53–63. doi:10.1105/tpc.1.1.53

95. Lester D, Sherman WB, Atwell BJ. Endopolygalacturonase and the Melting Flesh (M) Locus in Peach. J Amer Soc Hort Sci. 1996;121: 231–235.

96. Callahan AM, Scorza R, Bassett C, Nickerson M, Abeles FB. Deletions in an endopolygalacturonase gene cluster correlate with non-melting flesh texture in peach. Funct Plant Biol. 2004;31: 159–168. doi:10.1071/FP03131

97. Gu C, Wang L, Wang W, Zhou H, Ma B, Zheng H, et al. Copy number variation of a gene cluster encoding endopolygalacturonase mediates flesh texture and stone adhesion in peach. J Exp Bot. 2016;67: 1993–2005. doi:10.1093/jxb/erw021

98. Tatsuki M, Haji T, Yamaguchi M. The involvement of 1-aminocyclopropane-1-carboxylic acid synthase isogene, Pp-ACS1, in peach fruit softening. J Exp Bot. 2006;57: 1281–1289. doi:10.1093/jxb/erj097

99. Verde I, Bassil N, Scalabrin S, Gilmore B, Lawley CT, Gasic K, et al. Development and evaluation of a 9K SNP array for peach by internationally coordinated SNP detection and validation in breeding germplasm. PLoS One. 2012;7: e35668. doi:10.1371/journal.pone.0035668

100. Verde I, Jenkins J, Dondini L, Micali S, Pagliarani G, Vendramin E, et al. The Peach v2.0 release: high-resolution linkage mapping and deep resequencing improve chromosome-scale assembly and contiguity. BMC Genomics. 2017;18. doi:10.1186/s12864-017-3606-9

101. Alexander DH, Lange K. Enhancements to the ADMIXTURE algorithm for individual ancestry estimation. BMC Bioinformatics. 2011;12: 246. doi:10.1186/1471-2105-12-246

102. Alexander DH, Novembre J, Lange K. Fast model-based estimation of ancestry in unrelated individuals. Genome Res. 2009;19: 1655–1664. doi:10.1101/gr.094052.109

103. Lipka AE, Tian F, Wang Q, Peiffer J, Li M, Bradbury PJ, et al. GAPIT: Genome association and prediction integrated tool. Bioinformatics. 2012;28: 2397–2399. doi:10.1093/bioinformatics/bts444

104. Kang HM, Sul JH, Service SK, Zaitlen NA, Kong SY, Freimer NB, et al. Variance component model to account for sample structure in genome-wide association studies. Nat Genet. 2010;42: 348–354. doi:10.1038/ng.548

105. Liu X, Huang M, Fan B, Buckler ES, Zhang Z. FarmCPU manual. PLOS Genet. 2016;12: e1005767. doi:10.1371/journal.pgen.1005767

106. Barrett JC, Fry B, Maller J, Daly MJ. Haploview: Analysis and visualization of LD and haplotype maps. Bioinformatics. 2005;21: 263–265. doi:10.1093/bioinformatics/bth457

107. Van Ooijen JW. JoinMap ® 4, Software for the calculation of genetic linkage maps in experimental populations. 2006;Kyazma B.V: Wageningen, Netherlands.

108. Van Ooijen JW. MapQTL 6, Software for the mapping of quantitative trait loci in experimental populations of dipoid species. Kyazma BV, Wageningen, Netherlands. 2009;

109. Dal Cin V, Danesin M, Rizzini FM, Ramina A. RNA extraction from plant tissues: the use of calcium to precipitate contaminating pectic sugars. Mol Biotechnol. 2005;31: 113–9. doi:10.1385/MB:31:2:113

110. Andrews S. FastQC: A quality control tool for high throughput sequence data. In: Http://Www.Bioinformatics.Babraham.Ac.Uk/Projects/Fastqc/. 2010 p. http://www.bioinformatics.babraham.ac.uk/projects/. doi:citeulike-article-id:11583827

111. Kim D, Pertea G, Trapnell C, Pimentel H, Kelley R, Salzberg SL. TopHat2: accurate alignment of transcriptomes in the presence of insertions, deletions and gene fusions. Genome Biol. 2013;14: R36. doi:10.1186/gb-2013-14-4-r36

112. Langmead B, Salzberg SL. Fast gapped-read alignment with Bowtie 2. Nat Methods. 2012;9: 357–9. doi:10.1038/nmeth.1923

113. Anders S, Pyl PT, Huber W. HTSeq-A Python framework to work with high-throughput sequencing data. Bioinformatics. 2015;31: 166–169. doi:10.1093/bioinformatics/btu638

114. Mortazavi A, Williams BA, McCue K, Schaeffer L, Wold B. Mapping and quantifying mammalian transcriptomes by RNA-Seq. Nat Methods. 2008;5: 621–628. doi:10.1038/nmeth.1226

115. Warnes G. gplots: Various R programming tools for plotting data. R package version 2.11.0.1. 2013. doi:citeulike-article-id:5194889

116. Li H, Durbin R. Fast and accurate short read alignment with Burrows – Wheeler transform. Bioinformatics. 2009;25: 1754–1760. doi:10.1093/bioinformatics/btp324

117. Goodstein DM, Shu S, Howson R, Neupane R, Hayes RD, Fazo J, et al. Phytozome: A comparative platform for green plant genomics. Nucleic Acids Res. 2012;40. doi:10.1093/nar/gkr944

118. Reumers J, Maurer-Stroh S, Schymkowitz J, Rousseau F. SNPeffect v2.0: A new step in investigating the molecular phenotypic effects of human non-synonymous SNPs. Bioinformatics. 2006;22: 2183–2185. doi:10.1093/bioinformatics/btl348

119. Eduardo I, Pacheco I, Chietera G, Bassi D, Pozzi C, Vecchietti A, et al. QTL analysis of fruit quality traits in two peach intraspecific populations and importance of maturity date pleiotropic effect. Tree Genet Genomes. 2010;7: 323–335. doi:10.1007/s11295-010-0334-6

120. Boudehri K, Bendahmane A, Cardinet G, Troadec C, Moing A, Dirlewanger E. Phenotypic and fine genetic characterization of the D locus controlling fruit acidity in peach. BMC Plant Biol. 2009;9: 59. doi:10.1186/1471-2229-9-59

121. Serra O, Giné-Bordonaba J, Eduardo I, Bonany J, Echeverria G, Larrigaudière C, et al. Genetic analysis of the slow-melting flesh character in peach. Tree Genet Genomes. Tree Genetics & Genomes; 2017;13. doi:10.1007/s11295-017-1160-x

122. Lurie S, Friedman H, Weksler A, Dagar A, Eccher Zerbini P. Maturity assessment at harvest and prediction of softening in an early and late season melting peach. Postharvest Biol Technol. Elsevier B.V.; 2013;76: 10–16. doi:10.1016/j.postharvbio.2012.08.007

123. Li X wei, Jiang J, Zhang L ping, Yu Y, Ye Z wen, Wang X min, et al. Identification of volatile and softening-related genes using digital gene expression profiles in melting peach. Tree Genet Genomes. 2015;11. doi:10.1007/s11295-015-0891-9

1450